Power Transmission Engineering®

SEPTEMBER 2016

BEARINGS
BASICS AND BEYOND

- VIBRATION
- SPECIAL APPLICATIONS
- CARE AND HANDLING
- BEARING LIFE

www.powertransmission.com

Power Transmission Engineering®

SEPTEMBER 2016

[28]

[20]

FEATURE ARTICLES

TECHNICAL ARTICLES

Vol. 10, No. 6. POWER TRANSMISSION ENGINEERING (ISSN 2331-2483) is published monthly except in January, May, July and November by Randall Publications LLC, 1840 Jarvis Ave., Elk Grove Village, IL 60007, (847) 437-6604. Cover price $7.00. U.S. Periodicals Postage Paid at Elk Grove Village IL and at additional mailing offices. Send address changes to POWER TRANSMISSION ENGINEERING, 1840 Jarvis Ave., Elk Grove Village, IL 60007.

Power Transmission Engineering

VOL. 10, NO. 6

www.powertransmission.com

PTE Videos

Boca Bearing supplies components for the Wild Goose Canning Company, Boulder, CO. Check out a short video at **www.powertransmission.com/videos/Boca-Bearing-Spotlight.**

This video is part of the Spotlight series by Boca Bearings. **(www.youtube.com/channel/UCvc3Fd47QtOiPWGGE0p0zPA).**

Photo courtesy of Bosch Rexroth

IMTS Recap

Want a recap of everything IMTS, MDA and IANA? Check out *PTE*'s e-newsletters as well as the website for all the new technologies and products presented in the power transmission, motion control and fluid power sectors.

Back to Basics:

Check out ***www.powertransmission.com/subjects/basics*** for our library of Back to Basic articles on bearings, motors, lubrication, couplings, gears and more.

Buyers Guide Spotlight:

Mach III Clutch Inc.

Mach III designs and manufactures air and spring applied friction brakes, clutches, combination clutch-brakes, and mechanical torque limiters for power transmission applications to 5,000 lb.ft.

MACH III
Clutches • Brakes • Torque Limiters

More than 2,000 different models are available. We have been in business for more than 40 years and work directly with all levels of clients: OEM, distributor and user. Get listed in the PTE Buyer's Guide here: ***www.powertransmission.com/getlisted.php***

Stay Connected

Follow us on Twitter
twitter.com/#!/PowerTransMag

Connect with us on LinkedIn
www.linkedin.com/groups/Power-Transmission-Engineering-PTE-2950055

Subscribe Online
www.powertransmission.com/subscribe.htm

Power Transmission Engineering

Randall Publications LLC
1840 Jarvis Avenue
Elk Grove Village, IL 60007
Phone: (847) 437-6604
Fax: (847) 437-6618

EDITORIAL

Publisher & Editor-in-Chief
Michael Goldstein
publisher@powertransmission.com

Managing Editor & Associate Publisher
Randy Stott
wrs@powertransmission.com

Senior Editor
Jack McGuinn
jmcguinn@powertransmission.com

Senior Editor
Matthew Jaster
mjaster@powertransmission.com

News Editor
Alex Cannella
alex@geartechnology.com

Editorial Consultant
Paul R. Goldstein

ART

Art Director
David Ropinski
dropinski@powertransmission.com

ADVERTISING

Advertising Sales Manager & Associate Publisher
Dave Friedman
dave@powertransmission.com

China Sales Agent
Eric Wu
Eastco Industry Co., Ltd.
Tel: (86)(21) 52305107
Fax: (86)(21) 52305106
Cell: (86) 13817160576
eric.wu@eastcotec.com

Materials Coordinator
Dorothy Fiandaca
dee@randallpublications.com

DIGITAL

Content Manager
Kirk Sturgulewski
kirk@powertransmission.com

CIRCULATION

Circulation Manager
Carol Tratar
subscribe@powertransmission.com

Circulation Coordinator
Barbara Novak
bnovak@powertransmission.com

RANDALL PUBLICATIONS STAFF

President
Michael Goldstein

Accounting
Luann Harrold

BPA WORLDWIDE℠ BUSINESS

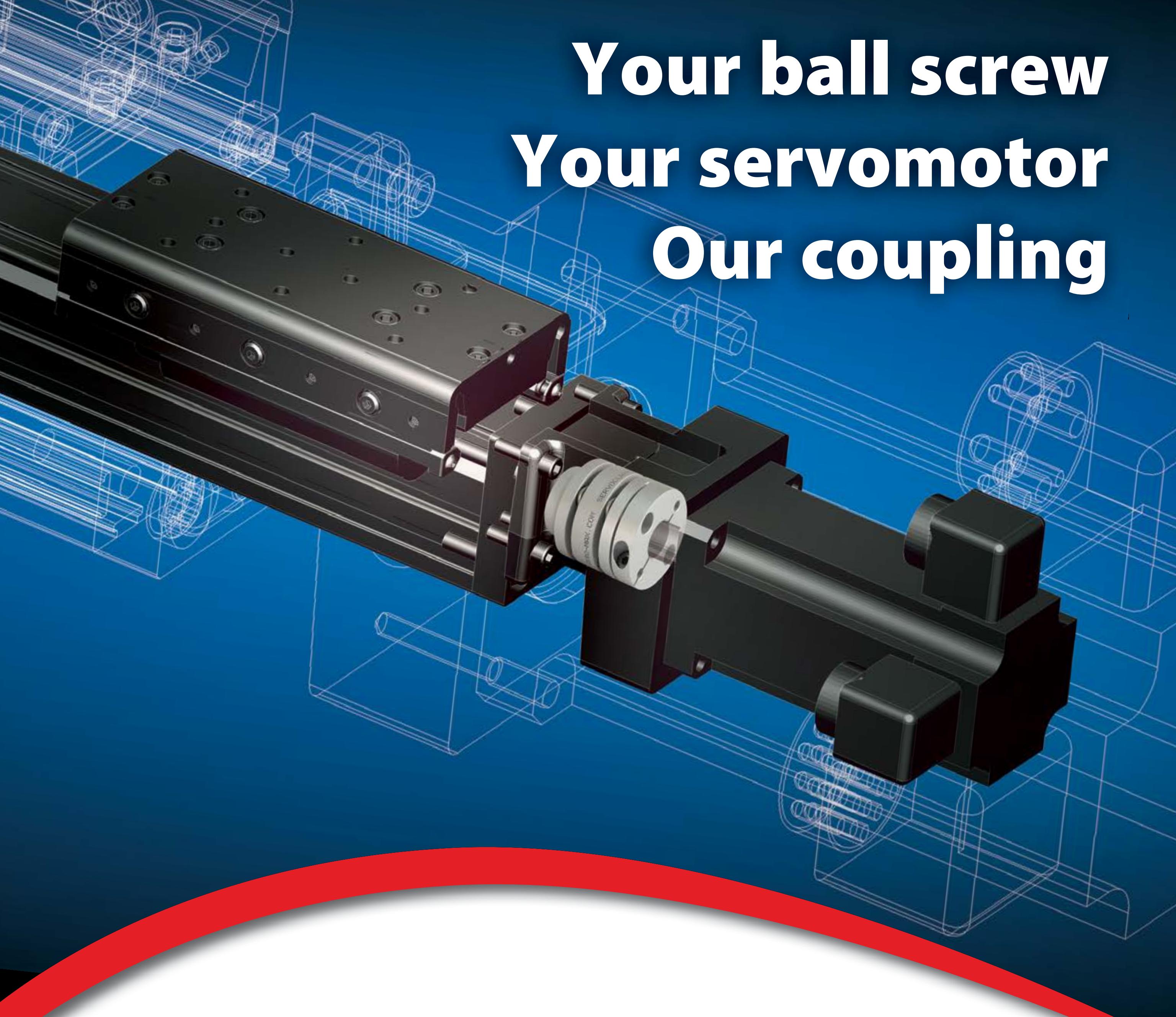

Your ball screw
Your servomotor
Our coupling

Together a winning combination for today's servomotor applications.

Our ServoClass® couplings have been recently redesigned to enable your actuator to go even faster and achieve the positional accuracy that will take your designs to the next level. Our couplings will do all this with low bearing loads.

3 New sizes now available.

Now, size, select and see the right ServoClass® coupling solution for your application with Zero-Max 3D CAD files.

Check our FAST deliveries.

ZERO-MAX®

www.zero-max.com 800.533.1731

Randy Stott, Managing Editor

Applications Abound

In a recent reader survey, you told us you wanted to see more specific examples of mechanical power transmission products and how they're designed, upgraded, maintained and used in a wide variety of industries. In the business, we call that type of article an "application story," and in this issue we've answered the call with several application stories that show how smart choices are being made about motion components in a wide variety of industries.

In "Mining for Solutions," (page 28) Chris Medinger of Leeson Electric explores the roles electric motors play in the overall success of a mining operation, especially considering the importance of energy efficiency and predictable maintenance. In this issue's *BSA Field Notes* column (page 32), Ernest Head of Motion Canada tackles some problematic bearings in a lumber mill. And Bruce Stephan's article (page 34) explains how the right pump technology—coupled with sophisticated software—helped solve a leak problem in adhesive dispensing application.

This issue also focuses on bearings, with a number of important features and technical articles. "Proper Handling of Bearings" (page 30) is this issue's *BSA Bearing Brief*. It includes important handling and lubrication tips for maintenance professionals. Chris Hansford's article, "Opening the Envelope on Bearing Vibration," (page 26) describes how advanced analysis techniques, along with the proper sensors, can be used to cut through the noise to determine problems in bearings, gearboxes and more. Will Cannon of Baldor Electric describes the lubrication theory and critical design parameters for applications that use hydrodynamic bearings and operate at slow speeds in "Minimum Design Considerations for Sleevoil Bearings for Industrial Fan Applications" (page 36).

Our centerpiece technical article this issue deals with a topic that's important both for system designers and those responsible for maintenance: bearing life. In "A Model for Rolling Bearing Life with Surface and Subsurface Survival—Tribological Effects," (page 44) the authors explore models that separate the risk of subsurface fatigue from the other factors that contribute to bearing life estimation, giving designers and manufacturers one more tool toward understanding which bearings are the right choice for their applications.

Finally, I'd like to call your attention to Senior Editor Jack McGuinn's article on Ethernet fieldbus technology and the various protocols that are enabling faster, better communication at the device level, using standardized, easily implemented technology. Read "The Brave New World of Industrial Automation," beginning on page 20, to learn how EtherCat and other protocols are helping to make better, smarter machines in a wide variety of industries.

Thank you to those of you who participated in our reader survey. We appreciate the feedback, and we promise we'll continue to deliver more of what you ask for. If you didn't get a chance to participate in the survey, but you'd still like to make suggestions or comments, my inbox is always open at *wrs@powertransmission.com*.

As always, thanks for reading.

Voith Turbo

PROVIDES TORQUE LIMITER TECHNOLOGIES FOR THE MODERN WORLD

TODD LEHMAN, VOITH TURBO, PRODUCT SALES MANAGER

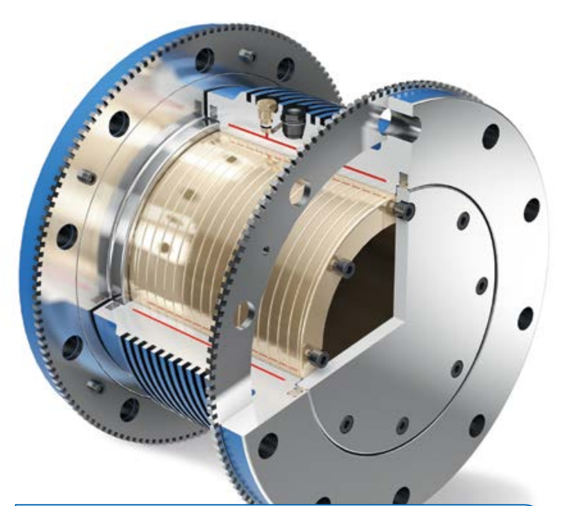

The Voith Turbo SlipSet is a mechanical fault ride through coupling that slips to trim or shave off torque peaks.

In today's world, the attitude of doing more with less extends to all areas of business. When considering machine productivity, doing more with less isn't a good idea. Working a machine past its designed factor of safety will limit the longevity of the machine and will single out the weakest link in its drive chain. In every case, a machine pushed past its design limits will fail when least expected (even though failure should be expected). Likewise, a machine whose drive chain design doesn't fully account for high amplitude torque spikes caused by sudden machine jams or electrical supply faults will expose the weak link either during the occurrence of the torque spike or sometime later when the fatigued link finally breaks unexpectedly.

There are several methods currently in use that attempt to maximize a machine's productivity without exceeding its design capacity. One method partially achieves the objective by monitoring the supply amperage relative to the motor nameplate amperage. While this method keeps the machine from operating past its design point based on the motor feedback, it does little to protect the drive chain from torque overloads caused by sudden machine jams or electrical supply faults.

Another method is to purposefully design the drive chain with a weak link such as a flexible connection coupling. Some level of perceived protection may be achieved through this method, but it must be considered that a failed flexible connection coupling will require some level of parts replacement and could cause damage to the surrounding drive components and guards as well as requiring added downtime, parts, and labor. The idea of a weak link in the drive chain is a good one, but that weak link needs to provide torque accuracy to maximize machine productivity, be easy to reset and not require a lot of parts or manpower to do it. The solution for the problem of maximizing machine productivity without exceeding machine capacity is the use of a torque limiter.

Torque limiters have been in use for years and are available in many configurations and types.

Shear pin couplings are fatigue based limiters that use specifically sized pins to transmit a set amount of torque and require replacement after an overload or after they have experienced too much fatigue. Adjustment of the torque limiter capacity requires resizing of the shear pins.

The Voith Turbo SmartSet has the ability to slip without seizing due to its special friction surface.

Ball in detent couplings are spring loaded limiters that can be reset through counter rotation of the mounted parts or by re-engagement of the balls via taps of a mallet. Over a period of time, the detents wear and the spring's tension decreases. Adjustment of the torque limiter capacity can typically be done through adjustment of the springs that apply pressure to the balls.

Hydraulically pressurized, friction based couplings are backlash free torque limiters which utilize shear tubes and a shear ring for release of the hydraulic pressure during a torque overload event. As soon as the pressure is released the coupling freely spins without contact of the friction surfaces. The shear tubes are replaced and hydraulic pressure is re-applied based on the desired torque limitation to reengage the unit. Adjustment of the torque limiter capacity can easily be accomplished by referencing the pressure-vs-torque calibration diagram that is supplied with the unit.

Having addressed the issue of maximizing machine productivity without exceeding its capacity, the next issue often occurs after the release of the torque limiter. It's true that the torque limiter has done its job to protect the drive chain of the machine but it does not automatically reset to allow a machine start. This has been a dilemma faced by operators for years. The question becomes: Should they should push the machine and risk failure, or not push the machine and reset a torque limiter?

The answer to that question could be a torque limiter with the ability to slip during overloads. Rather than immediately releasing on overload, these solutions will either slip for a number of degrees before releasing or never release at all unless an external trigger is used or the machine monitoring controls forces a shutdown. These torque limiters are based on the hydraulically pressurized, friction based design but use specially selected friction surfaces to allow for extended periods of slip. To help understand these limiters, it's important to know more about their construction.

The basic hydraulically pressurized, friction based torque limiting coupling, such as a Voith SafeSet, is made up of an inner and outer sleeve that are assembled and welded at the ends. This assembly forms a twin-walled hollow sleeve which can be oil pressurized up to 1,000 bar/14,500 psi after the machining of the necessary pressurization and shear tube ports have been completed. The design of the shear tube and mating seat provides a reliably sealed system, while the size of the torque limiting coupling determines the size and quantity of shear tubes that are to be used. The friction surface is specially treated to prevent wear during the slip phase of the coupling release. Once the SafeSet coupling has released it rotates on bearings preventing wear on those friction surfaces.

During normal operation the bearings remain static. The bearings only rotate following a release due to torque overload, which makes bearing life a minor factor when considering the operational dependability of the coupling. The bearings and friction surfaces are separated from the pressurized sleeve and require lubrication oil. The lubrication oil is used for two things: Bearing lubrication during a release condition, and to maintain a predictable friction coefficient across the friction surfaces which results in a precise release torque relative to the applied pressure.

As noted earlier, hydraulically pressurized, friction based torque limiting couplings have no backlash and are not subject to material fatigue because the transmitted torque is through a friction surface. The applied hydraulic pressure generates a defined frictional force between the pressure sleeve and the shaft. The applied pressure determines the release torque of the coupling. Therefore, an increase or decrease of applied pressure, working within the torque limiters adjustment range, will result in an increase or decrease of the release torque.

If the operating torque exceeds the pressure-based release torque setting, the driving shaft will rotate relative to the pressure sleeve which is connected to the driven load. This results in an immediate reduction in applied torque when the friction force changes state from static to dynamic. The shear ring that is fixed to the driving shaft rotates relative to the pressure sleeve and breaks off the top of the shear tubes. Upon contact, the oil pressure in the coupling drops and the applied frictional force in the coupling is reduced releasing the torque limiting coupling and providing full separation of the driving and driven components of the drive chain.

Following a release, resetting of the coupling is simple. First the shear ring is aligned to allow removal of the shear tubes. Next the shear tubes are replaced and torqued to specification. Finally, the coupling is re-pressurized according to the calibration curve of the unit and following a simple pressurization procedure.

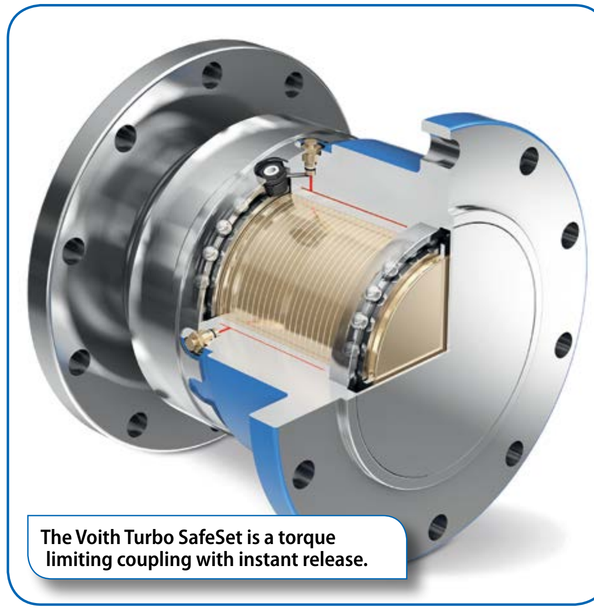

The Voith Turbo SafeSet is a torque limiting coupling with instant release.

With the basics of hydraulically pressurized, friction-based torque limiting couplings in mind, it is also important to understand the more advanced versions including: couplings that have the ability to slip as well as mechanical stops to prevent damage from excessive slip due to machine overloads; and permanently slipping torque limiting couplings which can only be influenced through external monitoring.

The Voith SmartSet torque limiter is a mechanical fault ride through coupling that slips to trim or shave off torque peaks caused by short duration overloads to protect the drive chain components. The SmartSet was originally designed as a start-up coupling for synchronous motors which generate transient torques of plus or minus ten times the motor nominal torque during acceleration and prior to grid synchronization. The SmartSet will also fully release in situations of extended over torques to protect the links of the drive chain and itself. The SmartSet technology and construction is based on the previously discussed design of the SafeSet torque limiting coupling. However, there are differences that make the SmartSet unique:

- The SmartSet has the ability to slip without seizing due to its special friction surface.
- The SmartSet device is centrifugally engaged by the shaft rotation of the application.
- The SmartSet design allows for a minimum slip before release of 30 degrees and a maximum of 120 degrees per start.

The slip angle before release is reset with each shut down of the machine and the full 30 to 120 degree slip angle becomes available once more. With this type of torque limiter the need for a machine shut down is limited to instances of multiple short duration overloads or a continuous overload. After a trip, the limiter must be reset and re-pressurized for the appropriate torque unless an active slip monitor like the Voith CMS 310 is used to provide feedback to the machine PLC to either stop the process or reduce the load before the SmartSet is mechanically forced to trip.

Much like the Voith SmartSet, the Voith SlipSet torque limiting coupling is a mechanical fault ride through coupling that slips to trim or shave off torque peaks caused by short or extended duration overloads to protect the drive chain components. The SlipSet will not release and therefore no resetting of the SlipSet is required. Once more, active monitoring of the slip with the CMS 310 or other active monitor is important. While the SlipSet is designed to slip, it is not designed for permanent slip. Slip makes heat and is an indicator that the machine is being pushed past its design parameters. The active monitor looks at the torque limiter slip and provides the machine PLC with feedback to make appropriate decisions such as feed reduction, feed stop, or machine shut down.

With trends moving toward more remote machine visibility and monitoring, several devices have been developed for use with any of the previously discussed hydraulically pressurized, friction based torque limiters. The Voith series of remote monitoring and control technologies provides an added level of safety and control to the machine and its torque limiter.

The CMS 310, Coupling Monitoring System, is a new generation of Voith Coupling Monitoring System, built on a PLC based platform. By continuous monitoring, the operator can get important information about the status of a coupling and driveline. The operator is able to supervise and monitor a torque limiting coupling over a web interface or HMI panel. This is possible because the system uses the Profinet communication standard for an easy integration to existing industrial process monitoring systems. The slip angle is continuously measured and calculated to determine how much the coupling has slipped. The status information can then be used to quickly identify any need for action.

The active monitoring system fits well within Industry 4.0 thinking by providing increased uptime, integration with existing process monitoring systems, potential driveline performance optimization, maintenance benefits and visual and audio warning indicators.

The active monitoring system works through calculation of the torque limiting coupling input and output rotational positions. The measurements are made by inductive sensors mounted on each side of the torque limiting coupling. If the coupling slips, there will be a pulse difference between the sensors, and the control system will inform the operator of the current situation via a web interface or optional HMI panel. Depending on the customer's preference, the machine PLC or the machine operator can then adapt the power input to reduce the load, or shut down the drive line depending on the information from the CMS 310 system. The CMS 310 also monitors the maintenance of the torque limiting coupling, since it will monitor the number and duration of releases and slips. When the limit defined for the installed torque limiter is reached, the CMS 310 will indicate that a service is needed by showing a service indicator light on the screen.

Demands on operators and machines continue to increase, as companies are focused intently on production and efficiency. As we've discussed in this article, these demands can lead to over-taxing machines, pushing them past their safe limits and tolerances — a practice that can lead to outcomes contrary to efficient production. Fortunately, we have also discussed vital systems — torque limiting technology — designed to help operators maximize their machine's productivity without exceeding design capacity or jeopardizing safety and efficiency.

For more information:
Voith Turbo
Phone: (717) 767-3200
www.voith.com

Svendborg

BRAKING CONTROL SYSTEM GOES MOBILE

SOBO iQ controls are now accessible from both Android and IOS mobile devices. This new level of convenient accessibility is significant since most SOBO iQ controls are installed in tough, hard-to-reach, isolated areas such as underground or overland mining conveyors.

Users can remotely access and monitor their Svendborg Brakes SOBO iQ controls by simply downloading the CERHOST app for Android mobile phones or tablets, available from Microsoft on GooglePlay. The iCERHOST app for use with iPhones and iPads is available via the iTunes App Store. Once downloaded, the app can be easily accessed using the "Remote Display" tool on any computer.

The SOBO iQ main menu allows users to access all control functions including startup, brake ramps, parking, hpU and diagnostics. The state-of-the-art SOBO iQ combines various cutting-edge technologies to provide significant flexibility, safety and durability on mine conveyors and other heavy-duty industrial applications.

The SOBO iQ features three-state digital modulation and a dual-loop PI control (pressure/speed). The pressure control is based not only on speed but also on deceleration. SOBO iQ controls braking torque by comparing a preset speed ramp with actual conveyor speed feedback. The unit can provide different braking profiles for different operational scenarios. Advanced functions including independent overspeed monitoring, rollback, gearbox and out-of-band monitoring are included.

The SOBO iQ provides only the torque needed for a safe, controlled stop. The controller can be used with a combination of brake types, mounted on both the high and low speed sides of the conveyor drive. Up to four hpUs can be connected to each controller.

For more information:
Svendborg Brakes (Altra Industrial Motion)
Phone: (303) 285-1271
www.svendborg-brakes.com

AutomationDirect

FORK SENSORS DESIGNED FOR EASY INSTALLATION

AutomationDirect's new PS series fork sensors, also referred to as "slot" or "U" sensors, are offered in visible red light and laser models. Available in PNP and NPN styles, and designed for easy installation, the rugged metal one-piece construction assures constant alignment. The high-resolution PS-series fork sensors feature glass optics, selectable light on/dark on operation, adjustable sensitivity potentiometers, high switching frequencies, and are fitted with M8 connectors with 360-degree viewable LED indicators. Starting at $86.00, the visible red light fork sensors feature easy setup and have a sensing range from 5mm to 220mm, depending on model. Starting at $137.00, the laser fork sensors feature a Class 1 laser to detect small objects

and have a sensing range of 30 mm to 120 mm, depending on model; certain models are available for transparent objects. All PS-series fork sensors are IP67-rated, have cULus approval and are CE, RoHs and REACH compliant.

For more information:
AutomationDirect
Phone: (800) 633-0405
www.automationdirect.com

MINExpo Preview

DAVID BROWN SANTASALO

David Brown Santasalo will showcase its AMF Series at the upcoming MINExpo International exhibition in Las Vegas, Nevada. The launch of the AMF series in February of this year attracted the interest of many equipment manufacturers and end users with applications for agitation, mixing and flotation. The AMF vertical gear unit provides high thermal capacity and eliminates the need for external cooling in extreme ambient conditions.

These two or three-stage vertically mounted helical gear units feature a power range of up to 750 kW and nominal output torque of up to 200 kNm, as well as a reversible operational direction. Their robust design ensures they're easy to transport

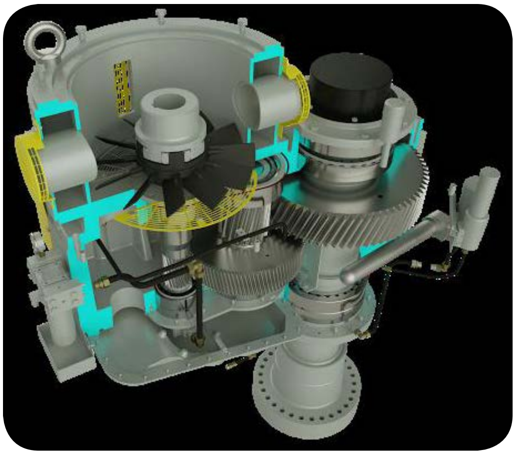

and install without risk of damages. More on the AMF features can be seen on the product animation at the website below.

Joe Sitta, director of sales for David Brown Santasalo's Americas business comments: "The AMF is the result of bringing the latest in gearing technology together with the unique features and benefits of our application proven designs into the most modern and highly adaptable product on the market today. The AMF is built rugged for long worry free operation in the most demanding applications."

To learn more about the AMF, visit David Brown Santasalo at MINExpo International: Stand 27513, South Hall 2, Las Vegas Convention Center, Las Vegas, Nevada.

For more information:
David Brown Santasalo
http://santasalo.com/products/flotation-drive/

Stafford Manufacturing

DEVELOPS COLLARS AND COUPLINGS FOR MAINTENANCE, REPAIR AND RETROFIT

A new group of shaft collars, couplings, thrust assemblies and repair kits especially developed for maintenance applications is being introduced by Stafford Manufacturing Corp.

The Stafford Maintenance Group features eight families of products born from special repair and retrofit requirements to add capabilities such

MINExpo Preview

STIEBEL-GETRIEBEBAU GMBH

Stiebel-Getriebebau has developed advanced pump drives which combine an improved energy balance, greater flexibility and performance. Visitors to this year's MINExpo will be able to discover these technologies at the Stiebel-Getriebebau exhibition Stand 28900 in the South Hall.

For mid-size mining excavators and above (from around 300 t), the Stiebel Type 4462 pump drive provides the driving force. The drive is connected to the engine (800 kW) via an SAE 0 bell housing adapter. The available range of transmission ratios varies between i_1= 0.9 and 2. The integrated oil pump and the oil distribution system used by Stiebel ensure optimum lubrication and cooling of the pump drive. This means that sloping positions — of up to 30° in all directions — are possible during operation. Overall, a maximum of six pumps can be fitted on both sides which actuate the swivel and reach operation together with the other hydraulic functions. Furthermore, the hydraulic pump attachments also provide a separate oil chamber to ensure operating reliability for the hydraulic unit system.

as wrenching flats to collars for applying torque, conversion couplings and adapters for joining dissimilar shafts, and the Stafford Prototype and Repair Collar System (SPARC) that lets users create their own working models of special-purposed shaft collars and components within a few hours.

Developed to reduce downtime and costs, the Stafford Maintenance Group of shaft collars also includes weldable- and paintable-shaft collars, along with collars and couplings that are available in kits. Conversion couplings allow for the joining of inch-metric and different size shafts and thrust collar assemblies, including micro-adjustable end stops and axial thrust designs for releasing frozen shaft components are also offered.

Stafford Products for maintenance, repair, and retrofit are priced according to configuration and quantity. Price quotations are available upon request.

For more information:
Stafford Manufacturing Corp.
Phone: (800) 695-5551
www.staffordmfg.com

With the Type 4382 single-stage pump drive from the P2000 range, Stiebel-Getriebebau has created a special solution for a wide range of mobile hydraulic applications. The robust, torsionally-stiff drive employs the proven modular system to offer a comprehensive range of attachment variants. The unit is connected using an SAE bell housing or cardan flange. Three pump connections at the take-off with freely selectable SAE connector are available. The maximum torque per take-off is 1,500 Nm and a maximum speed of up to 3,000 min^{-1} is possible. At an engine power of 530 kW the pump drive is available with a transmission ratio of i = 0.6572 to 1.5217. The design — with a weight of 200 kg and block casing — is particularly compact, allowing space-saving integration. Thanks to a special lubrication system, which utilizes customized internal ribbing and oil pockets, the lubrication of all necessary components is ensured.

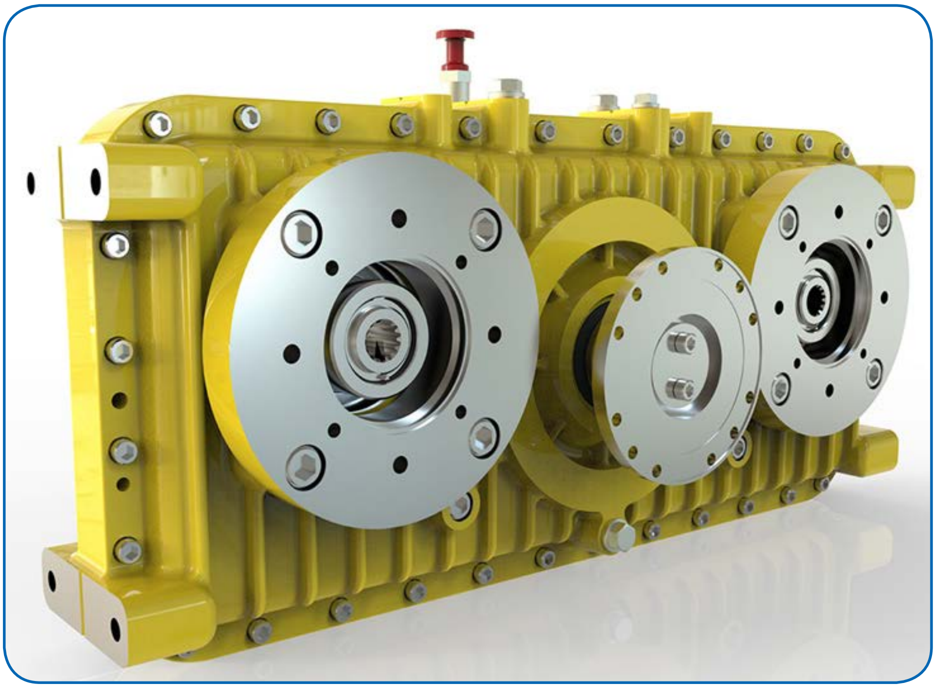

With its high degree of adaptability, the Stiebel Type 4652 pump drive provides an ideal drive solution — in particular for mobile tracked drilling rigs. This is because its particularly compact design allows easy underfloor installation. The geometric offset of the drive/take-off, the large oil volume and solid ribbing of the casing result in an outstanding energy balance for the pump drive. This means that an additional oil cooler is not usually necessary. The drive therefore ensures economical and sustainable operation with $P_{max} = 700$ kW, $T_{2max} = 3{,}300$ Nm and a maximum speed of $Nm_{ax} = 2{,}500$ min^{-1}.

For more information:

Stiebel-Getriebebau GmbH
Phone: +49 1802 78 43 235
www.stiebel.de

Brother Gearmotors

OFFERS 3D CAD DRAWINGS FOR 1-3 HP MOTORS

Brother Gearmotors now offers 3D Computer-aided Design (CAD) drawings of its 1–3 hp gearmotors on the company's website. With the new online tool, customers can easily access and search Brother Gearmotors' product catalog, using 3D technology to pan, zoom and rotate images of the 1-3 hp gearmotors. Offering realistic, high quality visuals and details, the panoramic images can be manipulated in a variety of ways to provide a comprehensive view of the products from various angles.

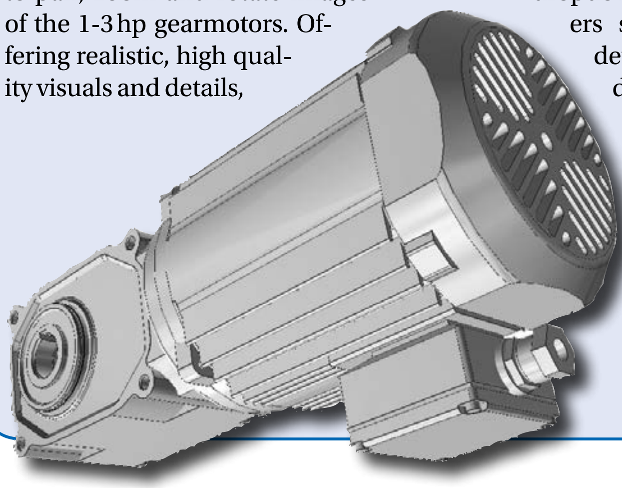

Site visitors can fully configure and download products in 150+ CAD and graphics formats. Additionally, a dropdown menu offers customers spec sheets containing detailed motor and brake dimensions.

All Brother Gearmotors in the 1–3 hp range are compliant with the new government (DOE) mandate for small electric motors that took effect June 1, 2016.

"Our 3D modeling technology offers customers the ability to more accurately see what a particular gearmotor will look like when it is placed in its intended application," said Matthew Roberson, senior director of Brother Gearmotors. "Brother is pleased to provide a way to enhance user education and simplify the overall selection process using this easy navigation tool."

For more information:

Brother Gearmotors
Phone: (866) 523-6283
www.brother-usa.com/gearmotors

Festo

SEMI-ROTARY VANE DRIVE DESIGNED FOR LONG LIFE AND FAST INSTALLATION

Festo has introduced a new pneumatic semi-rotary vane drive and matched contactless position sensor that transforms a relatively simple and low cost drive into a solution that lowers engineering and inventory overhead, is fast and easy to install, and delivers long service life due to its sealed housing.

Standard swivel angles for the DRVS semi-rotary drive are 90, 180, and 270 degrees. Custom swivel angles are possible with a stop bracket accessory. At six bar pressure, the seven different sizes in the DRVS line deliver a torque range of .15 Nm to 20 Nm. Festo sizing software makes ordering the optimum unit for the application fast and accurate. The company guarantees overnight shipping for standard DRVS drives, which lowers inventory requirements for OEMs and assures end use customers fast delivery of replacement parts.

The SRBS, a compact, contactless magnetic position sensor, attaches to the DRVS via a single cable and three screws. During installation, personnel simply move the vane to the drive's two positions and with a few clicks of the SRBS push button both positions are located for the position sensing unit. Repetition accuracy is <.0039 inches (.1 mm). Through its push button, the SRBS position sensor can be designated PNP or NPN and NO or NC, which means that one part number covers all the different combinations.

"Festo is fundamentally reshaping its product lines to engineer end-to-end productivity for customers," said Mike Guelker, Festo product manager. "Customers are going to like the fast, accurate ordering, delivery, and installation of the DRVS and the flexibility, ease of use, and accuracy of the SRBS."

For more information:
Festo Corporation
Phone: (631) 231-9215
www.festo.com/us

Portescap

EXPANDS ATHLONIX DCT MOTOR SERIES

Portescap expands the newly launched DCT range of Athlonix Brush DC motors with the introduction of the 17DCT brush DC mini motor. The 17DCT motor features Portescap's energy efficient coreless design with an optimized self-supporting coil and magnetic circuit which enables higher performance in a compact 17 mm diameter size.

With high torque carrying capabilities reaching up to 6.14 mNm, the 17DCT provides suitable performance with efficiency reaching up to 85 percent while providing a long lifetime. Due to the inherent design of the 17DCT motor, it can deliver higher torque per ampere resulting in better battery life. This makes it ideal for demanding applications such as medical and industrial pumps, drug delivery systems, miniature industrial power tools, tattoo machines, mesotherapy guns, dental tools, watch winders and more. Other applications, including lab automation, security and access and humanoid robots, can benefit from the features of the 17DCT Athlonix motor.

Athlonix 17DCT miniature DC motors are available in two variations, precious metal commutation and graphite commutation with a neodymium magnet inside. The unique constant force spring design for carbon brush provides consistent performance. An REE (Restriction of Electro Erosion) coil is an available option, which prolongs the life of the motor and provides an environment of intrinsic safety especially at high speed conditions.

"Athlonix motors are powered by a proprietary self-supporting coil resulting in maximized magnetic flux and ampere-turns for a given diameter," said Sunil Kumar, brush DC product line manager at Portescap. "In contrast, typical self-supporting coils have inherent ampere-turns limitations that affect the magnetic flux density in the magnetic circuit, which further limits power output and endurance of the motor."

Component standardization and design modularity allow quick customization capability for samples across various applications.

"Due to a lower motor regulation factor compared to comparable motors available in the market, our new 17DCT has a higher load carrying capacity at minimum reduction in speed leading to more uniform power," said Kumar.

Athlonix motors are available with encoders and gearheads of various sizes and ratios. They are manufactured in an ISO certified facility and are RoHS compliant.

For more information:
Portescap
Phone: (610) 235-5499
www.portescap.com

R+W

RELEASES NEWS MODELS AND SIZES FOR ST SAFETY COUPLINGS

High capacity torque limiters from R+W now have more customization and sizing options. After years of development, the ST line has added five sizes across the product line as well as four new models to better meet requirements in all industries.

The newly available sizes will broaden the range from 2 KNm to 250 KNm and remove the need to oversize a torque limiter in many applications. A smaller size will not only reduce costs, but also allow customers to downsize their machines and take advantage of lower moments of inertia.

Additional connection methods such as flange-to-flange, bellows, elastomer and disc pack will give people more variety to find the optimal solution for their overload protection. Custom combination style torque limiters will also be available for special applications.

For more information:
R+W
Phone: (630) 521-9911
www.rw-america.com

Lenze

LAUNCHES ENHANCED VERSION OF THE I500 FREQUENCY INVERTER SERIES

Lenze has launched an enhanced version of its i500 frequency inverter series, equipped with a WLAN diagnostic module for easy parameter setting when commissioning and diagnosing motor inverters for a range of machine applications, including pumps and fans, conveyors, formers, winders, traveling drives, tool and hoist drives.

A keypad, USB interface, and the new WLAN module are now standard on the entire Lenze i500 frequency inverter series. Featuring a Lenze Easy Starter PC tool and WLAN diagnostics over a smart keypad app, the i500 frequency inverter optimizes programming control. The WLAN module communicates wirelessly with a PC or Lenze smart keypad app. The Android smart keypad app is available for free download over Google Playstore. A fully-fledged alternative to the functions of a hardware keypad, the smart keypad app offers numerous benefits, including intuitive user operation and display, and wireless communications.

A parameterization solution, the easy-to-use Lenze smart keypad app allows for i500 frequency inverter parameter settings to be conveniently downloaded, stored, and emailed for analysis. Adjustments can be performed from a safe distance during operation, even on a traveling drive or remote machine equipment. Parameter settings are able to be diagnosed remotely and returned electronically for easy upload.

The Lenze space-saving i500 frequency inverter series enables communication over EtherCAT, EtherNET/IP and PROFINET, in addition to compatibility with standard field buses. Modules are available in the 0.33 to 100 hp (0.25 to 75 kW) power range for scalable functionality. The wide-ranging modular system allows for various product configurations depending on machine requirements.

For more information:
Lenze Americas
Phone: (508) 278-9100
www.lenze.com

Custom Machine & Tool

EXPANDS CAPABILITIES WITH NEW TOOTH PROFILES

Custom Machine & Tool Co., Inc., recently announced it will be adding another metric profile to the company's line of pulleys and pulley stock. Joining the 72-hour guaranteed delivery on pulley stock program is the AT-3 Metric Profile. The AT-3 compliments this timing pulley stock program which also includes the AT-5 and AT-10 profiles.

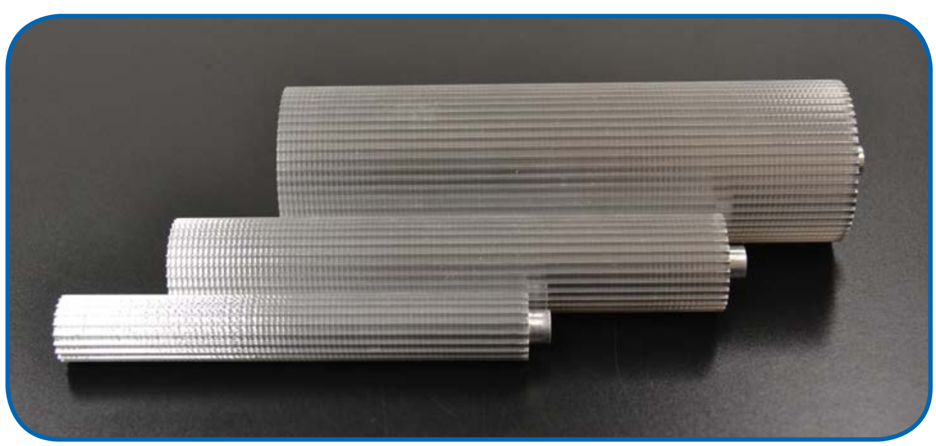

CMT is also adding the 3 mm, 5 mm, 8 mm Goodyear Super Torque Pd Profiles. Goodyear enthusiastically promotes the Super Torque Pd as "the next evolution in synchronous drive belt development from Goodyear." The Super Torque Pd belts have a unique modified round tooth design that minimizes tooth shear and operates quieter than traditional trapezoidal tooth profiles.

"We are thrilled to continue investing in manufacturing capital equipment which allows us to expand and showcase our products in the power transmission and motion control product industry," said Owner and President of Custom Machine & Tool Co., Inc., Robert Bennett.

For more information:
Custom Machine & Tool
Phone: (781) 924-1003
www.cmtco.com

The Brave New World of Industrial Automation

Real-Time Ethernet-Based Fieldbus Technology Revolutionizing Industries

Jack McGuinn, Senior Editor

One of the best things about being a journalist — whether for example it be reporting on manufacturing, politics, show business, or anything else — is being paid to "go to school" and learning about any number of things that you were perhaps ignorant of at the outset.

Sometimes, however, you catch an assignment to write about a subject that, at least at first blush, seems frighteningly intimidating due to its scope and complexity.

For this reporter, at least, real-time Ethernet fieldbus industrial automation is one of those subjects. Graze the Internet for information on this burgeoning smart manufacturing development and you'll quickly see that there is certainly no shortage of technical papers, supplier information, governmental input, etc. The only problem is trying to make a layman's sense out of it. There are seemingly countless, devilish details concerning hardware, software and standards (protocols) — not to mention a phalanx of competing views as to which iteration is best for this or that application. We're talking about discerning the differences between the five most applied (since 2001) protocols/standards — in use on factory floors, i.e. — EtherCat (*www.ethercat.org*); EtherNet/IP (*www.odva.org*); Powerlink (*www.ethernet-powerlink.org*); Profinet IRT (*www.profibus.com*); and Sercos III (*www.sercos.de/en*). And while there are other technologies that leverage Ethernet as well, "their components are not sufficiently published, downloadable or promulgated in the open source community to be considered standard and open." (*Source*: *kingstar.com*)

But then I received some brief but exceedingly sensible advice, to wit:

Focus on the big picture: what does it do, how does it do it — and worry less about the details.

In case you were wondering, fieldbus is a family of industrial computer network protocols used for real-time distributed control, standardized as IEC (International Electrotechnical Com-

Twenty-first-century industrial automation utilizes control systems — e.g., computers or robots — and other now-available information technologies for coordinating a variety of industrial processes and machineries (Photo courtesy Beckhoff).

mission) 61158. It is an industrial network system for real-time distributed control that connects instruments in a manufacturing plant. Fieldbus works on a network structure that typically allows daisy-chain, star, ring, branch, and tree network topologies.

And "industrial automation," in Ethernet fieldbus form, is use of control technology such as computers or robots, and information technology for handling different processes and machineries in an industry to replace a human being. It is the second step beyond mechanization in the scope of industrialization (*SureControls Inc.; surecontrols.com*).

Note the absence of any concern over eliminating "the human being" in the equation. But face it — that sort of sentiment is *so* last-century.

Anyone questioning the rapid spread of highest-tech industrial automation and motion control need only look at the lineup of high-tech automation-related exhibitors for this year's IMTS (*www.imts.com*). Beginning with the 2014 IMTS co-location of the IANA and MDA shows, and continuing with this year's event, industrial automation is becoming one of the show's lead players. According to Larry Turner, president & CEO of IMTS partner Hannover Fairs USA, Inc., "The single most important development in manufacturing in the past two years has been the overwhelming discussion around and movement towards investing in Industrial Internet of Things (IIoT) programs and initiatives to help accelerate the era of IT-optimized smart manufacturing. As IIoT solutions providers better frame, define and create IIoT strategies, many organizations have started to look at what is possible in the age of Industry 4.0. Manufacturers around the world are now embracing the Internet of Things and smart manufacturing. Digital factory solutions will be showcased across all of the 2016 shows."

Industrial automation in today's high-tech, world economy-competitive context is much more than simply making more things and making them faster. Today it is also all about making those same things more cheaply, yet with higher quality.

The Ethernet and TCP/IP protocols have in the past been used in manufacturing to network control systems, management systems, and manufacturing cells on the shop floor, but *not* for the controlling communications *inside* the actual machines and equipment. (*Transmission Control Protocol is a core protocol of the Internet protocol suite. It originated in the initial network implementation in which it complemented the Internet Protocol (IP). Therefore, the entire suite is commonly referred to as TCP/IP.*) The machine controller itself and the communications to the actuators invariably demand use of deterministic fieldbus, so TCP/IP is not suitable. Essentially, the use of the "traditional" TCP/IP protocol — from machine control to the sensors and actuators — has failed, as it is incapable of satisfying deterministic, real-time demands.

But machine-builders — including CNC machine tool builders — recognized an inherent, value-added opportunity to *retain* those hardware components typically used in the accepted TCP/IP network setting. That, coupled with explosive growth of the Internet, led to a universal standard for communication cards and cabling. For example, a network interface card (NIC) and a TCP are a mere fraction of the cost of an industrial fieldbus cable and DAQ card. Indeed, the ability to "recycle" this existing hardware can provide savings of at least 50% above a traditional, proprietary fieldbus configuration.

Example — the economics of adopting Ethernet as a fieldbus are compelling because Ethernet components offer dramatically lower costs and are universally available. But in order to implement a *proprietary* fieldbus motion assembly, an IO card at up to $400, proprietary cables at up to $30/linear foot, and servo drives and premium motors must be purchased.

However, if an Ethernet-based standard protocol is used, the IO card can be replaced by the onboard NIC card ($0 additional cost) that comes installed on the PC; the proprietary cables can be replaced by inexpensive CAT5 cables; and the servo drives will be dramatically lower if the standard is strong enough to support multiple vendors. Equipment assembly for Ethernet components is much simpler too. Rather than having cable harnesses that are 4 inches in diameter at the PC interface, a simple CAT5 cable similar to the one that connects to your home PC is far more manageable; other economic benefits for Ethernet as well.

This NASA application required EtherCAT-protocol robotic transporters for moving rockets from place to place at NASA assembly facilities (Photo courtesy Beckhoff).

Beyond that, it was then decided that a new, real-time protocol could deterministically connect and communicate the machine controller to all the sensors and actuators in a machine, i.e. — *real-time industrial automation and motion control.*

While not as yet necessarily accepted as the gold standard, of the five real-time Ethernet fieldbus standards (protocols) EtherCAT appears capable of superior performance and winning market acceptance. Its performance, for example, is rated an order-of-magnitude better than Ethernet IP and Powerlink.

As for PROFINET IRT and SERCOS III, while they apparently offer near-equivalent performance characteristics, EtherCAT offers a more "open" solution. EtherCAT has been adopted by 10 times more servo drive and IO suppliers than any other standard. As a result, many machine builders adopting real-time fieldbus technology are opting for EtherCAT.

The EtherCAT protocol, developed by Beckhoff Automation LLC (*www.beckhoff.com*), prompted the formation of the EtherCAT Technology Group (ETG) (*www.ethercat.org*); machine builders will note that it is capable of processing 1,000 I/Os in 32.5 µs, or 100 axes in 125 µs.

What is driving this need for speed? Time-to-market and energy savings, for starters. Also, maintenance costs associated with machinery used for industrial automation are less because, reportedly, it does not often fail. But *should* it fail, only computer and maintenance engineers are required to repair it.

Today's increasingly complex, automated industrial systems, such as a manufacturing assembly line, typically require a "distributed control system" i.e. — an organized hierarchy of controller systems — to operate. In this hierarchy, there is usually a human machine interface (HMI) at the top where an operator can monitor or operate the system. This is typically linked to a middle layer of programmable logic controllers (PLCs) via a non-time-critical communications system (e.g. Ethernet). At the bottom of the control chain is the fieldbus that links the PLCs to the components that actually do the work, such as sensors, actuators, electric motors, console lights, switches, valves and contactors.

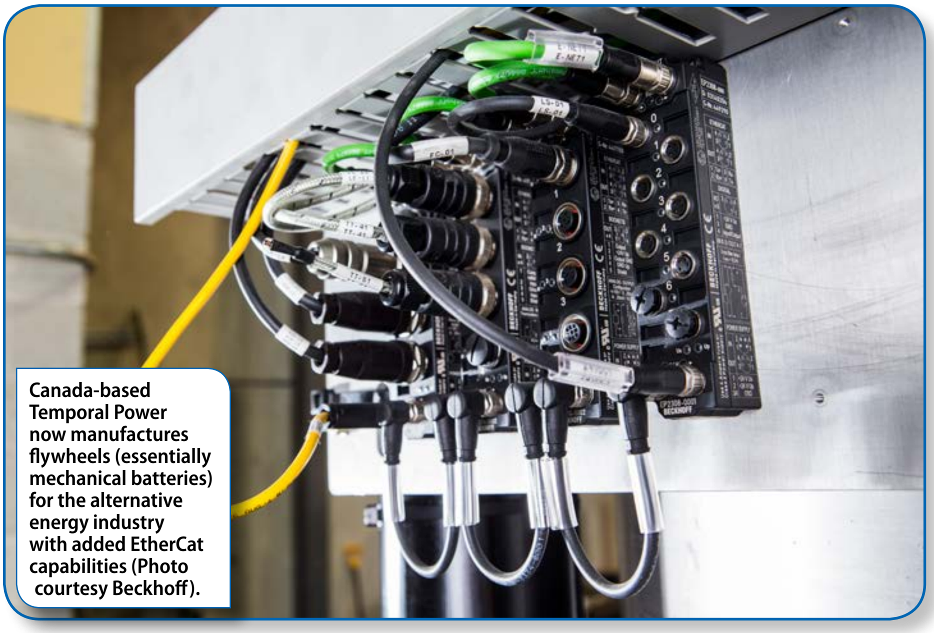
Canada-based Temporal Power now manufactures flywheels (essentially mechanical batteries) for the alternative energy industry with added EtherCat capabilities (Photo courtesy Beckhoff).

Q&A

Beyond the preceding, what follows is input from several company spokespersons invested heavily in fieldbus Ethernet industrial automation motion and control. They include: **Jeffrey D. Estes**, Certified Engineering Technologist (CET), Okuma America Corporation (*www.okuma.com*); **Joey Stubbs**, North American representative, EtherCat Technology Group (*www.ethercat.org*); and **Gale Lu**, Sr. Business Development Manager, Nexcom U.S. (*galelu@nexcom.com*).

PTE: What would be your layman's definition of industrial automation and real-time communication?

Jeffrey D. Estes (JDE). Simply put, being able to transfer, bi-directionally, information and data points over our IT technology. The IT technology continues to evolve and become faster and more capable. Okuma's position is to connect through the most universally accepted manner, allowing data to flow to all areas of the organization, Big Data.

Joey Stubbs (JS). Industrial automation takes the inconsistencies, quality issues and labor costs out of the production of goods by utilizing manufacturing equipment specifically designed to produce those goods. Also, in many cases, industrial automation enables the manufacturing of products that *could not* be made by people.

Real-time communication can be defined as digital communication that is fast and offers predictable timing.

PTE: Would you say the following is accurate?

One of the five real-time Ethernet fieldbus standards has achieved a tipping point of acceptance. It appears that EtherCAT offers both superior performance and market acceptance. Its performance is an order-of-magnitude better than Ethernet IP and Powerlink. And while PROFINET IRT and SERCOS III offer nearly equivalent performance characteristics, EtherCAT offers a more "open" solution at far lower cost than both PROFINET IRT and SERCOS III. From a technology and price/performance standpoint, EtherCAT is far superior. And the market agrees. EtherCAT has been adopted by 10 times more servo drive and IO suppliers than any of other standard.

Joey Stubbs (JS). I wouldn't say that PROFINET IRT and SERCOS III offer nearly equivalent performance to EtherCAT, but they are definitely "higher performance" than Ethernet/IP and Powerlink. The remaining bulk of the above statement is very correct. There are currently 193 different EtherCAT master vendors, 155 different companies with at least one model of EtherCAT drive, 105 different vendors of EtherCAT I/O and 45 vendors providing Functional Safety over EtherCAT (FSoE) devices. These vendors contribute to the thousands of different EtherCAT components and controllers available today. Worldwide vendor acceptance is phenomenal, to say the least.

PTE: Does this industry also have trouble finding young replacement talent as an older workforce retires?

JDE: Finding talent that understands Big Data and willing to treat a $100,000+ computer in the machine tool control the same as the $1000 PC on most desks is challenging. Okuma is constantly learning and training on how to connect/communicate as the various manufacturing systems evolve. Much like smart phones, the technology is growing at a rapid pace and the knowledge of our workforce, of all ages, must learn and adapt in this environment. Very exciting time to be working in manufacturing!

PTE: What accounts for the high start-up cost of implementing fieldbus technology/automation? Are, for example, custom motors and other custom hardware a big-ticket item? Cabling?

JS: The term "high start-up costs" can be an oxymoron when examining the overall costs of a fieldbus technology implementation. It depends on the type of system specified by the user. EtherCAT does not require special fieldbus cards in the controller, and has no need for special cables, connectors or any Ethernet infrastructure devices such as switches, hubs, or routers.

Additionally, EtherCAT reduces overall costs due to the inherent noise immunity offered by CAT5e cables, and the protocol's incredible suite of pinpoint diagnostics tools, which help minimize downtime, while maximizing uptime and production.

PTE: Does preventive maintenance assume an entirely new dynamic regarding the hi-tech hardware/software? Who is qualified to do it?

JDE: Electronic hardware is extremely reliable. The amount of data coming from, and flowing through, the electronics is astounding. That same data is also providing the health of the electronic devices processing it. The hardware is able to self-diagnose its own health and efficiency. Example: much like our cars, a technician can obtain data from new electronics through connecting to the machine.

JS: Because of the high throughput and high levels of determinism, EtherCAT is well suited to data acquisition tasks, including very specialized services, such as local machine condition monitoring on the same communication network controlling the machine(s). This condition monitoring enables functionality such as vibration monitoring, which can indicate bearing wear on rotating motors and internal problems with pumps, as well as harmonics on gears and other rotating machinery. This makes it possible to perform corrective measures during regular maintenance downtime, as opposed to permitting equipment to fail and having to do corrective measures when the machine should be running. This amounts to a huge increase in overall throughput that cannot be ignored, especially in the long run.

PTE: Please speak to the energy savings tied to fieldbus automation, perhaps for machine tool builders as an example.

JDE: Okuma has a technology called Eco Suite that constantly reviews key energy usage of key components of the machine and reduces their energy consumption when not demanded by the machining process. Check it out at *www.Okuma.com*.

JS: Using a high-speed, highly efficient, highly responsive fieldbus and control system can certainly bring energy saving benefits, depending on the industry. Plastic injection molding equipment, for instance, can save energy and raw materials by achieving tighter control of the plastic melting process, thin down the walls of plastic products and create less waste. This all adds up to a considerable reduction in energy use and waste. EtherCAT power monitoring terminals can enable the machine to monitor its own power usage and, if set up to do so, modify power settings and turn off unused equipment or devices, again saving power and operating costs.

PTE: Of the fieldbus protocols available — EtherCAT, EtherNet/IP, PROFINET IO, Ethernet Powerlink, SERCOS III, etc., is one best suited for machine tool automation?

JDE: EtherCAT has positioned itself as the clear winner. The protocol is not intended for any particular industry or application, but has found its niche in a variety of different industries with many different types of users. EtherCAT offers a low-cost fieldbus option for embedded control systems

Unified EtherCat controllers enable PLC-CNC robotics collaboration for automated production lines (Photo courtesy Nexcom).

for embedded control systems and low cost PLCs. It is also a high-speed, highly deterministic bus for data acquisition systems that supports even the most demanding applications, such as to form the "nervous system" for advanced robotic controls. The protocol has even been applied in R&D for space applications, as EtherCAT is used by NASA in several vehicle applications. It also performs well in generic applications, such as machine tool automation, because of the high speed, low cost, flexibility and device variety.

PTE: What determines whether a machine tool builder's existing infrastructure is suitable for converting to fieldbus/industrial? Ethernet-driven control and automation? Put another way, is it usually a blank-sheet scenario or are a good portion of existing components retained?

JDS: One of the great things about EtherCAT, and one of the properties that has allowed it to achieve its current high level of acceptance, is that a user doesn't have to "start over" and use only EtherCAT devices in a network. There are gateways from EtherCAT to over 30 different fieldbuses, both in Master and Slave configurations, which facilitate communication to individual legacy devices, or complete non-EtherCAT networks, such as PROFIBUS, PROFINET and DeviceNet, among others.

PTE: How robust are the existing IEC standards? Has time spent developing these standards (some taking decades apparently to be written) over the years slowed the progress of industrial automation?

JDE: In my opinion, it is probably good that there are some lags due to standardization processes. Otherwise, the industry would be flooded with spur-of-the-moment technologies that are half-baked and not very well thought out. That alternative scenario would seriously confuse and degrade the industry.

PTE: What might be the next "automated" miracle? Glass half-full?

JDE: Simply connect your machine tool and start collecting data. This data can be used by planner/schedulers, maintenance, manufacturing engineers, finance, quality assurance and compliance, simulations, or six sigma project determinations, just to name a few. Big Data provides information that pieces can be extracted and used by everyone in the organization. What's so exciting is the data is *milliseconds* old. It's real time! Amazing!

For more information:

Josh Olson
Marketing Communications Specialist
Beckhoff Automation LLC
Phone: Direct — (952) 428-7320
Fax: (952) 890-2888
j.olson@beckhoff.com
www.beckhoffautomation.com

Gale Lu
Nexcom U.S.
2883 Bayview Drive
Fremont, CA 94538
www.nexcom.com

Jeffrey D. Estes, CET
Okuma America Corporation
1900 Westhall Dr.
Charlotte, NC 28278 U.S.

For Related Articles Search
automation
at www.powertransmission.com

Opening the Envelope on Bearing Vibration

A sophisticated signal processing technique pinpoints bearing failure at an early stage.

Chris Hansford, Managing Director, Hansford Sensors

Experienced operators can often tell if a machine is not working properly, on the basis that it does not 'sound right.' The same principle can be applied—using modern electronics—to identify the exact cause of the problem.

Sensitive accelerometers can detect and analyze the vibrations from industrial equipment, highlighting problems such as misalignment or bearing imbalance. The technique is known as vibration analysis. It can identify bearing failure in the very early stages, when there is a microscopic defect on the raceway, for example. The problem is that the identifying signal is usually drowned out in all the other noise emanating from the machine.

Sensitive accelerometers can detect and analyze the vibrations from industrial equipment, highlighting problems such as misalignment or bearing imbalance.

Filtering device

It is vital to catch these defects as early as possible to stop them from developing into more serious problems. One way of homing in on the signal of interest—and filtering out the 'noise'—is to use a signal processing technique called acceleration enveloping. It works by progressively filtering out unwanted parts of the vibration spectrum until the signal of a bearing defect can clearly be seen—extracting low level, repetitive vibrations from the noise around it.

It is vital to catch bearing defects as early as possible to stop them from developing into more serious problems.

The unfiltered waveform from a defective bearing is a mix of low and high frequencies, with no obvious pattern. The first step is to apply a band pass filter, which isolates only the frequencies in which the signal of interest is hiding. Some experience is needed in order to know how to choose the high- and low-pass frequencies.

The filtered output will identify repeating, high frequency signals, though more steps are required to pinpoint the one specific to the bearing defect. First, the waveform is rectified—inverting the negative part to positive. This is then enveloped (or demodulated) by tracing a line over the general shape of the rectified signal. This 'envelope' is now used as a true vibration signal—helping it to stand out from the noise. The envelope helps to contain regularly spaced signals, such as a single defect on a raceway. Other causes of noise, such as shaft rub, are random so they will not produce evenly spaced peaks.

Technique in action

Acceleration enveloping is most commonly used in roller bearing systems, but can also be applied in areas such as electric motors and gearboxes. It is a key factor in the success of condition-based maintenance (CBM) programs. While enveloping is most commonly used with signals in the acceleration spectrum, it can also be used to improve other measurements such as a shock pulse.

Once the signal has been filtered, the information can be collected from the accelerometer using a data collector, ready for review and interpretation by a specialist, who can decide whether or not maintenance work is required immediately or can be planned as part of routine schedules.

While acceleration enveloping may seem to be the definitive answer to detecting bearing failure, it cannot be universally applied to any machine. The technique detects faults involving repetitive, metal-to-metal interactions. Anything that masks this, such as gaskets or dampers, may put a machine outside its scope of use.

Success factors

If an application is suitable for enveloping, several factors will help to ensure better results. Firstly, accelerometers to measure the low-level signal should be selected carefully (in the proper frequency range) to suit the needs of the particular machine or application.

Secondly, accelerometers should then be correctly mounted (close to the component being monitored) on a flat, clean surface to guarantee consistent results. Poor mounting reduces reliability and can make collected data redundant.

Once accelerometers have been installed and calibrated, data readings should then be taken at regular intervals over a period of time to allow accurate trend analyses to be produced. This allows a steadily deteriorating condition to be identified, for example.

It is important to understand that the information provided is not a simple 'yes/no' answer and requires some skill and experience to interpret. The amplitude of a worsening condition can actually reduce over time, for example, as the imperfection becomes slightly smoother.

The potential benefits of acceleration enveloping are clear, but it would be unwise to rely on the technique alone. Implementing it as part of a wider monitoring and analysis regime can be far more effective, helping plant engineers to safeguard the health, performance and productivity of all the assets under their care. **PTE**

For more information:

Hansford Sensors
Phone: +44 (0) 845 6801 957
www.hansfordsensors.com

Acceleration Enveloping in Action

According to the Global Wind Energy Council (GWEC) there were 268,000 wind turbines in operation at the end of 2014, with each turbine having an average of 8,000 separate components. Of these, a large number are associated with the drivetrain, which has separately been recognized as the major cause of extended downtime. Gearbox and bearing wear, in particular, is known to cause problems. Although wear tends to be gradual rather than catastrophic, it can nonetheless lead to expensive repairs that—in terms of downtime plus the possible need for heavy lifting equipment, gearbox replacement or generator rewinds—cost far more than simply the cost of a replacement bearing or gear unit. Regular vibration monitoring can prevent these issues occurring.

The complexity of a typical wind turbine does, however, present a challenge for vibration monitoring. For example, the main turbine, gearbox and generator often have more than 15 rolling element bearings installed, while the gearbox incorporates a series of stages, each with multiple gears. These components generate unique vibration signatures, with different amplitudes and frequencies, which can be difficult to isolate from each other and that can be masked by noise from surrounding systems.

This is where a technique such as acceleration enveloping can play a crucial role, enabling vibration analysts and maintenance engineers to separate vibration signatures and identify the changes in signal conditions, which can indicate increasing wear.

To be effective, acceleration enveloping requires the use of multiple accelerometers, fitted to all key rotating parts. These include the main bearings, planetary, intermediate and high-speed gear stages, the generator (inboard and outboard bearings) and ideally the nacelle traverse and axial movements.

In each case, there are several critical factors that must be considered. In particular, each accelerometer must be mounted securely on a clean and solid base, and as close to the component being monitored as possible; normally, standard M8 mountings are used. It is also important to collect data consistently, to enable any change in operating conditions or trends over time to be accurately identified at the earliest possible stage.

It should also be noted that the frequency of enveloping signals is related directly to the speed of shaft rotation. On wind turbine drivetrains—for example, on the generator output shaft—rotational speeds can be relatively slow and may therefore require the use of special purpose, low-frequency AC accelerometers, with a sensitivity of between 100 mV/g and 500 mV/g. The sensors are generally hard wired back to a junction box within the nacelle and then to a switch box mounted at ground level. Signals can either be monitored on-site using hand-held data collectors, which feature software capable of automatically calculating acceleration enveloping, or are transmitted to a remote monitoring center for subsequent analysis. **PTE**

Mining for Solutions

High-efficiency, heavy-duty motors offer key to reducing energy consumption and downtime

Chris Medinger, product marketing specialist, Leeson Electric

Increasing pressure on many fronts is compelling mine operators to thoroughly examine every phase of their operations. Fluctuating demand that whipsaws mineral prices, government-imposed environmental regulations and rising operating costs related to maintenance downtime all pose serious challenges for the mining sector. Add pressure from customers and stakeholders for more sustainable operations as well as union demands for higher wages, and you have a scenario that requires mine operators to exercise every possible option to achieve more efficient operations.

Variable costs of doing business affect the bottom line

To achieve sustainable operations as well as long-term viability and profitability, mining must do everything it can to conquer the myriad variables affecting operating expenses, two significant ones being reducing energy costs and downtime. Let's examine these two and how high-efficiency, heavy-duty motors address these challenges.

Reducing energy costs

A typical mining environment is notorious for being one of the harshest working environments on the planet. Critical ambient conditions, solid contamination (dust) and severe processes are just some of the major factors present at a mine site. Motors are used above and underground in non-hazardous mines and open pit quarries that typically mine iron ore, platinum, gold and rare earth metals. Applications include conveyors, pumps, fans, smaller winches, crushers, smaller mills and flotation tank agitator motors. High-efficiency, heavy-duty motors can extend the life and performance of mining equipment while reducing the downtime and costs associated with ongoing maintenance. Using the latest technology, some motor manufacturers are able to engineer energy-efficient designs that also stand up to the hostile mining environment.

Mining and metals production is an energy-intensive process, with a significant proportion of energy consumption coming from purchased electricity. According to the Southwest Energy Efficiency Alliance, a metal mining company's energy expenditures can consume between 20 percent and 40 percent of its total production costs in American mining. However, today's highly efficient motors, drives and mechanical power transmission products can significantly reduce this energy consumption.

The U.S. Department of Energy's (DOE) manufacturing and mining energy analysis study explored and compared main industrial market verticals and energy use by major process systems. The study noted that the mining industry was ranked as the third-highest energy user of motor driven systems among 10 major industry verticals.

Mining projects that may involve the upgrade to high-efficiency motors include:

- Retrofitting or replacing underground support systems such as ventilation fans and air systems
- Upgrading motors or replacing conveyor systems
- Efficiency improvements to crushing, separating or materials transportation processes
- Retrofitting pumping systems in mine dewatering, slurries transportation and tailings disposal
- Improvements in extraction and refining processes
- Improvements in control systems or sensors
- Installing variable speed drives for pumps, compressors and operating fans at part load capacity

To encourage mining companies to retrofit standard motors to high-efficiency motors, many incentives and rebates are offered. For example, in 2010, U.S. Senator Blanche Lincoln introduced legislation to create a rebate program to boost the manufacturing sector and promote energy efficiency by encouraging the sale of high-efficiency industrial motors. The program provided a $25 per-horsepower rebate for customers who purchased a high-efficiency motor for industrial and commercial use in everything from fans and compressors to food processing, mining, water pumps and commercial buildings.

Pacific Gas & Electric (PG&E) has developed a Retrofit Incentive Program for its industrial customers. This involves the installation of energy efficient motors or systems customized to their facilities. Additionally, PG&E offers rebates to customers who install qualified high efficiency products.

As a minimum requirement, electric motors for the mining and mineral sector need to:

- Meet global mining industry requirements, yet be flexible for adaptation to local legislation
- Be robust to meet the aggressive nature of the environment
- Be highly reliable and never be the component in the drive train responsible for unplanned downtime

Reducing downtime costs

Mining equipment is the lifeblood of the operation. Consider these staggering costs of downtime: According to Caterpillar, it's estimated that the total cost of unscheduled downtime can be as much as 15 times that of a scheduled event. Mining companies are susceptible to $180,000 in lost production per incident. This includes lost production time accumulating in $3,000 an hour per incident, and 60 hours of downtime per incident. Maintenance, because of its impact on return on capital, is a key driver of performance. By reducing maintenance costs, companies can improve their performance.

Motors

The mining segment is very diversified and has different processes for mining of assorted minerals or stones. In all these processes, electric motors are used as driving energy in a large scale to extract, transport, crush and separate metals. Peripheral systems such as pumping and recycling of fluids, treatment and control in the emission of pollutants like toxic dust and gases also use motors.

Mincom's 2010 annual survey of executives at the leading North American mining companies found that 67 percent of them are concerned about improving performance and operational effectiveness. To that end, high-efficiency, heavy-duty motors can play a key contribution.

There are well over 1.2 billion electric motors, of all types, used throughout the United States. However, electric motors are often out-of-sight, out-of-mind until production is down due to a burnout or catastrophic bearing failure.

Preventive maintenance and regular analysis of motors' load test performance are essential keys to a reliable motor. Selecting the right high-efficiency, heavy-duty motor for mining equipment is also a critical step for OEMs and end-users. When a motor is put into an application that it was NOT designed for, it will cause many kinds of repetitive repair issues that even the best preventive maintenance practices will not correct.

Various type series helps in the selection of the right motor for each operating mode required, whether constant speed, variable, or direct drive. Robust, reliable motors are perfect for belt conveyors and for modernizing existing systems.

Common motor failures

More motors fail due to bearing problems than for any other reason. The leading cause of bearing failures relates to a variety of issues surrounding lubrication. Antifriction bearings should be re-lubricated on a regular basis. The lubrication schedule depends greatly on the motor's operating environment and service conditions. While failures may occur due to lack of lubrication, bearings may also fail due to grease contaminated by water or other materials.

The second most common cause of motor failures is stator-winding failures. To ensure long motor life, it is important the motor operate within the temperature class of its insulation system and be kept clean and free of particle build up on the frame surface, air inlet and fans.

Conclusion

Mining companies are looking at cutting costs by, among other things, using more efficient equipment to ease energy demand and reduce downtime. Increasing investment in high-efficiency, heavy-duty motors would separate profitable, growth-oriented companies from the pack and equip them with a sustainable competitive advantage.

The payback times for motor investments can be within a couple of years and offers a positive impact on both the environment and the operation. The mining community is being challenged to find electrical equipment and systems solutions that make mining operations reliable, efficient and continuous; safer and protected. Sustainable, high-efficiency, heavy-duty motors are one way to achieve these goals.

For more information:
Leeson Electric
Phone: (262) 377-8810
www.leeson.com

Chris Medinger is product marketing specialist with Leeson Electric and may be reached at (262) 387-5410 or *chris.medinger@leeson.com*. Leeson is a Regal brand located in Grafton, WI. Regal Beloit Corporation is a leading manufacturer of electric motors, mechanical and electrical motion controls and power generation products serving markets throughout the world. Regal is headquartered in Beloit, Wisconsin, and has manufacturing, sales and service facilities throughout the United States, Canada, Mexico, Europe and Asia.

For Related Articles Search
motors
at **www.powertransmission.com**

Proper Handling of Bearings

Tips on Storage, Installation and Lubrication

Power Transmission Engineering is collaborating with the Bearing Specialists Association (BSA) on a special section within the magazine. *Bearing Briefs* will present updated reports on bearing topics for each issue in 2016. Complimentary access to all BSA Bearing and Industry Briefs is available on the BSA website at *www.bsahome.org/tools*.

BEARING SPECIALISTS ASSOCIATION ®

We build relationships

Rolling-element bearings are high-precision components that need to be stored and handled carefully to perform as designed. Proper storage and handling of a bearing before, during and after installation is important because once debris enters a bearing, it reduces the life.

Bearings should be stored in a clean and dry location with the bearing lying on its large, flat side. By placing the bearing this way, the chances of false brinnelling are reduced along with the potential of damage due to falling over.

Bearings should remain in their original packaging until they are ready for installation.

All assembly areas should be free of sources of contamination. Workbenches, tools, clothing and hands should be free of dirt, dust and other contaminants that may harm the bearing.

Mechanics handling clean bearings should wear latex gloves. This prevents oils from the skin from leaving a deposit that can stain the bearing surface, leading to etching and corrosion. If gloves are not available, hands should be clean and dry.

During installation, cleanliness extends beyond the bearing, to shafts, housings, and retaining devices. Debris on the shaft or housing can be pushed to the shoulder during bearing mounting, preventing proper seating. The contamination can become dislodged during service, allowing the bearing to work back against the shoulder, resulting in excessive bearing looseness. Contamination in the housing can result in wear and bruising damage in the bearings.

Lubrication

Antifriction bearings must be lubricated to prevent metal-to-metal contact between the rolling elements, raceways and retainers. In addition, lubrication protects the bearing against corrosion and wear, helps dissipate heat, helps seal out solid and liquid contamination and reduces bearing noise. A properly lubricated bearing has the best chance of reaching its maximum service life.

Hand Packing a Tapered Roller Bearing

Hand packing is one method to lubricate a tapered roller bearing. Below we will describe the process to hand pack a bearing:

- Mechanic should clean and dry hands or wear clean latex gloves.
- Place grease about the size of a walnut into the palm of one hand.
- Using your other hand push the large end of the bearing cone into the grease. This action will move the grease between the rollers, cage and cone.
- Begin rotating the cone assembly while pushing grease until the grease is forced out evenly around the small end of the bearing.
- Smear excess around the outside of the cone assembly.
- Additional grease may need to be added to the housing, depending on the application requirements.

Using a Mechanical Grease Packer

Using a mechanical grease packer to lubricate a tapered roller bearing is another method. Below we will describe the process to using a mechanical grease packer:

- Mechanic should clean and dry hands or wear clean latex gloves.
- Place the bearing cone assembly, small end down, into the grease packer funnel.
- Plug the bore of the large end of the bearing cone assembly with the conical retainer.
- Firmly press down on the conical retainer. This enables to grease to be forced between the rollers, cage and cone.
- Smear excess grease on the outside of the bearing cone assembly. **PTE**

For more information:

Bearing Specialists Association (BSA)
Phone: (630) 858-3838
info@bsahome.org
www.bsahome.org

Cutting Downtime in Lumber Application

Certified Bearing Specialist (CBS) Adapts Bearing Solution for Mill Operation

Ernest Head (Arnie), CBS and technical sales representative at Motion Canada helped save a lumber industry customer time and money by adapting a bearing solution for another client. Here's how:

According to Statistics Canada, the Canadian lumber industry has experienced significant economic pressure starting most recently in 1999, but has managed to rally in large part through plant closures and restructuring, resulting in financial gains in production.

Though the industry has seen some signs of recovery since 2010, the forecast today remains unclear. This is why it is so important that mills run efficiently, with as little unplanned downtime as possible. Motion Canada understands the pressure lumber customers face and consider their challenges one of its top priorities.

One particular mill was experiencing breaking motor mounts on a C-face flange reducer used to guide rolls for chip-n-saw production, a process where trees are cut into lumber, and then the waste material is converted into chips for fuel or paper production.

Continued breaking motor mounts could lead to expensive damage to the motor or the reducer. Many mill maintenance crews are fully capable of maintaining day-to-day issues and ensuring production continues to flow. However, at this particular mill, each time a motor mount on a C-face flange reducer breaks, it can potentially shut production down completely—an extremely time consuming and expensive situation.

The mill knew they needed a permanent and sustainable solution to ensure their production line ran efficiently. Head knew his customer was right to be concerned. The C-face flange reducer is a key element to the system because it increases adaptability and allows the reducer to be mounted to any industry standard motor. However, if the mounting is off even just a little, the mobility of the system is hindered and the production rolls will temporarily slow or stop. When the rolls don't work, downtime can be substantial.

Thankfully, Head had recently viewed a similar challenge at a different mill. Though not exactly the same issue, with a little creativity and over 30 years of experience in the industry, he was able to quickly adapt the previous solution to the current issue and share his proposal with the customer. Because the application is very rough, the motor needed to be slightly separated from the reducer to increase mobility, which would solve the breaking problem, according to Head. The customer agreed, and Head went to work.

First, Head worked with the Motion Canada Alberta service team to mount a stationary motor above the drive and design the proper drive shaft to connect the motor to the reducer. The challenge was in making sure the drive shaft had enough float to properly run the reducer without any problems. With the motor stationary, the drive shaft needed to be flexible enough to still run the reducer properly while it moved around with the feed rolls to position the logs.

That's where Motion Canada's Alberta engineering team came into play. Head shared the drive information from the application and the rough range of the feed roll with the engineering team so they could help identify how much movement the drive shaft would require to be truly successful. After a few tests to ensure the system was perfect, the team completed the drive shaft with enough flexibility and enough horsepower rating to do the job.

The updated system was installed at the mill on time and on budget. The chip-n-saw production line ran smoothly and Head's customer was satisfied with the quality, cost and effectiveness of the solution. **PTE**

Certified Bearing Specialist

BSA's Certified Bearing Specialist (CBS) program is the only bearing industry-specific program that identifies and quantifies the specific skill sets to certify an industry professional as a bearing specialist. The CBS program is all about developing the expertise to help customers and end users make the best bearing decisions. Take advantage of this complimentary access to a Certified Bearing Specialist. Please email your question to *info@bsahome.org*. An expert CBS will respond to your inquiry and it may appear in this article.

For Related Articles Search
bearings
at www.powertransmission.com

Ernest Head (Arnie) joined the BC Bearing Engineers family at the British Columbia Prince George branch in August 1987 as a shipper receiver. He has held several positions including inside sales representative, outside sales representative, branch manager and office manager. He became a technical sales representative when BC Bearing was acquired by Motion Canada in 2010. He will soon become a quotation specialist with Motion Canada in Kamloops, British Columbia.

Graco Pump Technology Solves Long-Term Pump Leaking, Dosing Issues

Superior quality pump components and advanced dispense software allow utility instrument manufacturer to dispense highly abrasive bonding material in programmed shot sizes

Bruce Stephan, director of marketing, applied fluid technologies division, Graco Inc.

When trying to find a new bonding material dispense system, one manufacturer tested a series of pumps—all of which leaked due to the abrasiveness of the bonding material. The manufacturer also had been attempting to manage shot size manually with their previous system, and was not able to keep dispense consistent. The company searched for a system that could accurately dispense programmed shot sizes while also eliminating the leaking issues they had experienced with previous pumps. Graco provided a Check-Mate pump with SmartWare software, and the manufacturer is now able to automatically dispense shots of bonding material as small as one ounce without leaks.

Abrasive material leads to leaking pump issues. The manufacturer produces power transmission products for the utility industry and uses its own proprietary material as a bonding agent between different metal components. The material features a high tabular alumina content and is therefore highly abrasive; in the past, it caused a number of piston pumps to leak and fail when their seal kits and throat packings, which are designed to stop pumps from leaking, could not stand up to the abrasive nature of the material.

The manufacturer was also relying on manual shot size measurement to dispense this bonding material, which made it difficult for users to maintain a consistent shot size. The company wanted to find a pump that would be able to withstand the abrasive medium with-

Graco was able to solve their customer's leak problem with a combination of robust seal technology, new software and some engineering adjustments (Photo courtesy Graco).

For Related Articles Search
pumps
at www.powertransmission.com

out leaking and would also automate shot size, but was unsure whether they would be able to find such a system. They reached out to Graco, from whom they had purchased other pumping equipment in the past, in the hopes that their experts from their Advanced Fluid Solutions (AFS) team would be able to solve the problem.

System designed to eliminate leaks and automate shot size. Graco offered the manufacturer a 30-day trial of the Check-Mate pump to prove that it could stand up to the material. The Check-Mate piston pump features advanced, severe-duty seal kits and throat packings that allow it to handle extremely abrasive materials without leaking. The Graco team also updated the pump size in order to further protect the system from leaks.

"The key in an application like this, with such an abrasive medium, is that engineers with experience in the industry must design the system with the correct-sized pump. All of this customer's pumps in the past had been undersized and so they had to work very quickly in order to keep up with customer volume demands. That rapid motion contributed to the pumps leaking and failing—often within about two weeks of installation," said Chris Lewis, Graco area sales manager who worked with this customer. "When we right-sized the pump we reduced the number of cycles-per-minute from about 60 to 20, and in doing so really reduced the wear and tear on the seals. Adding that to the higher-quality seal material used in the Check-Mate pump, we were able to prove to the customer that we could solve their leaking issues. The seal material used in competitive systems just can't compare."

After the first 30-day trial, the Graco team returned to the customer and installed *SmartWare* software on the pump. *SmartWare* takes the place of a flowmeter and regulator to measure shot sizes, and allows operators to program up to 100 different shot sizes for automated dispense. The *SmartWare* software package controls the piston in the Check-Mate pump, stopping it anywhere in its cycle, as necessary, to allow for dispense precision.

"The *SmartWare* software turns the Check-Mate pump into a highly precise dosing system, taking all of the guesswork out of dispensing. Whereas before operators were measuring shots by eye, now the operators just need to select a shot size from the programmed options," Lewis said. "What's more, the software compensates for the speed at which the pump can start up and stop, and functions with high accuracy, even though the piston frequently starts and stops partway through its stroke. Finally, the pump gets more accurate as time goes on because the software is continually learning, gathering more data with each dispense and adjusting itself accordingly."

SmartWare solves customer challenge. As the Graco AFS team predicted, the S*martWare* software was able to meet even this customer's demanding application.

"With the equipment we installed, this customer is now able to dispense shots as small as one ounce with an accuracy of about ± 2%," Lewis added. "That's basically unheard of in the industry, especially with this kind of extremely difficult, abrasive medium."

The *SmartWare* software can be installed in about two hours, and it dramatically increases the precision and accuracy of dispense, as well as the availability of dispense data. The software is user-friendly, with a display panel that shows amount of material being used in each shot, number of shots dispensed over time, and more. With *SmartWare* installed, the Check-Mate pump can be controlled with just a pedal and a button.

The system, which was installed in the summer of 2015, has been running smoothly since its installation.

"The durability and reliability of the Check-Mate pump, paired with the extreme dosing accuracy of our *SmartWare* software, has simplified this customer's application, reduced waste, and removed the major production headache that pumping had been for them for so long," Lewis said. **PTE**

For more information:

Stacie Marley
Publicist
McNeil, Gray & Rice Strategic Communications
One Washington Mall
Boston, MA 02108
(617) 367-0100 ext.107
www.mgr1.com

Bruce Stephan is director of marketing, applied fluid technologies division, Graco Inc.

Minimum Design Speed Considerations for Sleevoil Bearings for Industrial Fan Applications

Will Cannon, Application Engineer, Baldor Electric Company

Abstract

Applications that require slow speed operation and use hydrodynamic bearings can successfully operate in reduced film thickness conditions as long as the shaft hardness is adequate and the shaft surface finish is between 16–32 microinches. The reason is because a thinner oil film is sufficient as long as the shaft surface asperities are small and a minimal number of broken metallic fragments from metal to metal contact are allowed to pass through the oil film without causing damage. A small circulating oil unit will further increase the bearing reliability at slow speed operation by flooding the bearing with oil when the oil rings are delivering minimal oil from the slow shaft rotation and by providing continuous particle filtration.

**Disclaimer: *This paper and its contents are strictly concerning hydrodynamic bearings used in industrial fan applications; all suggested values are derived from years of experience.*

Introduction

Slow speed operation of fan systems within the air handling industry is generally performed due to two reasons: a coast down operation is required for hot (induced draft) fans to cool down before shutdown (often by using a turning gear), and operational efficiency improvements can be achieved during non-peak periods by slow speed operation using a VFD. In either case, when these fans are supported by hydrodynamic bearings, it is the oil film thickness developed from the bearing-shaft interaction that limits the minimum speed that can be maintained without causing premature wear and bearing failure. This paper will present a brief overview of lubrication theory and critical design parameters to achieve slow speed operation.

There is an extensive amount of technical literature available to describe lubrication and hydrodynamic theory; this paper is only intended to present a brief overview of public knowledge.

Lubrication Theory

There are four regimes of lubrication, and they are generally defined according to the film thickness parameter (Snyder, Ovaert, and Wedeven, 2014):

$$\lambda = \frac{h_{min}}{\sqrt{R_{journal}^2 + R_{bearing}^2}} \quad (1)$$

where

l = film thickness parameter, h_{min} = minimum film thickness, $R_{journal}$ = surface finish of shaft (rms), and $R_{bearing}$ = surface finish of bearing (rms) (Singhal, 2008).

Boundary Lubrication (l < 1)

Boundary lubrication implies that the two mating surfaces are not separated by the lubricant and that extensive contact between the surface asperities exists. High coefficients of friction and significant wear from metal to metal contact are notable characteristics within this lubrication regime.

Mixed Lubrication (1 < l < 3)

This regime maintains contact between the two surfaces but has a lower coefficient of friction than boundary lubrication. The lubricant provides some amounts of load support, but it is insufficient to separate the surfaces. Significant wear occurs in this regime.

Elastohydrodynamic (EHL) Lubrication (3 < l < 10)

In EHL lubrication, the lubricant provides substantial amounts of load support to separate the surfaces. Although the coefficient of friction drops to a minimum, fatigue wear such as pitting can still occur in this regime due to the distribution of stresses which still cause surface deformations (Gohar, 2001).

Hydrodynamic Lubrication (10 < l < 100)

In hydrodynamic lubrication, the entire load is supported by the hydrodynamic pressure developed within the lubricant film. The coefficient of friction is slightly higher than the EHL regime, but there is minimal wear that will occur on either surface, indicating infinite life can theoretically be achieved in this regime.

Lubrication Regimes

Another relation that is beneficial in understanding the regimes of lubrication is the Hersey number:

$$H_s = \frac{\eta\omega}{P} \quad (2)$$

where

h is the absolute viscosity, **w** is the rotational speed, and P is the pressure. A larger Hersey number would imply a thicker oil film (larger **l**) whereas a lower oil film thickness would be present at a lower Hersey number (Stribeck, 1902). This dimensionless parameter can be compared to the coefficient of friction as it increases and changes lubrication regimes, as shown in a Stribeck curve (Figure 1).

where

μ = coefficient of friction. The position and shape of the actual Stribeck curve is specific to each application and is dependent upon the composite surface roughness (factor of **l**), as well the contacting materials, lubricant, and other factors (Snyder, Ovaert, and Wedeven, 2014).

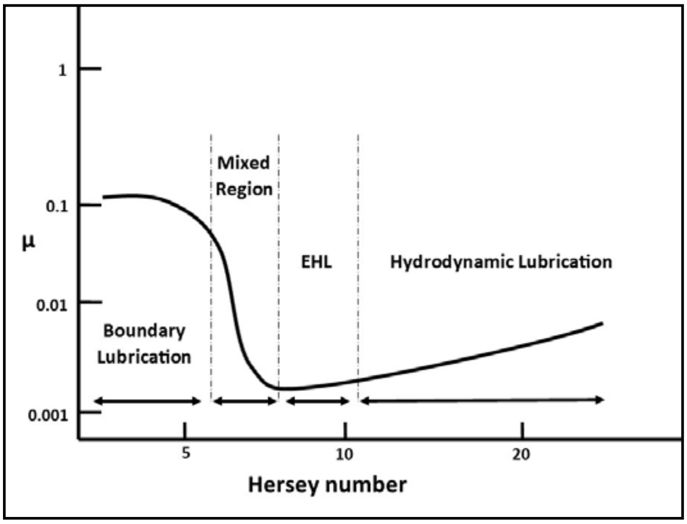

Figure 1 Stribeck curve comparing coefficient of friction with dimensionless Hersey number (Hamrock, Schmid, and Jacobson, 2004).

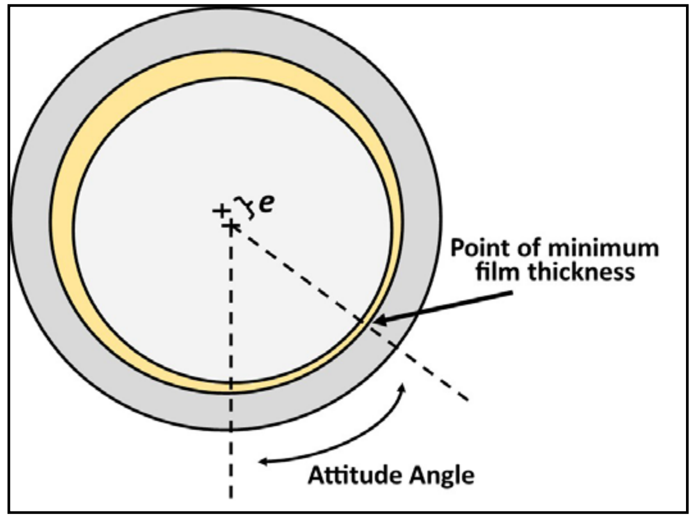

Figure 2 Illustration showing the attitude angle and point of minimum film thickness.

Hydrodynamic Theory

In addition to lubrication regimes, hydrodynamic theory must also consider application details in order to analyze the performance of a fluid film bearing at low speeds. The three requirements for the development of hydrodynamic pressure are: relative surface motion, converging geometry, and a viscous lubricant (He, 2005). One of the main governing parameters of hydrodynamic operation is the Sommerfeld number (S), also known as the bearing characteristic number, which is a dimensionless parameter that provides a relationship for dynamic stiffness and damping coefficients.

$$S = \frac{\upsilon NLD}{W}\left(\frac{R}{c}\right)^2 \tag{3}$$

where

ν = viscosity, N = shaft speed, L = bearing length, D = bearing diameter, W = rotor weight, R = radius of shaft, and c = radial clearance. The Sommerfeld number relates the geometric parameters of the bearing with the application specifics of weight, oil viscosity, and speed to determine the eccentricity ratio (ε):

$$\varepsilon = \frac{e}{c} \tag{4}$$

where

e = shaft eccentricity (distance between shaft and bearing centers). The eccentricity ratio is directly proportional to the attitude angle and both will vary with changes in the Sommerfeld number. The attitude angle will be the location where the shaft will ride on the oil film within the bearing at steady-state operation.

Understanding the fundamentals of hydrodynamic theory is critical to designing and producing a bearing that will continuously operate satisfactorily under various speed and load conditions and with extended bearing life.

Design Parameters

Shaft Surface Finish

The most critical design parameters in determining the minimum allowable speed while maintaining hydrodynamic lubrication are the oil viscosity and load (properties of the Hersey number [Eq. 2]), geometric tolerances of both the bearing and shaft (properties of the Sommerfeld number [Eq. 3]), and the composite surface roughness between the shaft and bearing (property of the film thickness parameter [Eq. 1]). Assuming that the pressure applied to the bearing from the rotor and shaft weight is constant, and also assuming that both the bearing and shaft geometries are adequately designed and manufactured (minimal run out and defects), then there are only two remaining factors that can be manipulated to decrease the minimum allowable speed while maintaining hydrodynamic lubrication: increasing the lubricant viscosity and decreasing the composite surface roughness. Selecting an oil with a higher viscosity grade would improve the minimum allowable operating speed, but at normal operating speeds, the higher grade viscosity would generate much more heat from oil shearing than a lower viscosity grade, as well cause the shaft to ride on the oil film at an attitude angle beyond the stability region which can cause instability and excessive vibration. Therefore, it can reasonably be concluded that the composite surface roughness from the bearing and shaft is the only variable that can be manipulated to improve the minimum allowable design speed. Furthermore, since the surface finish of the bearing load zone as provided by the manufacturer is constant, it is the shaft surface finish which can be improved that will lower the minimum allowable operating speed. However, experience has shown that there exists an optimal shaft surface finish range from 16–32 micro-inches; any less than this range has produced diminishing results in developing a hydrodynamic film.

Minimum Speed

Under normal operating conditions, the minimum recommended oil film thickness is 1 mil (thousandths of an inch), based on a shaft surface finish of 32 microinches. However, if a shaft is within this optimal surface finish range of 16-32 microinches, then the minimum allowable film thickness can be reduced to accommodate slow speed operating conditions (Table 1).

For example: if the minimum operating speed of an application was 100 rpm for a shaft with a 32 μ-in surface, then with a 16 μ-in surface, the minimum operating speed could

Table 1 Reduced acceptable film thickness values based on optimal shaft surface finish ranges. **These values are based on experience.

Shaft Surface Finish [μ in]	Acceptable Minimum Film Thickness [mils]	Approximate Percentage of Minimum Operating Speed
16	5/10	60%
24	7/10	80%
32	1	100%

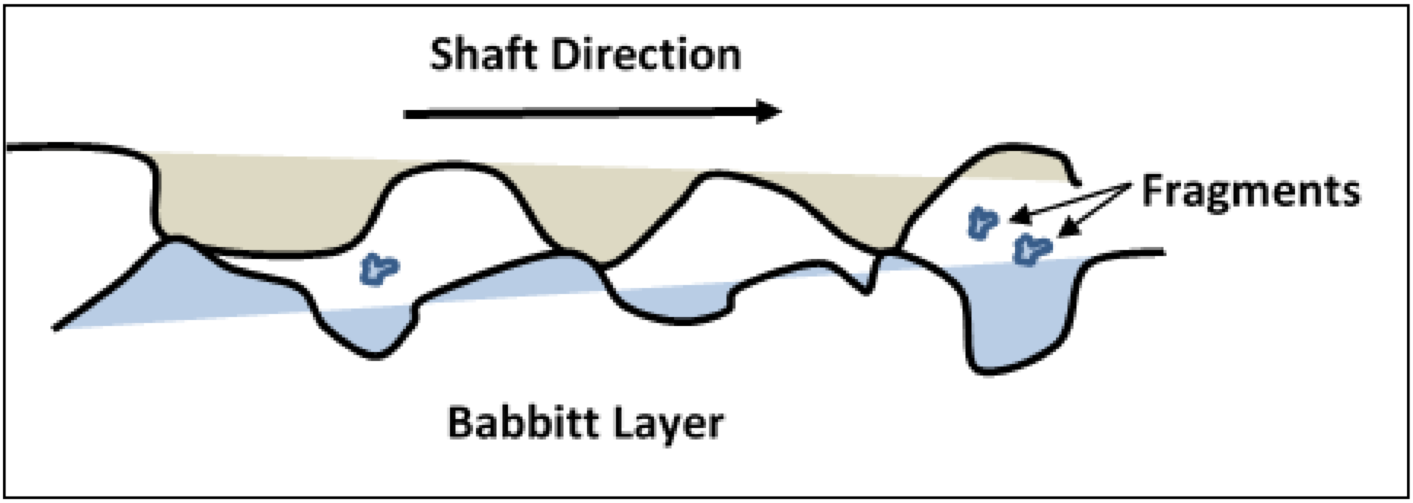

Figure 3 The shaft surface asperities will break the liner surface asperities and leave broken fragments that can advance bearing wear and failure.

be approximately 60%, or 60 rpm. The justification for this is that there will still be a complete separation of surfaces (full hydrodynamic lubrication) since the surface asperities are considerably small. Shaft run-out must be kept to a minimum because any high spots on the shaft will lessen the minimum film thickness and possibly provide an area of contact between the surfaces, inducing friction heat and even causing pre-mature failure.

Additional Performance Improvements

The benefits of having a hard shaft within the recommended surface finish range is the constructive wear-in it that will occur on the liner surface. As the shaft rotates directly on the babbitt layer during start-up and shut-down when hydrodynamic lubrication is not possible and there is metal to metal contact, the contact between the shaft surface asperities will break the surface asperities of the liner, since the shaft material is much harder than the babbitt material (Figure 3).

The broken fragments can accelerate bearing wear and the onset of bearing failure unless they are sufficiently small and minimal in quantity, in which case the shaft will burnish the babbitt layer and improve the liner surface. A sufficiently small fragment (~25% of the size of the film thickness) implies that it is sufficiently smaller than the minimum oil film thickness once full hydrodynamic lubrication develops so that it can easily pass through the film without causing abrasive damage to either surface. The fragment size that will be broken off can be minimized by either decreasing the load or increasing the hardness of the shaft (Smart, 2009). Additionally, the condition of the oil should be continuously monitored to prevent a build-up of metallic fragments in the oil.

Since slow speed applications generally require a minimum oil film thickness less than 1 mil, it is of critical importance to the life of the bearing that the shaft is both hard and within the optimal surface finish range, which ensures the fragments broken off will not be abrasive during hydrodynamic lubrication and a proper oil maintenance schedule is in place.

Additional Reliability at Slow Speeds

However, since shaft surface defects are inevitable, additional reliability can be incorporated into slow speed applications by using a small circulating oil unit. Self-lubricating hydrodynamic bearings are entirely dependent on oil rings to rotate on the shaft to deliver oil to the bearing (Figure 4).

This means that during start-up, shut-down, and slow speed operation, the oil rings are rotating at slower speeds and the quantity of oil being delivered is reduced which can cause the bearing to run in starved conditions. Since the reli-

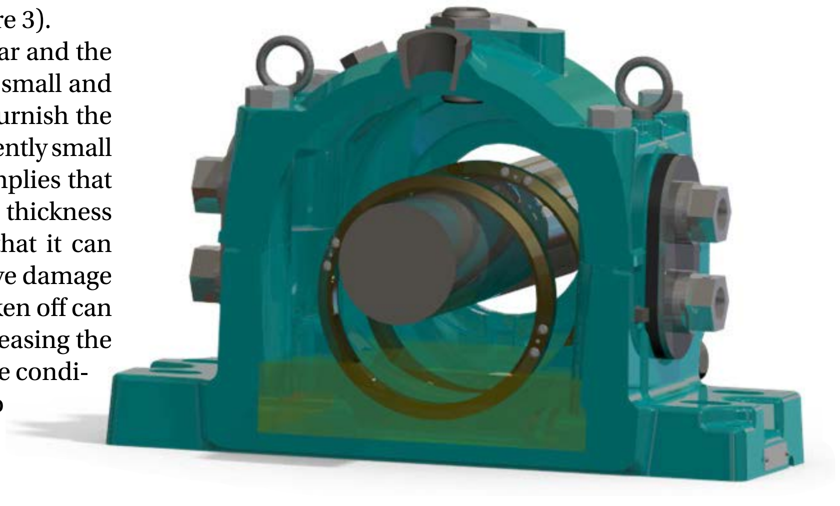

Figure 4 Oil rings rely on shaft rotation to deliver oil to the bearing.

able operation of the bearing is entirely dependent upon the shaft and bearing surfaces being separated by a film of oil, it is best practice to use a small circulating oil unit to ensure adequate oil supply when the oil rings are not rotating sufficiently often.

Conclusion

Hydrodynamic lubrication is dependent upon many factors, and with careful design and manufacturing, hydrodynamic bearings can adequately support applications that require slow speed operation. In order to design an application to continuously operate in a film thickness region below the recommended 1 mil, the shaft surface finish and hardness are critical parameters that determine whether the bearing will survive or fail in these conditions. Circulating oil units enhance the reliability of slow speed operation, as they deliver oil to the bearing and prevent starved conditions when the oil rings are turning at a reduced speed and are limited from providing an adequate oil supply for full hydrodynamic lubrication. **PTE**

William Cannon is an application engineer with Baldor Electric Company, a member of the ABB Group, with responsibility for Baldor·Dodge sleevoil bearings. Since joining the company in 2014, he has been involved in product development projects with hydrodynamic bearings, and he received a company-specific engineering achievement award for the Baldor·Dodge RTL-Spherical Bearing. William is a graduate of Clemson University.

References

1. Snyder, Dan, Tim Ovaert, and Vern Wedeven. "Lubrication, Friction, and Wear," Proc. of Essential Concepts of Bearing Technology, McDonald's Hamburger Campus, Oak Brook, IL. N.p.: AMBA, Sept. 9-11, 2014. 4-7.
2. Singhal, Sumit. "Sleeve bearing design for slow speed applications in cement plants," Cement Industry Technical Conference Record, 2008 IEEE. IEEE, 2008.
3. Gohar, Ramsey. "Film Thickness and Pressure Distribution in Elastohydrodynamic Lubrication," Elastohydrodynamics. 2nd ed. London: Imperial College Press, 2001. N. pag. World Scientific, 2001. Web. Dec.-Jan. 2015-16.
4. Hamrock, Bernard J., Steven R. Schmid, and Bo O. Jacobson. "Introduction." Fundamentals of Fluid Film Lubrication. 2nd ed. N.p.: Marcel Dekker, 2004.
5. Stribeck, R., "Second Report on Frication Experiments (Experiments on the Oil Pressure in a Bearing." Characteristics of Plain and Roller Bearings. Zeit. Ver, Deut. Ing. v. 46, 1902, pp. 1341-1348, 1432-1438, 1463-1470. Tower, B. (1885).
6. Budynas, Richard G. "Lubrication and Journal Bearings." Mechanical Engineering Design. By Joseph Edward. Shigley and Charles R. Mischke. 7th/8th ed. New York: McGraw-Hill, 2003. N. pag. KSU. Web. Dec.-Jan. 2015-16.
7. He, Minhui, C. Hunter Cloud, and James M. Byrne. "Fundamentals of Fluid Film Journal Bearing Operation and Modeling." TIB. Proc. Of Proceedings of the Thirty-Fourth Turbomachinery Symposium, George R. Brown Convention Center, Houston, TX. N.p., 2005. Web. Dec.-Jan. 2015-16.
8. Smart, Eric. "Fatigue and Wear in a Journal Bearing." High Power Media (n.d.): n. pag. 15 Nov. 2009. Web. Dec.-Jan. 2015-16.

For Related Articles Search
bearings
at www.powertransmission.com

An Open-And-Shut Case: Greases for Gear Applications

Dr.-Ing. Johann-Paul Stemplinger

Studies of Different Types of Greases in the FZG Back-To-Back Gear Test Rig

For the lubrication of *open gear drives* used in different industrial applications such as cement and coal mills, rotary furnaces, or where the sealing conditions are difficult, *semi-fluid greases* are often used in preference to fluid oils. For girth gear applications the greases are used with a splash or spray lubrication system. The selection of such greases influences pitting lifetime and the load-carrying capacity of the gears, as well as wear behavior.

Investigations have been carried out making comparisons between a fluid oil and different semi-fluid (NLGI 00) grease formulations, varying with regard to base oil viscosity, thickener type and the addition of both liquid and solid additives. The test runs for the determination of the different parameters were performed on FZG back-to-back gear test rigs; the schematic setup of the test rig is shown in Figure 1.

The FZG back-to-back gear test rig utilizes a re-circulating, power-loop principle — also known as a "four-square configuration" in order to provide a fixed torque (load) to a pair of test gears. The test gearbox and drive gearbox are connected through two torsional shafts; one shaft is divided into two parts and contains a load coupling used to apply the load through the use of weights hung on the loading arm.

Depending on the particular tests in question, different test gears and test conditions were selected and details of these are available for the reader interested in articles previously presented by this author (see references). The test runs for the investigation of pitting lifetime and pitting load-carrying capacity were performed on the test rig using splash lubrication. After certain test intervals the flanks of the pinion and wheel were visually inspected for damage. The test results show that gear greases of NLGI 00 consistency exhibit almost the same pitting lifetime as their base oil counterparts. Furthermore, the kinematic viscosity of the base oil shows a significant influence on pitting lifetime of such NLGI 00 grade greases. The addition of a special synthetic graphite to such a gear grease led to a decrease in pitting life and high wear. The test results also show that the pitting load carrying capacity of these greases correlates with the kinematic viscosity of the base oil. Using a higher base oil viscosity, longer pitting lifetime and higher pitting load carrying capacity were achieved. For semi-fluid gear greases, the calculation of pitting load carrying capacity according to ISO 6336 using the viscosity of the base oil correlates well with the practical test results.

The tests to analyze wear behavior of different semi-fluid gear greases were made in the wear test A/2.8/50 on the basis of ISO 14635-3 and ISO 14635-1. Four different wear categories were defined for the 100-hour endurance test and a classification made according to the wear sum on the pinion and wheel.

Generally speaking, almost all investigated lubricants, with the exception of greases containing solid lubricants, show low wear in all test parts. The influence of the base oil viscosity can be seen in that greases with higher base oil viscosities exhibit lower wear. The influence of the concentration of thickener and the type of thickener is almost negligible, but the grease with an aluminum complex soap does show just a very slight higher wear sum compared to its lithium soap-thickened counterpart. A much more significant difference can be seen in the influence of the amount and type of solid lubricant. Greases containing synthetic graphite exhibit much higher wear sums — correlating with the amount of graphite in the grease — compared to the same grease with no solid lubricants. At the end of the step test the grease containing 4.2% graphite shows a three-times-higher wear sum than the base grease. And with a higher amount of graphite — 11.1% —the wear sum increased to a level of eight times higher compared to the grease with no solids. This trend was also confirmed in the endurance test; i.e. — the more graphite, the higher the wear. On the other hand, the grease containing 4.2% of molybdenum disulphide displays comparable wear

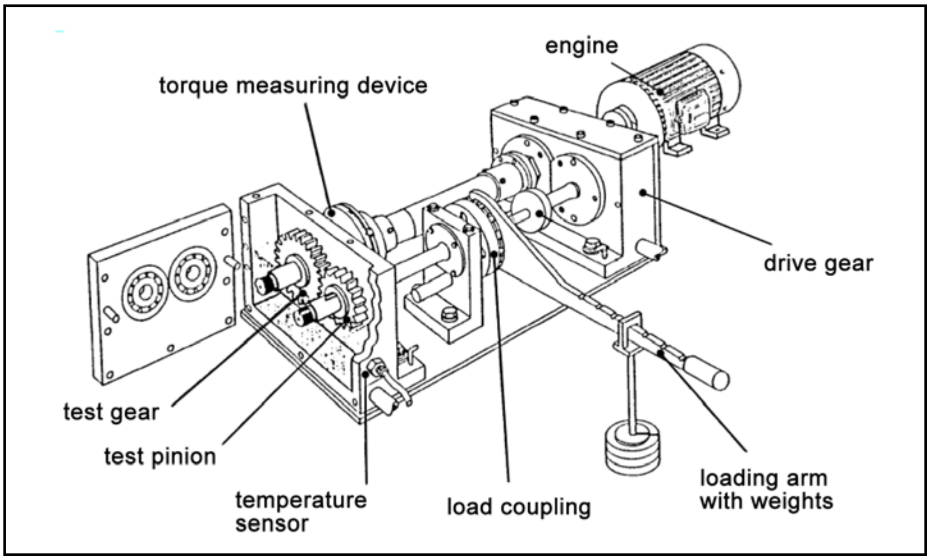

Figure 1 FZG back-to-back gear test rig.

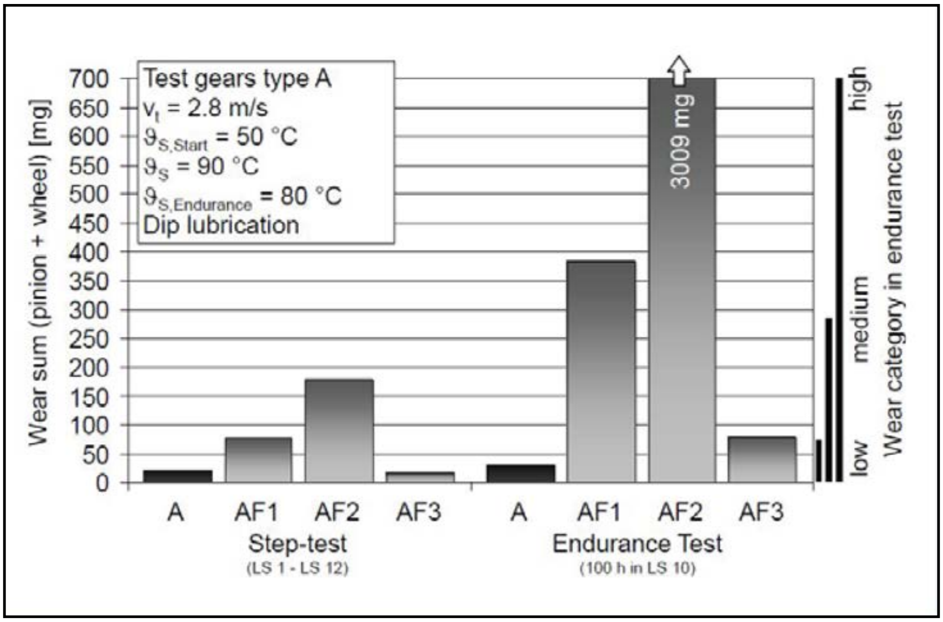

Figure 2 Wear behavior — influence of amount and type of solid lubricant.

A: Aluminum complex base grease
AF 1: Base grease + 4.2% graphite
AF 2: Base grease + 11.1% graphite
AF 3: Base grease + 4.2% molybdenum disulphide

to the base grease after the step test, and only slightly higher wear after the endurance test.

In a different context, for the lubrication of small, enclosed geardrives used in electrical tools or in medical applications, as well as for the lubrication of small gearboxes in difficult sealing conditions, stiffer greases are preferred, often of NLGI 1 or 2 grade consistency. The selection of grease type and the filling level influence efficiency, load-carrying capacity and heat transfer in a gearbox.

Investigations were performed with different greases of NLGI 1 and 2 consistency using different thickener types, lithium complex, aluminum complex, calcium complex and polyurea. Three types of base oils, all with kinematic viscosities approximately 100 mm^2/s@40°C, were used, i.e. — paraffinic, naphthenic, and a synthetic polyalphaolefin. All model lubricants were formulated with 4% of a typical EP package for greases.

The tests for the determination of efficiency and load-carrying capacity were, once again, performed on FZG back-to-back test rigs. The influence of different filling levels (e.g. — 40, 50, and 80%) in dip lubrication has been analyzed. Based on the results of comprehensive studies using NLGI 1 and 2 grade greases in the FZG test rig, different lubrication supply mechanisms — channeling and circulating — have been identified. Whether channeling or circulating occurs depends on various factors such as the interaction of torque, speed, filling level and the type of grease.

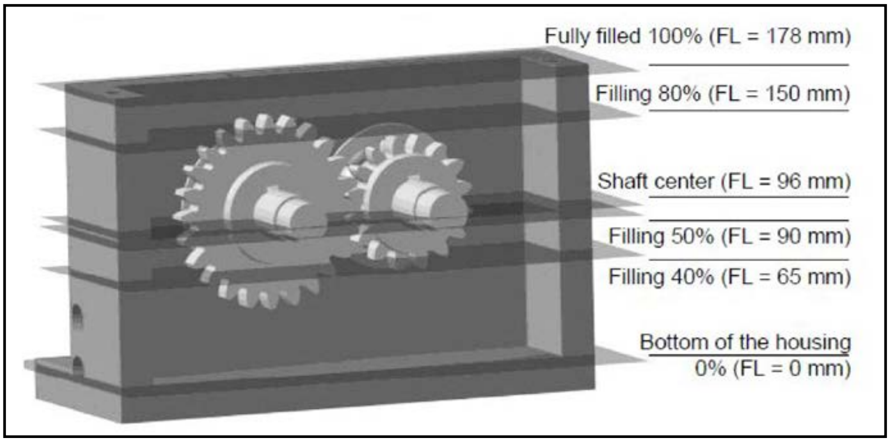

Figure 3 Filling of test gearbox.

Channeling. When the spur gearset starts to rotate, the grease next to the gearset is immediately discarded and does not return to that gearset due to the lack of a sufficient replenishment mechanism. A gap is formed between the rotating gears and the grease sump. No fresh grease flows from the sump to the gearset because of its solid consistency. A lack of lubrication and cooling can be observed that can lead to high bulk temperatures in the gears and, finally, to scuffing. Only a small amount of grease participates in the lubrication. Channeling occurs mainly at 40 and 50% filling levels and for stiffer products.

Circulating. In some cases, especially at high filling levels, a second, different lubricant supply mechanism can be observed. When the gears rotate, part of the grease in the sump rotates at a lower speed than the gears and, from time to time, fresh new grease flows from the sump in the direction of the gears. Compared to the situation with channeling, better lubricant supply to the gears, better cooling and thus lower bulk temperatures in the gears and higher sump temperatures can be observed. In total, more grease participates in the lubrication mechanism. Circulating occurs mainly at a filling level of 80%.

In general, the field of possible operating conditions with respect to load-speed combination is restricted by limited heat removal from the gears and, therefore, only high-speed, i.e. — low torque, low speed — high torque and medium speed — medium torque are possible operating conditions, thus limiting transmittable power without immediate scuffing failures. A lubrication-optimized, internal geometry of the housing without edges and corners, one which is tight-fitting to the gears, can improve heat transfer. And heat removal can, of course, be improved by cooling fans on the exterior of the gearbox.

Lubrication supply, efficiency and load-carrying capacity are somewhat influenced by the filling level. As a minimum filling level, it is necessary that all the gears are dipped into the lubricant. At the other extreme, a maximum filling up to 90–95% of the free volume in the gearbox is possible. A fully filled gearbox will leak due to the thermal expansion of the lubricants. A filling level of "shaft center" is a good compromise between low no-load losses, sufficient cooling, and adequate lubricant supply. When channeling occurs, low no-load losses, low sump temperatures, and high bulk temperatures can be observed with a high risk of wear and scuffing. On the other hand, circulating results in high no-load losses, better heat removal and thus lower bulk temperatures and higher sump temperatures.

When it comes to the optimal lubricant choice, the synthetic base oil shows advantages for frictional behavior and load-carrying capacity, whereas the naphthenic base oil cannot be recommended; the thickener type influences the lubricant supply to a minor degree. Lithium complex and aluminum complex greases show high oil separation and thus a good supply for channeling and circulating. Calcium complex shows the lowest oil separation of the greases and thus a lack of lubrication. Polyurea greases show the highest load-carrying capacity, the lowest frictional losses in the gear contact and good, high-temperature performance.

References:

1. Stemplinger, J.-P., B.-R. Höhn, K. Stahl, K. Michaelis and M. Hochmann. "Grease Lubrication — Pitting Load-Carrying Capacity of Gears," *STLE Annual Meeting & Exhibition* 2011, Atlanta/USA.
2. Stemplinger, J.-P., K. Stahl, B.-R. Höhn, K. Michaelis, H.-P. Otto and M. Hochmann. "Wear Behavior of Grease-Lubricated Gears," 2012, *ELGI–European Lubricating Grease Institute, 24th Annual General Meeting*, München.
3. Stemplinger, J.-P. K. Stahl, B.-R. Höhn, T. Tobie and K. Michaelis. "Analysis of Lubrication Supply of Gears Lubricated with Greases NLGI 1 and 2 and the Effects on Load-Carrying Capacity and Efficiency," 2013, *NLGI 80th Annual General Meeting*, Tucson/USA.

It Ain't Black — but It Works

The implementation of modern tribology offers substantial savings in wear, energy and, not least — money. According to Peter Jost in his presentation to the 2013 World Tribology Congress in Turin, "New materials and new technologies are cascading upon the world, but their tribological benefits are often not recognized by the end-users." Which is a pity, because there is so much to be gained by utilizing already-available lubrication technologies, not to mention the potential for developing new products with a focus on functionality rather than specification. Existing specifications are, in fact, often an impediment to progress; this is a dilemma for any new (lubricant) technology. Current specifications describe the old best practice products with emphasis on "old" — and, in many cases — reject a new and better product; new products need new specifications.

In grease-lubricated contacts it is accepted wisdom that thickener works only as a reservoir for the lubricant (the oil) that leaks out of the "sponge" into the contact zone and, after passing the zone, re-enters the grease matrix. We have now come to the conclusion that this theory does not fully correspond with reality. The thickener in soap-based greases contributes extensively to the formation of a lubricating film and, in some cases, the film can be twice as thick as it would have been when using an oil of the same viscosity as the base oil of the grease. We also found that at very high-contact pressures the friction decreased as the amount of thickener increased. The theoretical basis of calculations currently used for evaluating the thickness of a lubricating film do not consider the influence of the thickener and are therefore not applicable to lubricating greases. The Kappa value for greases is almost always higher than can be calculated for the base oils. At the same time, it is known that the tendency of the thickener to adhere to a metal surface is greater than that of an oil, which led us to postulate that it would be better to try to attach the additives to the thickening agent instead of dissolving them in the base oil. These new types of products have been designated "functional soaps."

Harbour Crane (Courtesy Bert Schenk, Lubricoat BV)

Functional soap-based greases have performed successfully in open gear applications in the mining and cement industries, as well as in traction motor gears on railway locomotives (even in Norway under frozen Arctic conditions). Even when used as semi-fluid gear greases they meet the specifications for most open gear applications, high adhesion to the surfaces; good pumpability; excellent corrosion inhibition; and extremely high load-carrying capacity (4-ball weld load > 7500N), FZG test > stage 12). In everything — *but* the stipulated content of solids! The advantages of excluding the solid particles are attractive to the end user if they can be convinced that a product that is not black will actually do the job. There is no build-up of solids in the gear teeth, thus reducing vibration and noise and, for the ambitious maintenance engineer, the surfaces are visible and can be monitored using, for instance, a stroboscope. And, the fact that the greases are not black has even some cosmetic advantages like, in the wind power industry, where it not considered environmentally attractive to see black oil running from the turning gears down on to the ground.

Mining Example/Case Study

One practical example from the mining industry is the use of such a product in ore processing and, in particular, rotary kilns. This functional soap was introduced in a kiln where the gear was in such bad condition that a replacement had been ordered. The gear had a diameter of about nine meters and was running at a speed of 2 rpm. The result, after about three months, was that the wear had been reduced dramatically to an acceptable level and, at the same time, the surface roughness had remarkably improved.

In addition to the mining industry, these products have been used with excellent results. Other examples are the lubrication of turning gears on wind turbines and even the swivel gears on large harbor cranes. According to Bert Schenk, Lubricoat BV, in the Netherlands, "This type of grease has been used successfully on the open gears of a slewing bearing of a floating bulk crane in the harbor of Amsterdam." He had received a phone call from the construction engineer of the company who built the crane to check the lubrication of the open gears because there was significant wear on the gear teeth. When he climbed the stairs of the crane to take a look at the open gears, he observed silver-grey grease on the open gears. "The pinion gear had a very rough surface and the gears of the slewing bearing were smooth," says Schenk. "In this particular case the hardened surface of the teeth on the pinion was discovered to be four times harder than the teeth on the slewing bearings, which were much softer. The harder pinion wheel was more or less 'grinding' on the softer slewing bearing. So the silver-grey color was caused by all the metal 'wear' particles in the grease. In addition, after recalculation of the gear geometries it seemed that the teeth did not have the right dimensions, so the teeth surfaces needed to be increased (for lower surface pressure). But remarkably, there was no pitting on the surface of the teeth, which had very smooth surfaces. This proved that the grease had lubricated perfectly during this grinding process. The customer is still using this grease because, even in extreme overload situations, it has proved to do its work."


Crane Gears
(Courtesy Bert Schenk, Lubricoat BV)

Yet another version, based on synthetic base oils, has been tested with great success on the traction motor gears of diesel electric locomotives.

The problem with these gears is that they originally were designed for oil lubrication. However, the seals are so poor that when oil is used, it is thrown out of the oil sump along the shaft. That is why most traction motor gears of today are grease-lubricated. Grease lubrication, however, has never worked satisfactorily — especially in winter. The types of greases predominantly used in such applications have been traditional bitumen-based lubricants with an addition of solid lubricants; e.g. — graphite and molybdenum disulphide. In winter these types of lubricants become very hard and elastic; they do not flow back down into the oil sump, but instead stay in the roof of the gearbox where they are thrown up by the gears. The PAO-based functional soap copes with the extreme loads and shock loads that occur in these spur gears as a result of rail joints and irregularities of the wheels caused by locked brakes. Still, the product remains smooth and fluid at very low temperatures and the re-flow to the oil sump is secured.

For more information, please visit: *www.axelch.com/wordpress/wp-content/uploads/2013/06/White-or-Black-Blues.pdf*

Dr.-Ing. Johann-Paul Stemplinger is a Research Group Manager at FZG, Gear Research Centre, Technische Universität München Germany — dedicated to working on gearbox efficiency as well as worm, bevel and hypoid gears. In 2012 he was responsible for gearbox efficiency at FZG, serving in the capacity of team leader. Stemplinger, with a M.Sc. in mechanical engineering from Technische Universität München, finished his doctoral thesis in the field of tribology of gear contacts at FZG in 2013. He has authored over 20 publications, including four patents in the field of powertrain and transmissions, focusing on tribology and lubrication of gears. While attending Technische Universität, Stemplinger in 2008 was awarded both the Oskar-Karl-Forster and Prof.-Dr.-Wilhelm-Wittman scholarships.

For Related Articles Search
grease
at www.powertransmission.com

A Model for Rolling Bearing Life with Surface and Subsurface Survival — Tribological Effects

Guillermo E. Morales-Espejel, Antonio Gabelli and Alexander J. C. de Vries

Until now the estimation of rolling bearing life has been based on engineering models that consider an equivalent stress, originated beneath the contact surface, that is applied to the stressed volume of the rolling contact. Through the years, fatigue surface–originated failures, resulting from reduced lubrication or contamination, have been incorporated into the estimation of the bearing life by applying a penalty to the overall equivalent stress of the rolling contact. Due to this simplification, the accounting of some specific failure modes originated directly at the surface of the rolling contact can be challenging. In the present article, this issue is addressed by developing a general approach for rolling contact life in which the surface-originated damage is explicitly formulated into the basic fatigue equations of the rolling contact. This is achieved by introducing a function to describe surface-originated failures and coupling it with the traditional, subsurface-originated fatigue risk of the rolling contact. The article presents the fundamental theory of the new model and its general behavior. The ability of the present general method to provide an account for the surface–subsurface competing fatigue mechanisms taking place in rolling bearings is discussed with reference to endurance testing data.

Nomenclature

A = Damage risk area (m^2)
$\hat{A}$ = Constant
$\overline{A}$ = Damage constant for volume, damage constant for a rolling contact
a_u = Fatigue limit load-life modifying factor; see Ioannides, et al. (Ref. 12)
a = Hertzian semi-width along the rolling direction (m)
$\overline{B}$ = Damage constant for surface
b = Hertzian semi-width across the rolling direction (m)
C = Dynamic capacity of the bearing (N)
c = Exponent in the bearing life equation
d_m = Mean diameter of the bearing (mm)
e = Exponent in the bearing life equation (standardized Weibull slope)
F = Radial bearing load (N)
$G(N)$ = Accumulated material degradation function from 0 to N load cycles
$\hat{h}$ = Thickness of the surface layer (m)
h = Exponent in the bearing life equation
I_s = Surface damage integral or surface damage parameter
I_{ss} = Subsurface damage integral
K = Constant for the surface damage function
L = Rolling contact life, bearing life (MR$_{ev}$)
$L_{10.BR}$ = Basic rating life (MR$_{ev}$)
m = Weibull slope for surface failure modes
N = Number of load cycles
P = Equivalent load in the bearing (N)
P_u = Fatigue load limit in the bearing (N)
p = Exponent in the bearing life equation
Δp = Pressure fluctuations due to roughness (Pa)
p_o = Maximum Hertzian pressure in the contact (Pa)
Q = Contact load (N)
R_q = r.m.s. value of the roughness (m)
R_s = Normalized surface damage function, $R_s = I_s u^e L^e_{10.\mathrm{BR}} / ([K \mathrm{Ln}(1/0.9)]$
S = Probability of survival
S = Sliding/rolling ratio in the contact, $S = u_s/\bar{u}$
S_R = Ratio of surface damage
u = Number of stress cycles per revolution, $L = N/u$
$\bar{u}$ = Mean speed of the contact surfaces (m)
u_s = Sliding speed (m/s)
V = Damage risk volume (m^3)
w = Exponent in the life equation
x = Coordinate (rolling direction) (m)
y = Coordinate (transverse to rolling direction) (m)
z = Coordinate (depth from the surface) (m)
η = Surface stress concentration reduction factor, $\eta = \eta_b \eta_c$ (Ref. 14)
κ = Viscosity ratio in the bearing (Ref. 15)
Λ = Lubrication quality factor $\Lambda = h_c/R_q$
σ = Amplitude value of stress-related fatigue criterion (Pa)
σ_u = Fatigue limit value of the fatigue criterion used (Pa)
τ_u = Shear stress fatigue limit (Pa)
τ_{xz} = Amplitude of the orthogonal shear stress (Pa)
Ψ_{brg} = Bearing-type characteristic number (Ref. 14)

Subscripts

e = Related to outer ring
i = Related to inner ring
s = Related to surface
v = Related to volume

Introduction

Since the pioneering work of Lundberg and Palmgren in 1947 (Lundberg and Palmgren (Refs. 1–2)), rolling bearing life has been modeled using basic principles of rolling contact fatigue based on an equivalent stress originated beneath the contacting surfaces and affecting the over-rolling material volume of the contact. This approach is focused on subsurface spalling fatigue because this was the dominant failure mode at the time the model was developed. In 1967, Tallian (Ref. 3) found that there are many different competing failure modes leading to fatigue failure of the bearing raceway. This is also the conclusion of a more recent investigation about this topic performed by Olver in 2005 (Ref. 4). In 1971, Chiu, et al. (Refs. 5–6), Tallian and McCool (Ref. 7), and Tallian (Ref. 8) also attempted to tackle the different failure mechanisms occurring at the surface and in the subsurface of the rolling contact using engineering crack mechanics concepts. The different failure modes that occur in rolling bearings and their effect on rolling bearing life are extensively discussed by Zaretsky (Ref. 9).

An exhaustive and up-to-date categorization and review of rolling contact fatigue models can be found in Sadeghi, et al. (Ref. 10).

A significant contribution and further extension of the Lundberg and Palmgren (Refs. 1–2) theory is provided by Ioannides and Harris (Ref. 11) and Ioannides, et al. (Ref. 12) with the introduction of an additional material parameter to characterize the fatigue strength of bearing steel at the very high number of stress cycles (Gabelli, et al. (Ref. 13)). The new model was found to give a better representation of the load-life performance of modern rolling bearings (Ioannides, et al. (Ref. 12); Gabelli, et al. (Refs. 13–14)). Furthermore, this model provides a consistent methodology to globally derate the life of the rolling contact in case the operating conditions are less than optimal as in case of reduced lubrication or presence of contamination particles (Ioannides, et al. (Ref. 12); Gabelli, et al. (Ref. 14)). Currently this approach is well supported by national and international standards (Ref. 15).

In the last few decades, the need to further increase energy efficiency in machines and reduce their environmental impact has created the tendency for rolling bearings to operate at higher rotary speeds, higher temperatures, and reduced lubricant film thicknesses. Furthermore, the presence of contaminants and aggressive additives in the lubricant has also contributed in making surface related failures a very common aspect of current service life of rolling bearings. Because of this, there is an increased need for more versatile or generalized rolling bearing life models, able to adapt and incorporate new developed knowledge about the tribology of surface initiated failures of the rolling contact.

Despite the progress achieved in the last few years in the numerical modeling of the tribology and surface performance of rolling contacts (e.g., Epstein, et al. (Refs. 16–17); Morales-Espejel and Brizmer (Ref. 18); Morales-Espejel and Gabelli (Ref. 19); Brizmer, et al. (Ref. 20); Warhadpande and Sadeghi (Ref. 21)), the integration of this new knowledge into an engineering model for bearing life estimation is, to some extent, hindered by the simplicity of present standardized life rating formulation (Ref. 15), which only relies on averaged global de-rating factors. This approach, although sufficient for most common situations, is not designed to give an account and differentiate among surface/subsurface competing failure modes that may occur in a bearing when exposed to a hostile environment and tough operating conditions.

Objective of this Article

The objective of the present article is to describe the basic equations of a probabilistic model for rolling contact fatigue life estimation tailored to better characterize bearing surface–induced damage from the subsurface rolling contact fatigue process of the bearing. This new formulation is designed to facilitate the incorporation into bearing applications of newly developed knowledge gained from testing, advanced numerical modeling, or even engineering field experience of the expected surface and subsurface performance of the rolling contact.

The article presents the fundamental theoretical aspects of the new model and its general behavior and does not intend, at this point, to describe an engineering methodology for bearing life calculation in applications; that aspect should come in further publications. The advantages of the present method in providing a specific account for the observed surface/subsurface competing fatigue mechanisms of the rolling contact is illustrated using a simple bearing application operating under various lubrication conditions and endurance test results.

Probabilistic Damage Approach

It is well known that under laboratory conditions, seemingly identical bearings operating under identical conditions have significantly different individual bearing lives. Because of this, the prediction of bearing life requires a probabilistic setting, in order to:

1. Represent the intrinsic local variability of the material matrix strength, geometrical parameters and stochastic properties resulting from the presence of random inclusions and other inhomogeneities; for example, Ioannides and Harris (Ref. 11), Lamagnere, et al. (Ref. 22), Lai, et al. (Ref. 23), Weibull (Ref. 24).
2. Provide a simple method for the nominal scaling of the life, conventionally rated at 90% reliability; that is, L_{10}, to a different value of reliability; that is, L_{50} (Lundberg and Palmgren (Ref. 1); ISO 281:2007 (Ref. 15); Weibull (Ref. 25)).

The present model will retain the standardized probabilistic approach used in rolling bearing life ratings based on a two parameter Weibull distribution, as discussed in Blachere and Gabelli (Ref. 26).

Weibull (Ref. 24), with the weakest link theory, introduced stochastic concepts in the determination of strength and rupture of structural elements.

If a structure is composed by n elements subjected to different stress states, thus with a different probability of survival $S_1 \cdot S_2 \cdots S_n$ following the product law of reliability, the probability that the whole structure will survive is:

$$S^n = S_1 \cdot S_2 \cdots S_n = \prod_{i=1}^{n} S_i \tag{1}$$

which can be expressed also in the equivalent form:

$$\ln(S^n) = \ln(S_1) + \ln(S_2) + \cdots + \ln(S_n) = \sum_{i=1}^{n} \ln(S_i) \tag{2}$$

Contact damage model. Lundberg and Palmgren (Ref. 1), in their classic original formulation of the dynamic capacity of rolling bearings in 1947, applied the product law of reliability of Weibull Equation 2 to derive the survival function of a structure made of n independent physical elements accounting for the degradation process from 0 to N load cycles:

$$\ln\left[\frac{1}{S(N)}\right]=\ln\left[\frac{1}{\Delta S_1(N)}\right]+\ln\left[\frac{1}{\Delta S_2(N)}\right]+\cdots+\ln\left[\frac{1}{\Delta S_n(N)}\right] \quad (3)$$

The volume V can be divided into two or more independent sources of damage risk for the structure; consider that G is a material degradation function accounting for the effect of the accumulation of load cycles (fatigue). Therefore, regions can be characterized by different material degradation functions that could describe different (or a single) degradation processes, $G_{v.1}$, $G_{v.2}$,…,$G_{v.n}$. Their combined effect on the survival of the complete structure can be expressed by using Equation 3, from which the following can be derived:

$$\ln\left[\frac{1}{S(N)}\right]=\sum_{i=1}^{n}G_{v.1}(N)\,\Delta V_{v.1.i}+\sum_{i=1}^{n}G_{v.2}(N)\,\Delta V_{v.2.i}+\cdots+\sum_{i=1}^{n}G_{v.n}(N)\,\Delta V_{v.n.i} \quad (4)$$

for an infinitesimal volume $\Delta V \rightarrow 0$ this becomes:

$$\ln\left[\frac{1}{S(N)}\right]=\int_{V_{v.1}}G_{v.1}(N)\,dV_{v.1}+\int_{V_{v.2}}G_{v.2}(N)\,dV_{v.2}+\cdots+\int_{V_{v.n}}G_{v.n}(N)\,dV_{v.n} \quad (5)$$

which is a generalized type of survival function for a structure composed of n independent regions subjected to the risks associated to the accumulation of material damage.

Surface and subsurface survival. In the present formulation for a rolling contact life, two independent degradation functions are introduced to express the survival probability of the rolling contact. The first function describes the damage taking place in the bulk volume of the rolling contact; that is, the subsurface damage accumulation function or $G_v(N)$. The second function represents the damage occurring in a thin material layer at the very surface of the rolling contact; that is, the surface damage evolution function or $G_s(N)$. Thus, the survival function (Eq. 5) for a rolling contact can be written as:

$$\ln\left[\frac{1}{S(N)}\right]=\int_{V_v}G_v(N)\,dV_v+\int_{V_s}G_s(N)\,dV_s \quad (6)$$

This formulation of the survival of a rolling contact allows the surface to account for the different probabilistic failure modes independently from the subsurface region of the contact. Indeed, surface phenomena such as surface distress, wear, indentations, frictional heating, etc., in general affect the fatigue of a very thin material layer whose mechanical properties may differ from the bulk properties of the Hertzian contact (Fig. 1). Therefore, it is advantageous to analyze the damage developed in this region separately from the rest of the contact. For instance, surface traction and roughness-induced surface stresses will not, in general, affect the subsurface smooth Hertzian stress or the amplitude of the fatigue stress criterion of the rolling contact (Ioannides, et al. (Ref. 12)).

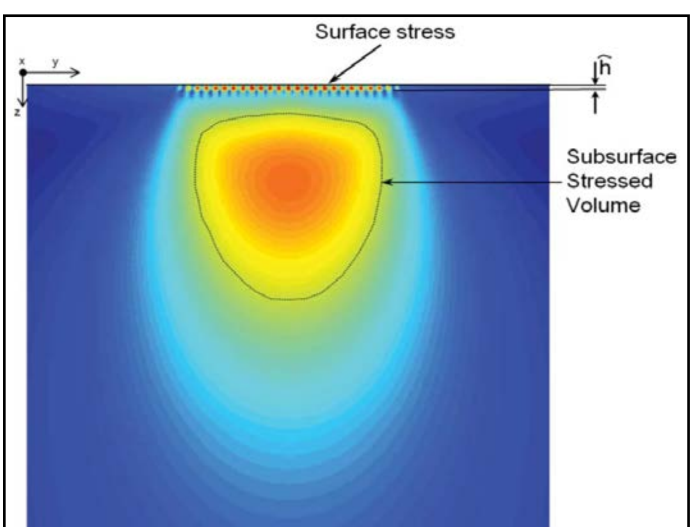

Figure 1 Schematics of surface and subsurface von Mises stress fields of Hertzian contact; surface stresses are related to surface microgeometry and lubrication conditions of rolling contact. Typically, surface stresses are constrained in narrow layer at raceway of depth, comparable to surface roughness.

Furthermore, in situations where surface traction is dominant, the stresses very close to the surface appear to be almost independent of the depth. Therefore, a further approximation is possible; consider a surface material volume $V_s=\hat{h}\cdot A$ as a thin layer on the raceway, then G_s applies to the surface region A, up to a depth $\hat{h}$ of the order of the depth of the microgeometry maximum stress (Fig. 1). For rolling bearings, raceway microgeometry (Refs. 14, 27) $\hat{h}$ can be assumed small and constant for similar classes and types of bearings. The probability of survival (Eq. 6) can then be rewritten in the following form:

$$\ln\left[\frac{1}{S(N)}\right]=\int_{V_v}G_v(N)\,dV_v+\hat{h}\int_{A}G_s(N)\,dA \quad (7)$$

Material degradation functions — subsurface damage. It is well established that subsurface damage in rolling bearings is caused by rolling contact fatigue (Lundberg and Palmgren (Refs. 1–2); Sadeghi, et al. (Ref. 10)). Cumulative fatigue damage models are expressed by a stress power law to account for the portion of life spent in the initiation and the short macropropagation phase of the crack that will ultimately determine the life time of rolling contacts (Lundberg and Palmgren (Ref. 1); Weibull (Ref. 24)). Many authors believe that the power function generally used to describe fatigue processes is not a mere empirical equation, but it is recognized as having the characteristics of a general physical law for damage accumulation processes of more universal applicability (Basquin (Ref. 28); Kun, et al. (Ref. 29)). A power law for rolling contact fatigue damage can be found in Lundberg and Palmgren (Ref. 1), Ioannides and Harris (Ref. 11), and Ioannides, et al. (Ref. 12). Using the approach of Ioannides and Harris (Ref. 11), the power law for subsurface rolling contact fatigue reads:

$$G_v=\bar{A}N^e\frac{\langle\sigma-\sigma_u\rangle^c}{z^h} \quad (8)$$

More advanced formulations of the same basic model are also available. In Ioannides (Ref. 30), σ_u is not constant but it is assumed to be function of N; that is, $\sigma_u(N)$. A similar methodology can be adopted in case the material undergoes changes of the original fatigue strength due to some extreme thermo-mechanical conditions during the stress cycling history of the rolling contact. When variable operating conditions are used in a bearing, the damage accumulation can be followed up by using the Palmgren-Miner rule (Ref. 31). Therefore, when the fatigue limit changes due to an extreme event — for example, overloading, overheating etc.—Equation 8 can still be used with the current, derated fatigue limit.

Material degradation functions—surface damage. Several surface-related failure modes and related mechanisms can be identified in rolling bearings (e.g., surface distress, indentations, wear-related stress concentrations, micropitting, surface chemistry, etc.). Under severe operating environmental conditions, surface damage leads generally to failures that are quite independent from the subsurface fatigue strength. Contrary to that, surface survival is more related to the operating conditions and raceway microgeometry e.g., metal-to-metal contact, local friction, film thickness, etc.). It is therefore difficult to generalize all different mechanisms using a single damage function as proposed for the subsurface fatigue case. Specific damage functions should be related to the expected failure modes. Tribological models can be used to derive these damage functions. When several mechanisms are present—for example, surface distress and mild wear—the damage function should account for possible competitive mechanisms (Ref. 18) and the statistical treatment should follow (Ref. 32). As an example of surface fatigue (Ref. 33), the following damage function is considered:

$$G_s = \overline{B} N^e \langle \sigma - \sigma_u \rangle^c \tag{9}$$

Generalizing Equation 7 for various independent surface regions (flanges, raceways, etc.) and/or independent surface damage mechanisms (surface distress, surface chemistry, etc.), one has:

$$\ln\left[\frac{1}{S(N)}\right] = \int_{V_v} G_v(N)\, dV_v + \hat{h}\int_A G_{s1}(N)\, dA + \ldots + \hat{h}\int_A G_{s_n}(N)\, dA \tag{10}$$

Note that to facilitate the use of the Weibull statistics (Weibull (Ref. 25)), the survival Equation 10 would require the adoption of a common standardized Weibull shape parameter (slope) for all different degradation functions. Failure modes with a tendency to be deterministic (very large Weibull slope) may represent a problem when combined with the more probabilistic classical rolling contact fatigue; for those cases (e.g., severe smearing, very severe wear, or contamination), the current approach may show limitations.

Model Behavior

Following Ioannides and Harris (Ref. 11) and Equation 8, the fatigue damage volume integral can be obtained by using the stress amplitude s originated from the Hertzian stress field:

$$\int_{V_v} G_v(N)\, dV_v = \overline{A} N^e \int_{V_v} \frac{\langle \sigma_v - \sigma_u \rangle^c}{z^h} dV_v \tag{11}$$

In a similar manner one can rewrite the surface damage function. If the constant $\hat{h}$ is included into the surface damage proportionality constant $\overline{B}$, one obtains:

$$\hat{h}\int_A G_s(N)\, dA = \overline{B} N^m \int_A \langle \sigma_s - \sigma_u \rangle^c dA \tag{12}$$

In the surface damage function (Eq. 12) the stresses σ_s must be obtained from the actual surface geometry of the contact and frictional stresses. Furthermore, for the sake of generality, the fatigue failure distribution of the surface of the rolling contact will be allowed to have a different Weibull slope (m) compared to the fatigue failures distribution of the subsurface volume (e). If different Weibull slopes are introduced when combining surface and subsurface damage models, the resulting statistics will not follow a standard Weibull failure distribution model. Substituting in Equation 7 and rearranging gives:

$$\ln\left(\frac{1}{S}\right) = N^e\left[\overline{A}\int_{V_v} \frac{\langle \sigma_v - \sigma_{uv} \rangle^c}{z^h} dV_v + N^{(m-e)}\overline{B}\int_A \langle \sigma_s - \sigma_{us} \rangle^c dA\right] \tag{13}$$

Substituting $N = uL$ in Equation 13 and solving leads to:

$$L^e = \frac{\ln\left(\frac{1}{S}\right)}{u^e\left[\overline{A}\int_{V_v} \frac{\langle \sigma_v - \sigma_{uv} \rangle^c}{z^h} dV_v + (uL)^{(m-e)}\overline{B}\int_A \langle \sigma_s - \sigma_{us} \rangle^c dA\right]} \tag{14}$$

Performing the reciprocal of Equation 14 provides the following:

$$\frac{1}{L^e} = \frac{1}{L_v^e} + \frac{1}{L_s^e} = \frac{u^e \overline{A}}{\ln\left(\frac{1}{S}\right)} \int_{V_v} \frac{\langle \sigma_v - \sigma_{uv} \rangle^c}{z^h} dV_v + \frac{u^m L^{(m-e)} \overline{B}}{\ln\left(\frac{1}{S}\right)} \int_A \langle \sigma_s - \sigma_{us} \rangle^c dA \tag{15}$$

It is easily recognized that in Equation 15 the reciprocal of the first term (at the right side of the equation) corresponds to the original Lundberg-Palmgren (Ref. 1) model (basic rating) modified with the additional effect of the fatigue limit (L_v) as introduced in Ioannides and Harris (Ref. 11), and the reciprocal of the second term (at the right side of the equation) corresponds to any additional effect introduced by damage accumulation at the surface of the rolling contact (L_s).

From Equation 14 it is possible also to derive an expression of the rolling contact life:

$$L = \frac{\left[\ln\left(\frac{1}{S}\right)\right]^{1/e}}{u}\left[\frac{1}{\overline{A}\int_{V_v} \frac{\langle \sigma_v - \sigma_{uv} \rangle^c}{z^h} dV_v + (uL)^{(m-e)}\overline{B}\int_A \langle \sigma_s - \sigma_{us} \rangle^c dA}\right]^{1/e} \tag{16}$$

Notice that in order to obtain the calculated life from Equation 16, a calculation based on an iteration scheme is required because the rolling contact life is also included in the right-hand side of Equation 16. However, if $m = e$, then the $(uL)^{m-e}$ term reduces to 1 and the solution for the life L becomes fully explicit.

Surface model behavior. In the current formulation, the treatment of the surface stresses and damage can be accomplished by using an advanced surface distress model for elasto-hydrodynamically lubricated (EHL) rolling–sliding rough contacts developed by Morales-Espejel and Brizmer (Ref. 18); further description of this model is given below.

In the current section, the use of this model will be limited to the calculation of the stress terms in the integrals of Equation 11 for the subsurface and Equation 12 for the surface. As a simple indication, consider maximum values of the stress amplitudes. For the case of $m = e$ the ratio of these stress amplitude terms should be proportional to the life ratio surface/subsurface to the power e/c, from which a consistency check and verification of the behavior of the present model can be obtained. With the model, it is possible to calculate the local pressures and stresses from mixed-lubrication conditions using as input a 3-D digital map of the surface topographies of the two rolling contact surfaces. The model can also calculate the local surface tractions from the mixed lubrication conditions.

This model was applied to a sample area of the raceway of a single-contact case of a radial ball bearing 6217 (Fig. 2). In general, this type of calculation is performed on a statistical significant number of area samples. However, for the present demonstration case, one area sample was found sufficient. The calculations were performed using the set of load cases as given in Table 1 and the roughness topography sample displayed in Figure 2. In Figures 3 and 4 some examples of the numerical calculations are shown (at the maximum pressure point in time); the sample area is at the center of the rolling contact; load case $P_u/P=0.5$ and with the assumption of reduced bearing clearance it is found a maximum contact pressure of $p_0=1.66\,GPa$ in the heaviest loaded contact (used as mean pressure in the micro-EHL analysis). The Hertzian contact semi-widths for this case are 0.24 and 2.4 mm. At this point it is important to introduce a common bearing-related term to describe the lubrication quality of the bearing, named κ, defined as the viscosity ratio between the actual used lubricant viscosity in the bearing and the required viscosity for proper lubrication (Ref. 15). This viscosity ratio can be related to the commonly used Λ parameter in the lubrication of other machine elements, as discussed in (Ref. 27). At the top of Figures 3 and 4 are displayed the distribution of the surface traction resulting from the frictional condition of the contact. In the poor lubrication case, surface traction values are substantially higher as boundary lubrication conditions dominate. In contrast, for the full-film case, values are low and there is no boundary (or dry) contact at all. At the center of Figures 3 and 4 the contact pressure and the τ_{xz} shear stress distribution for $y=0$ are also shown. Finally, at the bottom of Figures 3 and 4 the map of τ_{xz} at the surface of the sample area is displayed. Also in the case of the shear stress, the poor lubrication condition provides significantly higher stress values compared to the full-film conditions.

Table 1 Comparative surface and subsurface stress ratios for the example of the 6217 bearing, stress amplitude (*pa*)

		Subsurface Stress Amplitude	Surface Stress Amplitude, Poor Lubrication	Surface/Subsurface Life Ratio, Poor Lubrication	Surface Stress Amplitude, Good Lubrication	Surface/Subsurface Life Ratio, Good Lubrication
P_u/P	p_o, (GPA)	$\langle\tau_{xz}-\tau_u\rangle$	$\langle\tau_{xz,s}-\tau_{u,s}\rangle$, $\kappa=0.1$	$\left[\frac{\langle\tau_{xz,s}-\tau_{u,s}\rangle}{\langle\tau_{xz}-\tau_u\rangle}\right]^{c/e}_{\kappa=0.1}$	$\langle\tau_{xz,s}-\tau_{u,s}\rangle$, $\kappa=4$	$\left[\frac{\langle\tau_{xz,s}-\tau_{u,s}\rangle}{\langle\tau_{xz}-\tau_u\rangle}\right]^{c/e}_{\kappa=4}$
0.005	7.74	1.7×10^9	0.43×10^9	2.806×10^{-6}	0.32×10^9	1.798×10^{-7}
0.05	3.59	0.599×10^9	0.45×10^9	6.99×10^{-2}	0.25×10^9	0.294×10^{-3}
0.2	2.26	0.25×10^9	0.47×10^9	3.54×10^2	0.20×10^9	0.125
0.5	1.66	0.09×10^9	0.45×10^9	3.16×10^6	0.14×10^9	60

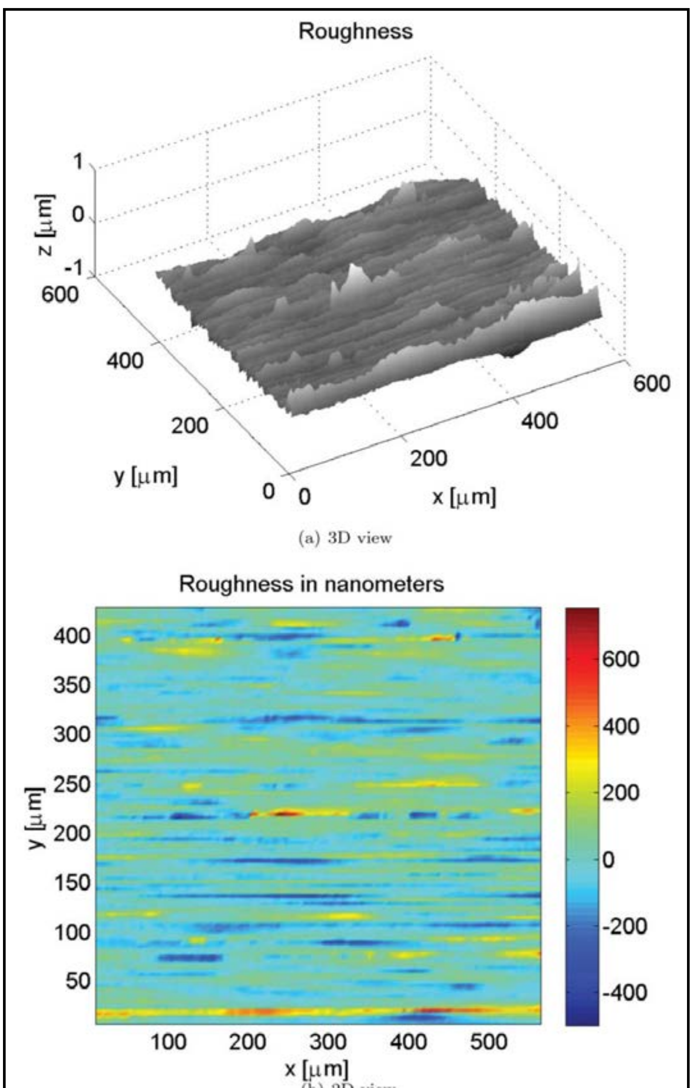

Figure 2 Inner ring sample roughness of radial ball bearing 6217, as used in the calculations; the ball surface was assumed smooth.

In Table 1 the results of several calculations are summarized. The calculations were performed using the advanced numerical model for surface distress discussed earlier (Ref. 18), the surface roughness sample was subjected to four loads and two lubrication conditions; that is, lubrication conditions, high film ($\kappa=4$) and low film ($\kappa=0.1$). Furthermore, considering the manufacturing machining of the surface and other chemical absorption processes of the material, it can be safely assumed that $\tau_{u.s}=0$ (conservative calculation).

Table 1 shows that at very high loads (i.e., low P_u/P values) the subsurface volume stress is dominant, providing a very low value of surface over subsurface damage ratio. As the load is reduced, the surface stress effect becomes more significant in defining the bearing performance. This is indicated in Table 1 by the continuous increase in the life ratio for both poor and good lubrication conditions. Comparing the two cases, it is found, as expected, that in the poor lubrication case the ratio surface over subsurface damage is always significantly larger than in the case of high kappa conditions. The maximum difference of the life ratio between the two lubrication conditions is about of three orders of magnitude, which is consistent with the expected variation of bearing life found in today's rating standards for the kappa range $0.1<\kappa<4$.

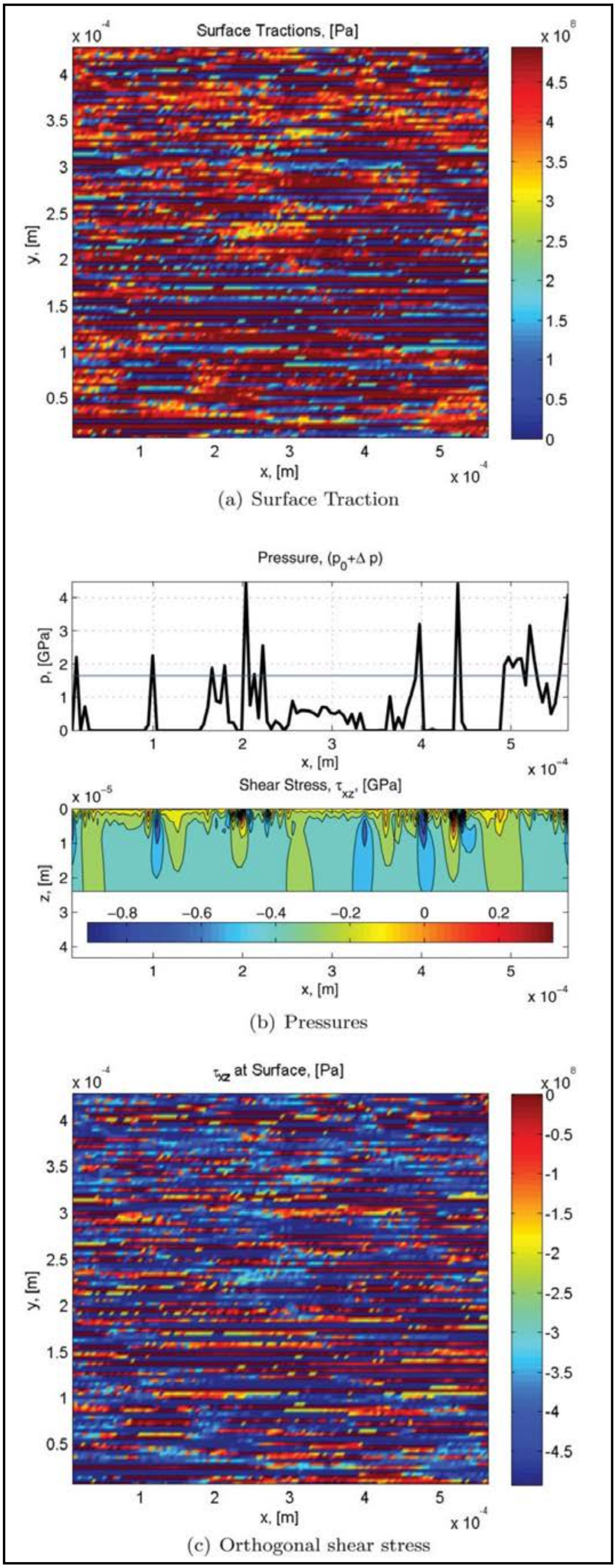

Figure 3 Calculated surface traction (along rolling direction), pressure, and stress τ_{xz} profile at $y=0$; surface stress τ_{xz} at over-rolling position of maximum mean pressure; low kappa case, $\kappa=0.1$; rolling direction from left to right.

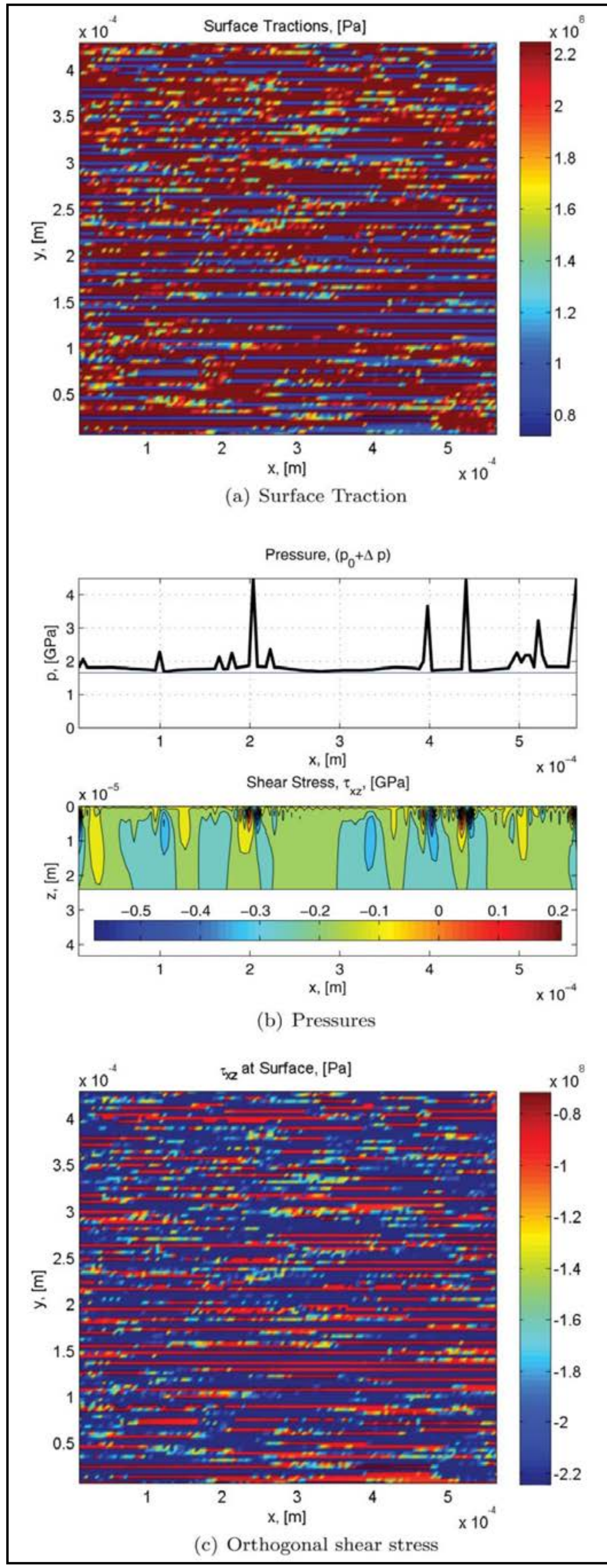

Figure 4 Calculated surface traction (along rolling direction), pressure, and stress τ_{xz} profile at $y=0$; surface stress τ_{xz} at over-rolling position of maximum mean pressure; high kappa case, $\kappa=4$; rolling direction from left to right.

Bearing Model Formulation

The transformation of the single-contact model Equation 16 into a rolling bearing life equation can be done by following the work of Lundberg and Palmgren (Ref. 1). Starting from Equations 44 and 46 of Lundberg and Palmgren (Ref. 1), after some algebraic manipulation to account for the load distribution and internal geometry in a bearing, Equation 81of this reference gives the transformation into bearing load. For a bearing load F applied radially on the rolling bearing, the heaviest loaded contact rolling- element (inner ring, RE-IR, subindex i) and for the contact rolling-element (outer ring, RE-OR, subindex e), one has:

$$\ln(1/S_i) = k_i m_i^{-w} F^w L^e \qquad \ln(1/S_e) = k_e m_e^{-w} F^w L^e \tag{17}$$

where the contact load of the heaviest loaded rolling element (Q) and the bearing load (F) are related by $F = m_i Q_i$ and $F = m_e Q_e$ and the exponent $w = pe = (c - h + 2)/3$. The parameters m_i, m_e are internal geometry functions of the bearing and can be calculated from Equations 89 and 95 of (Ref. 1). Finally, k_i and k_e are proportionality constants defined according to the reference and with the use of the nomenclature given in the reference; thus:

For point contact —

$$k = \ln(1/S)(A_1\varphi)^{\frac{-(c-h+2)}{3}} D_w^{\frac{-(2c+h-5)}{3}} \tag{18}$$

For line contact —

$$k = \ln(1/S)(B_1\psi)^{\frac{-(c-h+1)}{2}} D_w^{\frac{-(c+h-3)}{2}} l_a^{\frac{-(c+h-1)}{2}} \tag{19}$$

Combining the probabilities $S = S_i S_e$ leads to:

$$\ln(1/S_i) = (k_i m_i^{-w} + k_e m_e^{-w}) F^w L^e \tag{20}$$

Solving for L one obtains:

$$L = \left[\frac{\ln(1/S)}{k_i m_i^{-w} + k_e m_e^{-w}}\right]^{1/e} \frac{1}{F^p} \tag{21}$$

Now, following Ioannides, et al. (Ref. 12; Eq. 8), the damage volume integral can be obtained by a mean approximated value (avoiding in this way the integration):

$$\int_{V_v} G_v(N)\, dV_v \approx \overline{A} N^e \frac{\langle \sigma - \sigma_u \rangle^c}{z_o^{h-1}} ab \tag{22}$$

For the surface the stress integral can be derived from Equation 12 as:

$$\hat{h} \int_A G_s\, dA = \overline{B} N^m \int_A \langle \sigma_s - \sigma_u \rangle^c dA = N^m I_s \tag{23}$$

where, I_s represents the unknown surface damage integral, which includes a constant layer thickness $\hat{h}$ in the constant $\overline{B}$.

Substituting in Equation 7 and rearranging gives:

$$\ln\left(\frac{1}{S}\right) - N^m I_s = \overline{A} N^e \frac{\langle \sigma - \sigma_u \rangle^c}{z_o^{h-1}} ab \tag{24}$$

From Equation 24 it follows that Equation 21 can be modified with a surface integral by replacing $\ln(\frac{1}{S})$ by $\ln(\frac{1}{S}) - N^m I_s$, so replacing F with the more general bearing notation, P, and introducing a fatigue limit load-life modifying factor (Ref. 12), here it will be named a_u. Notice that this function becomes Â in case of zero fatigue limit.

$$a_u = \frac{\hat{A}}{\left[1 - \left(\psi_{brg} \frac{P_u}{P}\right)^w\right]^{c/e}} \tag{25}$$

Therefore, following Equation 21:

$$L^e = \left[\frac{\ln(1/S) - N^m I_s}{k_i m_i^{-w} + k_e m_e^{-w}}\right] (a_u)^e \left(\frac{1}{P^p}\right)^e \tag{26}$$

and with $N^m = u^m L^m$.

$$L^e = \left[\frac{\ln(1/S) - u^m L^m I_s}{k_i m_i^{-w} + k_e m_e^{-w}}\right] (a_u)^e \left(\frac{1}{P^p}\right)^e \tag{27}$$

Similarly, with existing bearing life equations the square bracket in Equation 27 without the I_s term and with $S = 0.9$ represents the dynamic capacity of the bearing to the power pe; thus:

$$L_{10}^e = \left[C^{ep} - \frac{u^m L_{10}^m I_s C^{ep}}{\ln(1/0.9)}\right] (a_u)^e \left(\frac{1}{P^p}\right)^e \tag{28}$$

Finally, solving for L_{10} gives:

$$L_{10} = \frac{1}{\left[1 + \frac{u^m L_{10}^{(m-e)} I_s}{\ln(1/0.9)} \left(\frac{C}{P}\right)^{ep} (a_u)^e\right]^{1/e}} a_u \left(\frac{C}{P}\right)^p \tag{29}$$

Equation 29 represents a new general semi-analytical form for bearing life calculation, based only on the modifying factor a_u with no surface damage components. It introduces an additional new surface damage function (or integral) I_s to account for only the surface effects in bearing life, calculated from Equation 23 or back-calculated with the use of an advanced surface distress models.

Advanced surface distress model. An advanced surface distress model (fatigue and mild wear) was introduced in the past (Ref. 18); this model has been validated with experiments and has been used with success in the description of indentation failures in rolling contacts (Ref. 19). The model will not be described here in detail as it is described elsewhere, but for completeness of the current article the key elements of the model are described below; the model will be used later on to illustrate the potential of the current formulation.

Modeling of the surface–fluid interactions (pressure and surface shear stress) is carried out by using a mixed-lubrication model that solves the transient Reynolds equation (with non-Newtonian behavior) for the fluid part and

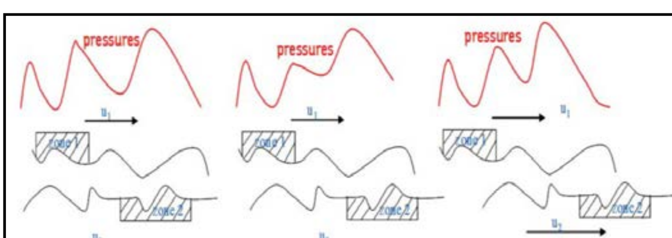

Figure 5 Illustration of roughness relative movement inside the contact; local analysis of the topography is done by varying the mean pressure following to local Hertz value (Ref. 18).

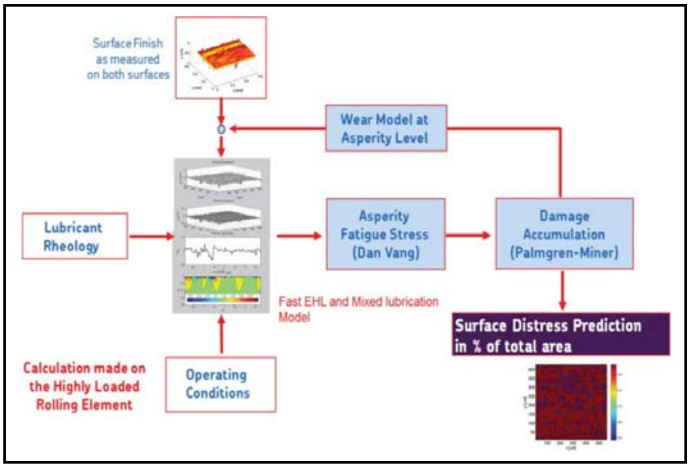

Figure 6 Flowchart of the advanced surface distress model used to solve the surface related failure modes (Ref. 18).

the half-space elasticity for the solid component with a fast fourier transform technique. For every macrocycle (Fig. 5), the scheme simulates the relative movement in time of the microgeometry inside the contact due to sliding (including moving pressures and stresses) and accumulates the damage via a fatigue criterion. Because at every passage in the contact the local operating conditions and the topography itself may change; thus, a simple damage accumulation law is used. Figure 6 summarizes the general modeling scheme and the computer program flowchart. The process begins with measured virgin 3-D surface samples for the two contacting bodies. Once both rough surfaces enter into the contact in the first cycle, the transient mixed-elastohydrodynamic lubrication problem is solved by means of the Reynolds equation for the different time steps until the roughness samples exit the contact. In the neighborhood of the surface the full stress tensor is calculated and used in the fatigue damage criterion (Ref. 18), which is applied for the current cycle, then the damage is accumulated according to an accumulation law (i.e., Palmgren-Miner) for the calculated number of cycles. Next, if the accumulated damage parameter exceeds the crack initiation limit, a crack or a micropit will be generated. The surface topographies then are fed into a lubricated wear model (based on a local Archard approach) that will modify the asperities microgeometry. The topography is updated only after a certain number of contact cycles to reduce computer time. The calculation process restarts and continues until the number of desired simulated contact cycles is reached. At the end of the simulation the modified surface topography is obtained together with the accumulated damage map on the surface and near subsurface; the micropitted area can be evaluated at this point as a percentage of the total area.

Surface distress modeling. In a calculation exercise with the advanced surface distress model (Ref. 18), several measured bearing topographies including rolling elements and raceways from bearings of different sizes from medium to large-size roller bearings. Lubrication conditions and load in the model were varied and the range of parameters varied in the model are summarized (Table 2). From the many numerical simulations with the described model it was concluded that the number of load cycles needed to generate

Table 2 Range of parameters used in the advanced model for surface distress for the derivation of Equation 31

Parameter	Minimum Value	Maximum Value
Mean Bearing Diameter d_m (mm)	87.5	400
Hertzian contact pressure, p_o (GPa)	0.3	3.55
Lubrication quality parameter κ	0.1	4
Sliding/rolling ratio, S	0.02	0.05
Number of loading cycles, N	10^5	10^9

surface distress (within 1.5% damage area at the surface of the total simulated area) could be calculated from the following curve-fitted equation:

$$N_{1.5\%} = \exp\left\{\frac{1}{\log_{10^e}}\left[\frac{c_1}{p_o^2} - (c_2 p_o)^{c_3} + c_4\right]\right\} \quad (30)$$

where, c_1, c_2, c_3, and c_4 are curve-fit constants that depend on the lubrication quality parameter of the bearing κ and the bearing mean diameter d_m.

The core of Equation 30 can be rearranged in terms of bearing load ratio rather than pressure and simplified to represent a surface damage function; therefore:

$$u^m I_s \approx f_1 \exp\left[\frac{f_2}{(P/P_u)^{f_3}} + \frac{f_4}{(P/P_u)^{f_5}}\right] \quad (31)$$

where,

f_1, f_2, f_3, and f_4 are curve-fitted constants that depend on the surface stress conditions (e.g., lubrication, contamination, etc.).

Finally, Equation 31 can be solved for f's using some calculated points of $u^m I_s$ obtained with the advanced surface distress model with the use of a collocation algorithm by fixing a number of locations in the abscissa P/P_u. An example of the obtained surface fatigue function for no contamination conditions is shown (Fig. 7) (R_s) normalized with respect to a constant; it can be seen that for better lubrication conditions (higher κ values), the surface fatigue function is substantially

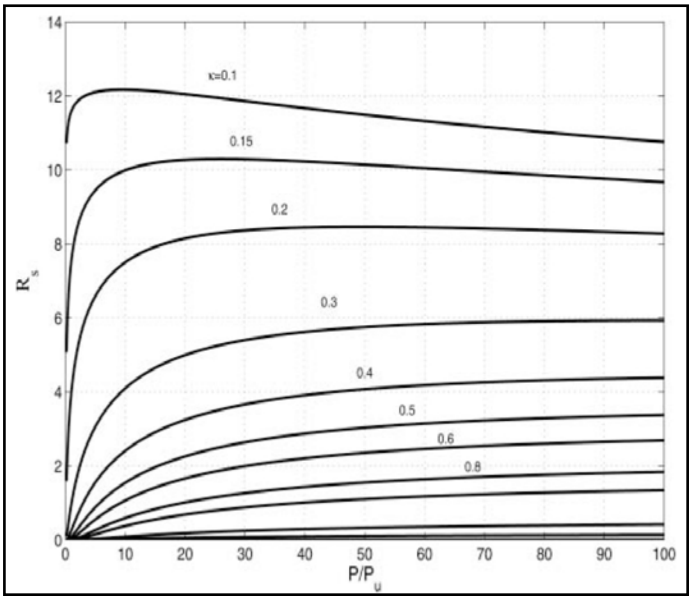

Figure 7 Normalized surface damage function ($R_s = I_s u^e L^e_{10.BR}/[KLn(1/0.9)]$) vs. bearing load ($P/P_u$) and the lubrication conditions (κ) as defined in ISO 281 (Ref. 15) for conditions of no contamination. Notice that, for higher values of κ better lubrication, the surface damage function is reduced, and it is also nearly constant with load.

reduced. This function is also nearly constant with load at high values of load.

Ratio of surface damage. To further explore the consistency of the new approach, the ratio between the surface and subsurface damage functions is calculated and discussed. Now, with introduction of the definition of the basic rating life (e.g. Ref. 15) $L_{10.BR} = (C/P)^p$, this ratio is calculated by:

$$S_R = (a_u L_{10.BR} - L_{10}) / (a_u L_{10.BR}) \tag{32}$$

In this equation L_{10} is calculated with the use of Equation 29 and the proposed surface damage diagram (Fig. 7).

Figure 8 shows the corresponding plots for S_R as a function of load P/P_u and κ. From the figure it can be observed that at very low loads the surface damage tends to low values; with an increase in load the surface damage becomes dominant with respect to the subsurface damage. However, with even higher loads the subsurface damage gains importance due to rolling contact fatigue, reducing the dominance of the surface damage.

Figure 8 also shows an approximate indication of when the damage is driven by the surface and when by the subsurface, depending on the load and the lubrication conditions, giving this a possible indication of where most likely the failure will occur at the end of the life of the bearing population. It can also be seen that the importance of the surface damage function with respect to the subsurface is reduced when the lubrication conditions are enhanced (higher κ values).

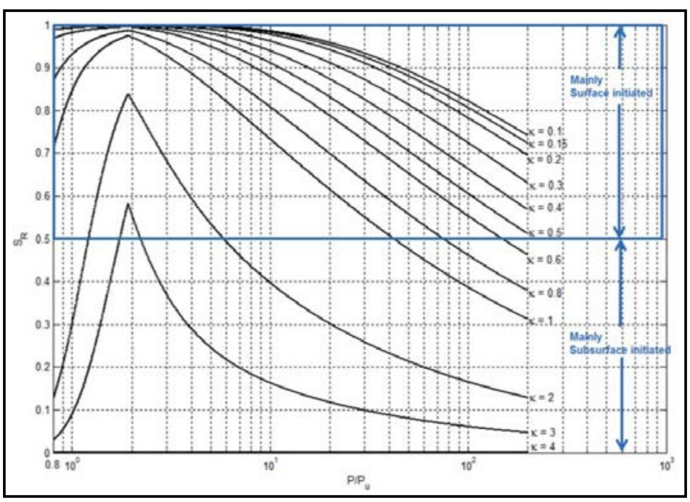

Figure 8 Calculated damage function ratio from Equation 32 for different κ values and for variable load P/P_u for a deep-groove ball bearing typical case. The importance of the surface damage function with respect to the subsurface is reduced when the lubrication conditions are enhanced.

Results and Discussion

In the present section, some results from the model will be compared with endurance tests carried out in-house; furthermore, a simple ball bearing example will be used to illustrate the methodology. The comparison with endurance tests will focus on the surface model, which is the novel part of the present approach. The subsurface model used here has been compared with endurance tests in the past (e.g., Refs. 11–12) and so will not be repeated here.

Endurance testing practice (Refs. 34–35) shows that the rate

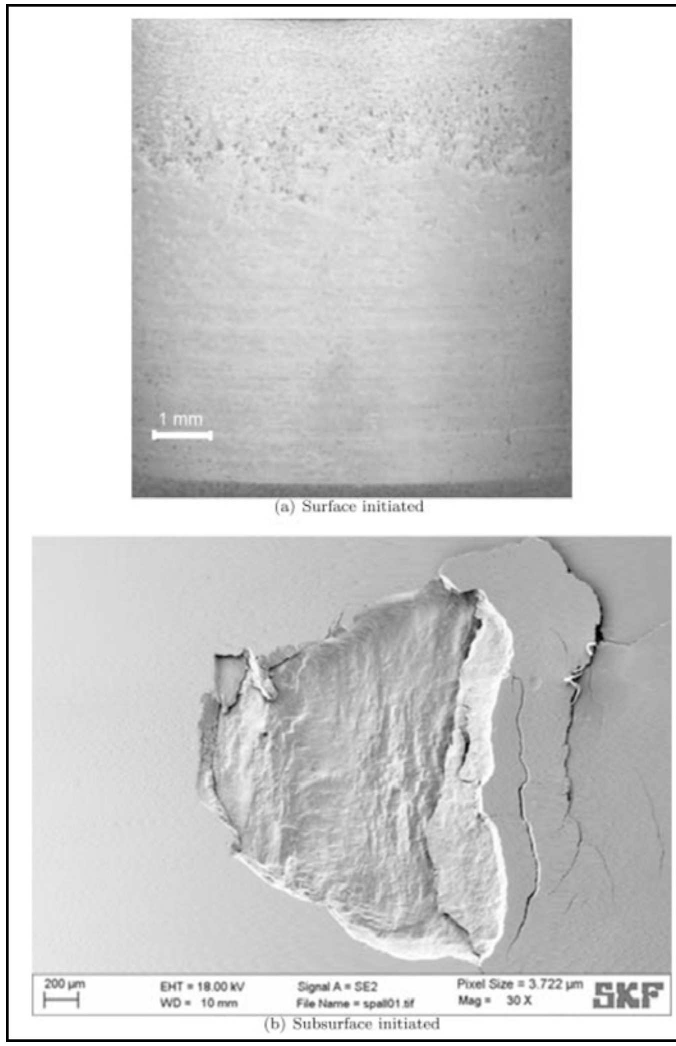

Figure 9 Pictures of in-house tested bearing raceways showing surface- and subsurface-initiated failures; over-rolling direction from left to right.

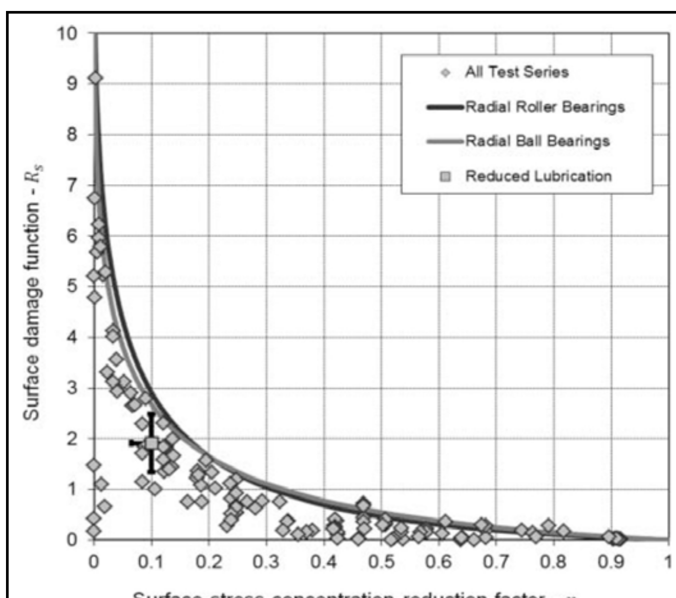

Figure 10 Comparison the surface damage limiting curves of the ball and roller bearings; for example, Equation 31 and the back-calculated surface damage obtained from endurance testing of bearing population samples.

Table 3 Test conditions used for bearing life testing, as given in (Ref. 14)			
Bearing Type	**Designation**	**Load Ratio, *C/P***	**Lubrication, *K***
Deep-Groove Ball Bearings	6305, 6205, 6206, 6207, 6309, 6220	1, 2.8, 2.4, 2.1, 3.1, 3.5, 4, 6	4, 3.4, 2.1, 2, 1
Cylindrical roller bearings	NU 207 E, NU 309 E	2.5, 2.77, 2.82	4, 1, 0.8
Spherical roller bearings	22220 E, 22220 CC	2.22, 2.3, 2.5, 2.7, 3, 4.7	4, 3.6, 1.8, 0.37, 0.28
Tapered roller bearings	331274, K-LM11749, K-HM89449, K-580/572	1, 1.1, 1.3, 2.5, 3.5	4, 2.9, 0.9

of bearing failure, either from the surface or from the subsurface (Fig. 9), is distributed in a very similar way (Ref. 34). This indicates that a common Weibull slope can be used in Equation 29. This equation can be used to back-calculate the surface damage parameter $R_s = u^e I_s / [K \ln(1/0.9)]$ corresponding to 90% reliability of a bearing populations that are endurance tested.

The methodology used is as follows:

1. Solve Equation 29 for I_s with known operating conditions and L_{10} lives from endurance tests.
2. Calculate the parameter R_s using I_s.
3. Repeat the calculation for every endurance test series and plot the results R_s vs. P/P_u and η in Figure 10 (points in the plot). As described in Gabelli, et al. (Ref. 14), the parameter η is a measure of the stress on the surface caused by poor lubrication and/or contamination conditions; for $\eta = 1$ there is no extra surface stress, for $\eta = 0$ the stress is maximum (Ref. 12).
4. Once the test series are plotted, plot the results of the surface distress model (solid lines) (Eq. 31). The dependence on η of this equation is implicit in the surface topographies and operating conditions used to obtain this equation. In this case, the extreme conditions of the tests have been used.

Typically a bearing population sample is formed by a set of 25–35 bearings, of which about one third may fail during the test (Ref. 36). For this evaluation, a set of 227 endurance population samples was used including a total of some 6,650 bearings, covering both ball and roller bearing geometries in equal proportion. A detailed description of the test used here is given in (Ref. 14), but for the sake of completeness a summary of the test conditions is given in Table 3. From the test, the mean point estimation of the L_{10} life is derived using Weibull statistics. In Figure 10 the surface damage parameter R_s back-calculated from a large set of endurance tests results (dots) is displayed alongside the surface damage parameter obtained from the surface distress model presented in Equation 31 (lines). The curves of the surface distress model represent the limit conditions of the endurance tests for both roller and ball bearings and are plotted vs. the surface stress concentration reduction factor η (Ref. 14) for description. Inspecting the results plotted in Figure 10, it is apparent that almost all test results are positioned below the limit curves obtained from Equation 31. From Figure 10 it can be concluded that the model theory provides a safe estimation of the raceway survival. Furthermore, given the large dispersion affecting endurance test results, an additional experimental evaluation was carried out. A more recent group of endurance test results was merged into a single pool of results formed by 445 roller and ball bearings tested under reduced lubrication ($\kappa \approx 0.4$–0.5). This test pool was statistically analyzed in order to gain information regarding the 90% confidence interval of the surface damage parameter derived from testing. The result of this analysis is indicated with the square symbol and the 90% confidence range is indicated with the error bars. The comparison with the model curves shows that also in this case the surface damage function has a proper safe setting compared to the statistical data of the survival of the raceway surface. The test series (points) follows very well the behavior of the surface model when the severity at the surface (η) is varied; higher values of η represent endurance tests with good lubrication and little or no contamination (less severity at the surface), and the surface model (lines) shows the corresponding behavior.

A full ball bearing example. Despite the fact that the objective of the present article is not to illustrate the use of the proposed model in bearing applications nor in comparison with other models, it is believed that a simple ball bearing example can help the reader to understand the methodology and the behavior of the model.

Consider a standard 6309 deep-groove ball bearing with a dynamic load rating of 55.3 kN and a fatigue load limit of 1.34 kN, working under a radial gravity load of 10 kN. The bearing is operating under constant lubrication and temperature conditions in different rotating speeds; thus, the lubrication parameter κ described in ISO 281:2007 (Ref. 15) can be readily calculated. The bearing works under very clean conditions so, the contamination parameter (see ISO 281:2007 (Ref. 15)) can be set $e_c = 1$.

Using the surface–subsurface rating life calculation method outlined in the present article, the rating life can be estimated using Equation 29 in conjunction with Equation 25 and Figure 7. For this calculation example, the surface–subsurface life rating life model can be set using similar constants and parameters as applied in the ISO 281 model (Ref. 15) and thereby similar results from the two models are expected.

Following this criterion it is assumed that the surface/subsurface survival distribution is characterized by similar, standardized Weibull exponents; thus the surface Weibull exponent m can be assumed to be equal to the Weibull exponent $e = 10/9$ as used in ISO 281:2007 (Ref. 15). Others exponents and constants used in Equations 29 and 25 can be taken from (Ref. 12), leading to the results of Table 4.

Table 4 Deep-groove bearing example (6309) results from the present approach to illustrate the use of the model			
ISO Viscosity Ratio κ	**Surface Damage Function R_s**	**Contribution of the Surface Eq. [32] (%)**	**Surface-Subsurface Life Eqs. [29] and [25] L_{10} *(Mrev)***
0.1	12.2	100	17
0.4	2.2	96	81
2.9	0.02	23	1,656

By inspecting Table 4 it can be recognized that the surface/subsurface life model (when positioned to the same settings as in ISO 281 (Ref. 15)) can provide rating lives that are similar to the standard.

However, the main ability of the present model is to treat fatigue damage developed at the surface of the raceway separately from the subsurface. This is the motivation behind the development of the present model, as this will open new and better capabilities in representing the performance and damage process taking place in rolling bearings.

Summary and Conclusions

New concepts for bearing life calculation based on the separation of different regions at risk have been investigated. A simple approach is proposed to separate the surface from the subsurface rolling contact fatigue based on the product law of reliability. In this way a more flexible and physical approach can be constructed to describe surface damage mechanisms in rolling bearings considering tribological effects on the surfaces. As an example of the potential of the new approach consisting of the separation of surface and subsurface, the effects of poor lubrication were considered in the current article and an advanced model for surface distress (Ref. 18) was used to describe these effects in a more general bearing life calculation. With similar techniques, it seems possible to include, for example, the effect of additives (Ref. 20), indentations (Ref. 19) and abrasive wear — to be discussed in future publications.

From the development of the model and its behavior, the following observations can be summarized:

- There are significant gains and increase in flexibility in bearing life modeling when other failure modes or regions in addition to the Hertzian rolling contact fatigue are incorporated into the formulation of the bearing life.
- The present approach represents a framework where different failure modes can be included for different regions at risk of the bearing contact. This approach allows for the incorporation of knowledge gained from the use of tribological models into bearing life estimation.
- The current approach can give an indication of the zone at higher fatigue risk in a bearing population.
- A potential target of the new approach is the physical modeling of several classes of bearing failure mechanisms, such as surface distress (surface fatigue and mild wear), lubricant contamination, lubricant additives, wear-related stress concentrations, etc., capturing some deterministic aspects of bearing surface topography, material properties, and local lubrication conditions.

A new more general model able to account for different failure modes has been proposed, and the surface term of the model is compared with a large set of experimental results of endurance testing of bearing population samples. With the use of advanced tribological models, curve-fitted equations are obtained to describe the surface damage functions (I_s) to consider; for example, surface distress effects from poor lubrication. Furthermore, a simple application example of a ball bearing has been used to illustrate the methodology.

From the obtained results the following conclusions can be drawn:

- In the present work, the separation of the surface and subsurface in bearing life calculations has been demonstrated to be a feasible and convenient way to model particular failure modes in the two separate regions.
- The proposed surface damage parameter R_s obtained from the advanced surface distress model represents a good conservative limit when compared with endurance tests results.
- According to the results of Table 1 and the ball bearing example, the subsurface and the surface fatigue models keep a consistent behavior when compared with existing bearing life models. **PTE**

Acknowledgements. The authors wish to thank the SKF Group for kind permission to publish this article. The authors also want to thank V. Brizmer for his help in the derivation of the surface distress function, Equation 30.

References

1. Lundberg, G. and A. Palmgren. "Dynamic Capacity of Rolling Bearings," *Acta Polytechnica, Mechanical Engineering Series*, 1947, 1(3), pp. 1–52.
2. Lundberg, G. and A. Palmgren. (1952), "Dynamic Capacity of Roller Bearings," *Acta Polytechnica, Mechanical Engineering Series*, 1952, 2 (4), pp. 96–127.
3. Tallian, T. E. "On Competing Failure Modes in Rolling Contacts," *ASLE Transactions*, 1967, 10 (4), pp. 418–439.
4. Olver, A. V. "The Mechanisms of Rolling Contact Fatigue: An Update," *Proceedings of the Institution of Mechanical Engineers: Part J - Journal of Engineering Tribology*, 2005, 219, pp 313–330.
5. Chiu, Y. P., T. Tallian, J.I. McCool and J.A. Martin. (1969), "A Mathematical Model of Spalling Fatigue Failure in Rolling Contact," *Transactions of the ASLE*, 1969, 12, pp 4106–4116.
6. Chiu, Y. P., T.E. Tallian and J.I. McCool. , J. I. "An Engineering Model of Spalling Fatigue Failure in Rolling Contact — The Subsurface Model," *Wear*, 1971, 17, pp 433–446.
7. Tallian, T. E. and J.I. McCool. , J. I. "An Engineering Model of Spalling Fatigue Failure in Rolling Contact — The Surface Model," 1971, *Wear*, 17, pp 447–461.
8. Tallian, T. E. "An Engineering Model of Spalling Fatigue Failure in Rolling Contact Engineering Discussion and Illustrative Examples," *Wear*, 1971, 17, pp 463–480.
9. Zaretsky, E. V. *STLE Life Factors for Rolling Bearings*, 2nd Ed., Society of Tribologists and Lubrication Engineers, 1999, Park Ridge, IL.
10. Sadeghi, F., B. Jalalahmadi, T.S. Slack, N. Raje and N.K. Arakere. "A Review of Rolling Contact Fatigue," *Journal of Tribology*, 131, pp 041403-1-15.
11. Ioannides, E. and T.A. Harris. "A New Life Model for Rolling Bearings," *Journal of Tribology*, 1985, 107, pp 367–378.
12. Ioannides, E., G. Bergling and A. Gabelli. "An Analytical Formulation for the Life of Rolling Bearings," *Acta Polytechnica Scandinavica, Mechanical Engineering Series*, 1999, 137, pp 1–80.
13. Gabelli, A., J. Lai, T. Lund, K. Ryden, I. Strandell and G.E. Morales-Espejel, "The Fatigue Limit of Bearing Steels. Part II: Characterization for Life Rating Standards," *International Journal of Fatigue*, 2012, 37, pp 155–168.
14. Gabelli, A., G.E. Morales-Espejel and E. Ioannides. "Particle Damage in Hertzian Contacts and Life Ratings of Rolling Bearings," *Tribology Transactions*, 2008, 51, pp 428–445.
15. ISO 281. "International Standard, Rolling Bearings — Dynamic Load Ratings and Rating Life," 2007, Geneva, Switzerland.
16. Epstein, D., T. Yu, Q.J. Wang, L.M. Keer, H.S. Cheng, S. Liu, S.J. Harris and A. Gangopadhyay. "An Efficient Method of Analyzing the Effect of Roughness on Fatigue Life in Mixed-EHL Contact," *Tribology Transactions*, 2003, 46 (2), pp 273–281.
17. Epstein, D., L.M. Keer, Q.J. Wang, H.S. Cheng and D. Zhu. "Effect of Surface Topography on Contact Fatigue in Mixed Lubrication," *Tribology Transactions*, 2003, 46 (4), pp 506–513.
18. Morales-Espejel, G. E. and V. Brizmer. "Micropitting Modeling in

Rolling–Sliding Contacts: Application to Rolling Bearings," *Tribology Transactions*, 2011, 54, pp 625–643.
19. Morales-Espejel, G. E. and A. Gabelli. "The Behavior of Indentation Marks in Rolling–Sliding Elastohydrodynamically Lubricated Contacts," *Tribology Transactions*, 2011, 54, pp 589–606.
20. Brizmer, V., H.R. Pasaribu and G.E. Morales-Espejel. "Micropitting Performance of Oil Additives in Lubricated Rolling Contacts," *Tribology Transactions*, 2013, 56 (5), pp 739–748.
21. Warhadpande, A. and Sadeghi. "Effects of Surface Defects on Rolling Contact Fatigue of Heavily Loaded Lubricated Contacts," Sadeghi, F. (Ed.), *Proceedings of the Institution of Mechanical Engineers: Part J - Journal of Engineering Tribology*, 2013, 224, pp 1061–1077.
22. Lamagnere, P., R. Fougeres, G. Lormand, A. Vincent, D. Girodin, G. Dudragne and F. Vergne. "A Physically Based Model for Endurance Limit of Bearing Steels," *Journal of Tribology*, 1998, 120, pp 421–426.
23. Lai, J., T.Lund, K. Ryden, A. Gabelli and I. Strandell. "The Fatigue Limit of Bearing Steels Part I: A Pragmatic Approach to Predict Very High Cycle Fatigue Strength," *International Journal of Fatigue*, 2012, 37, pp 155–168.
24. Weibull, W. "A Statistical Theory of Strength of Materials," *Proceedings of the Royal Swedish Academy of Engineering Sciences*, 1939, 151, pp 1–45.
25. Weibull, W. "A Statistical Distribution Function of Wide Applicability," *Journal of Applied Mechanics*, 1951, 18 (3), pp 293–297.
26. Blachere, S. and A. Gabelli. "Monte Carlo Comparison of Weibull Two and Three Parameters in the Context of the Statistical Analysis of Rolling Bearings Fatigue Testing," J. Beswick, (Ed.), 9th Volume, *Bearing Steel Technologies: Advances in Rolling Contact Fatigue, Strength Testing and Related Substitute Technologies*, 2012, 1548, pp 382–407.
27. Morales-Espejel, G.E.A. Gabelli and E. Ioannides. "Microgeometry Lubrication and Life Ratings of Rolling Bearings," *Proceedings of the Institution of Mechanical Engineers: Part C - Journal of Mechanical Engineering Science*, 2010, 224, pp 1965–1981, London, UK.
28. Basquin, O.H. "The Exponential Law of Endurance Tests," *Proceedings of American Society of Testing Materials*, 1910, 10, pp 625–630.
29. Kun, F., H.A. Carmona, J.S. Andrade and H.J. Hermann. "Universality behind Basquin's Law of Fatigue," Physical Review Letters, 2008, 100 (9), p 094301.
30. Ioannides, E. "Component Reliability Analysis — A Fatigue Life Model Common to Rolling Bearings and Structural Components," *SEECO 85 Conference Transactions*, 1985.
31. Miner, M. A. "Cumulative Damage in Fatigue," *Journal of Applied Mechanics*, 1945, 12, pp A159–A164.
32. McCool, J.I. "Competing Risk and Multiple Comparison Analysis for Bearing Fatigue Tests," *Tribology Transactions*, 1978, 21, pp 271–284.
33. Lubrecht, A. A., B.O. Jacobson and E. Ioannides. "Lundberg Palmgren Revisited," *Proceedings of the Japan International Tribology Conference*, Nagoya, Japan, 1990.
34. Andersson, T. "Endurance Testing in Theory," *Ball Bearing Journal*, 1985, 217, pp 14–23.
35. Goss, R. and E. Ioannides. "Performance Testing: Facilities and Opportunities," *Ball Bearing Journal*, 1989, pp 12–21.
36. Leenders, P. "Endurance Testing in Practice," *Ball Bearing Journal*, 1985, 217, pp 24–31.

For Related Articles Search
bearing life
at www.powertransmission.com

Antonio Gabelli is senior scientist working at SKF on tribology and rolling contact fatigue life of rolling bearings. He joined the Engineering and Research Center of SKF in Netherlands in 1981, since than he published many research papers on fatigue and lubrication of rolling bearings. He was one of the key contributors to the new bearing life theory, developed by SKF in the 90's He is also author of several patents on rolling bearings. He holds a mechanical engineering degree from the University of Padua (Italy) and a PhD degree in from Chalmers Technical University of Gothenburg (Sweden).

Guillermo E. Morales-Espejel is principal scientist, SKF Engineering & Research Centre, The Netherlands, and a visiting professor at LaMCoS, INSA de Lyon. He holds a PhD in tribology from the University of Cambridge, a "Habilitation à Diriger des Recherches (INSA-Lyon)," and has15 years of experience in rolling bearings. Morales-Espejel has authored more than 50 scientific papers and several book chapters with a focus on bearing life, friction, lubrication and surface life.

Antonio & Guillermo were awarded by STLE for their tribology publications of 2010 ("Particle Damage in Hertzian Contacts and Life Ratings of Rolling Bearings") & 2013 ("The Behaviour of Indentation Marks in Rolling-Sliding Elasto-hydrodynamically Lubricated Contacts.")

ETEL

ASSISTS IN SOLAR IMPULSE 2 FLIGHT AROUND THE GLOBE

Recently the Solar Impulse 2 airplane finished its flight around the globe, with airtime lasting over 500 hours and is the first plane to do so relying entirely on Solar Energy. With an ETEL motor inside, the Solar Impulse 2 successfully started in Abu Dhabi and flew across Asia, the Pacific Ocean, the United States, Atlantic Ocean, and Europe before heading right back where it started. This is a remarkable achievement, not just in the industry of aviation but for the idea of clean energy as a technological driving force.

The Solar Impulse 2 airplane was designed to have optimum performance-per-weight ratio so every component, down to the smallest of screws was made to be as light as possible. The task of contributing a proper motor that met these demands was a goal ETEL was more than able to achieve. A number of years ago ETEL was asked to contribute its expertise in direct drive technology to create a motor capable of an efficiency above 95 percent which proved vital in ensuring the solar power absorbed by the panels was made the most out of. ETEL proved to be the supplier that was able to provide the highest quality motor and that expertise continues to be incorporated into their own standard product line of direct drive motors and motion stages.

Photo courtesy of Solar Impulse | Revillard | Rezo.ch

Through a partnership with many vendors, the Solar Impulse 2 team was able to achieve their goals and ETEL is proud to be a part of this accomplishment. In the end, the airplane proved to successfully combine the most advanced scientific knowledge in terms of aeronautics, materials, photovoltaic energy and electrical motors.

The ETEL motor used in the Solar Impulse 2 airplane is a torque motor characterized by having an optimized force density and unmatched current efficiency. It is based on the same technology as the parts every ETEL customer receives. The motor in the Solar Impulse 2 is obviously slightly modified to support the extreme environmental conditions that are unique to this challenge, but the heart of the motor and its magnetic technology is currently ensuring the proper operation of thousands of machines around the world.

CTI Shanghai

SET TO CONTINUE DISCUSSION ON DEDICATED HYBRID TRANSMISSIONS

Stricter legislation and more environmental awareness among drivers, including those in China, are causing a radical rethink in the automobile industry; all the experts agree that hybrid drives will become more important. A new transmission category is particularly outstanding: Dedicated Hybrid Transmissions (DHTs), which are developed specifically for use in hybrid drives.

A DHT is a hybrid transmission that performs key transmission functions (such as matching the ICE's rpm and torque to vehicle operating conditions) with the assistance of an electric motor. So in a DHT, electric motor components handle essential tasks, and are 'baked in' to the concept. "This distinguishes DHTs fundamentally from add-on solutions, and follows the current way of thinking. "It doesn't matter whether legislation or driving enjoyment is the stimulus," says Mario Brunner, head of passenger car transmission, AVL List GmbH. "Either way, there is no doubt that electrification will significantly change the future of drive technology. Most of today's hybrid drives use conventional transmissions with add-on hybrid solutions, but that means extra costs. For an optimal balance of functionality and cost, we need dedicated solutions instead."

However, the efficiency of traditional transmission concepts is also being improved. "Audi is currently launching a new, sustainable S-tronic generation of its all-wheel drive system," reveals Michael Schöffmann, head of transmission development, Audi AG. "It still has all the typical Quattro characteristics, but is much more efficient." Efficiency is an issue all through drive development work, and DHTs score high marks in this respect.

Three advantages stand out when discussing DHTs. Firstly, DHTs can be designed to be far more compact and efficient. Unlike conventional automatic shifts, for example, where gear step numbers are progressively increasing, DHTs can actually reduce the gear step count. Secondly, DHTs support very economical, eco-friendly driving because the electric motor's support enables the ICE to stay within its optimal performance window. Thirdly, the extra power from the electric motor can be used to tangibly boost two factors that are key for the acceptance of hybrid automobiles: driving dynamics and enjoyment. Hybrid drive automobiles are still a rarity, but a turnaround is in sight.

"On the one hand, there is growing pressure to factor in environmental protection more strongly; on the other, there are stricter emission rules. These have advanced the development of energy-saving drive technologies in the world as a whole, as well as in China," explains Hanbing Yang, president automotive of the Schaeffler Group Greater China.

China in particular is seen as a pioneer of electric mobility. "In the last decade, the world changed the Chinese automobile market. In the next decade, China will assume leadership in the automobile world. So 'Developed for China' means 'Developed for the world' too," says Prof. Dr. Frank Zhao, director of Tsinghua Automotive Strategy Research Institute (TASRI), Tsinghua University. The ambitious targets of the Chinese central government confirm that assessment: the plan is to put around 5 million electric automobiles on the road by 2020.

The first time people presented and discussed DHTs for a broad specialist audience was at the 14th International CTI Symposium Berlin in early December 2015; the initiative came from Prof. Dr.-Ing. Ferit Küçükay, the Symposium chairman, and Dr. Robert Fischer (AVL and member of the advisory board). Since then, this born-in-Berlin acronym has been widely adopted by specialists, and the industry eagerly awaits the next International CTI Symposium 'Automotive Transmissions, Hybrid & Electric Drives". From September 21-23 2016, an estimated 500 experts will meet up in Shanghai to continue their discussion of DHT, as well as other topics.

The International CTI Symposium is a meeting place for experts from around the world who wish to discover and discuss the latest technologies and developments in automobile transmissions and alternative drives. The Symposium presents the people who drive the transmissions market, and indicates technically and financially interesting developments. Apart from the development of DHT, topics for Expert Talks in Shanghai will also include cost reduction potential, higher efficiency and comfort optimization, CO_2 emission reductions, integration, connectivity and the influence of automated driving on transmissions.

Baldor

NAMES WAITE MOTOR PRODUCT MANAGEMENT DIRECTOR

Baldor Electric Co. recently named Ryan Waite director of motor product management for its global NEMA motor business. Waite is responsible for the rapid global growth of Baldor•Reliance motors sales as well as implementing the strategic vision for the business. Waite joined Baldor in 1990 and has experience in operations, engineering and customer service. His previous positions have included manufacturing engineering manager, plant manager, director of Lean Flex-Flow, and most recently, director of manufacturing. Waite has a bachelor's degree in mechanical engineering from Southern Illinois University. He will be located in Fort Smith, Arkansas.

ICP

SPEAKS TO NACD MEMBERS ON TODAY'S HIRING AND RECRUITING CHALLENGES

Responding to a request from the National Association of Chemical Distributors (NACD) to help member companies with their hiring challenges, Industrial Careers Pathway (ICP) arranged for retired industrial manufacturing executive Terry Knight to make a presentation to an NACD leadership meeting in Philadelphia, Pa., recently. Knight, who served as chair of the ICP Steering Committee for five years until January 2016, has been actively involved with ICP since its inception in 2002 as a leading advocate and contributor.

Knight spoke to about 30 executives from the chemical distribution industry about ICP resources to help with the challenge of recruiting, hiring and managing employees from generations Y and Z, and successfully engaging five generations in the workplace. Surveys of industrial distribution executives consistently show that filling open positions and managing younger employees continue to occupy a top trouble spot. ICP, having been at this issue's forefront for the past decade, is a go-to resource for insights and solutions.

Knight said, "The opportunity to speak to this highly professional level of chemical distribution industry leaders was very valuable and worthwhile. The excitement in the room regarding the programs ICP offers was real."

Of specific interest to the group was the introduction of a new program, dubbed Team ID, which is aimed at raising awareness of and attracting entry-level employees to careers in industrial distribution. The program consists of an online "personality" quiz for job seekers to discover how their own personality will match up with a specific entry-level career path in the field: inside or outside sales, customer service or warehouse work. In addition to the quiz, videos illustrate the process of these jobs, with Team ID "superheroes" swooping in to save the day with on-time, helpful and accurate problem solving as industrial distribution workers. Job seekers are then linked to the ICP website to learn more and to the ICP Job Board, the only online job board specifically focused on industrial distribution careers, to apply for posted jobs.

Access to the resources available for distributor companies (many for no charge or at very low cost) is at the website below. These resources include free "How-To-Guides" for everything from starting an internship to organizing a company tour for the community.

Any company belonging to one of the nine supporting Alliance Partner organizations, of which NACD is one, can take advantage of these free resources and receive discounted rates when posting open positions to the aforementioned job board. Member companies are highly encouraged to urge employees to register as volunteer ICP Ambassadors in order to help ICP spread the word about industrial distribution in their local communities. Many opportunities identified by ICP, such as classroom presentations and career fair appearances, are awaiting volunteers for 2016.

Smart Automation Group

BRINGS TOGETHER CUSTOM AUTOMATED EQUIPMENT MANUFACTURERS

The world's leading suppliers of custom automated manufacturing equipment recently launched the Smart Automation Group, a collaborative partnership designed to disrupt the custom automation services industry.

This unique partnership—which includes Eclipse Automation, Insys Industriesysteme AG, Transmoduls Ltd, SMZ Wickel-und Montagetechnik AG, JULI Technology, and ITE Automation—are joining together to share best practices, industry IP, experience, and know-how to provide customers with automation solutions in a way unlike anything on the market today.

Thanks to the collective expertise of its member companies, Smart Automation Group will be able to produce technologies that are the lynchpins of manufacturing processes across every industry, including automotive, consumer, health sciences, nuclear, electronics, energy, and industrial, to help clients grow today, and build for tomorrow.

"Our vision is to collectively disrupt the traditional way of providing custom automation services, putting the customer at the core of everything we do," said Steve Mai, president of Eclipse Automation. "Smart Automation Group's collaborative approach means we can automate any manufacturing process, and that through a commitment to quality, and operational excellence, there is no challenge we can't solve for our clients, no matter where they are in the world."

As part of this new joint venture, each partner is taking a team-oriented approach, significantly increasing the overall capabilities that enhance automation solutions for clients. Each company will review its own client requests, but if a particular project requires additional capabilities, the collaborative project team can be tapped to bring the best value to the table.

All of this seamlessly takes place in the background, ensuring the client maintains a single point of contact. The result: enhanced value of all automation solutions for customers.

In any given case, one of Smart Automation Group's partners could be called on to contribute with its global reach, intellectual property, employee know-how, resources, or relationships, all with the sole goal of providing value-added solutions to each project scope.

With offices in Canada, the United States, Hungary, Switzerland, and China, Smart Automation Group works with strategic partners in every region of the world, to provide unique, cost-effective, and scalable solutions through collaboration and shared innovation, with a global support network.

Kollmorgen

RELEASES AUTOMATION AND MOTION CONTROL CATALOG

Kollmorgen's new Automation and Motion Control catalog details the features, benefits and specifications of the company's complete range of motion control solutions, including: Direct Drive motors, servo motors and drives, Safe Motion, distributed and central servo amplifiers and the complete Kollmorgen Automation Suite. The catalog also includes stepper motors and drives, PMDC motors, linear actuators and planetary gearboxes.

More than 100 diverse and scalable product and solution ideas are covered in the catalog, making it much more than a simple guide for selecting individual products used in next-generation machine design. The Kollmorgen catalog helps OEM engineers find the highest performance control and drive combinations for their machines. High-performance motion differentiates machines, enhancing energy efficiency and accuracy and reliability, which delivers a marketplace advantage and improves Overall Equipment Effectiveness (OEE) for OEMs and their customers.

The new catalog is now available in two easy-to-use formats, a downloadable PDF and an interactive, easy-to-navigate, digital catalog for online browsing.

Comet Solutions and Romax Technology

ANNOUNCE DISTRIBUTION AGREEMENT

Comet Solutions, Inc., a leading provider of simulation automation technology, recently announced a new distribution agreement with Romax Technology, a U.K.-based global leader in analytical solutions for transmission, axle and driveline systems. This partnership combines Comet's automation platform, which enables organizations to quickly build integrated, robust, multi-tool simulation automation templates (combining CAD, FEA, Romax and other tools), with Romax's software and award-winning engineering team's expertise in developing optimized driveline and gearbox systems.

ROMAX TECHNOLOGY

For over 25 years, *RomaxDESIGNER* (Romax's flagship simulation program) has enabled users to quickly and accurately perform detailed analyses of critical performance attributes for improvements in durability, efficiency and dynamics, including advanced features such as consideration of manufacturing variation and planetary sideband analysis.

Comet provides simulation automation and standardization processes by integrating the variety of tools used by gearbox/transmission product engineers, including CAD, finite element meshers, *RomaxDESIGNER*, structural analysis tools, fatigue life tools, packaging/tolerancing tools, and other detailed gear design tools. By integrating data and tools within a single automation environment that includes optimization capabilities, Comet enhances the system analysis aspects of *RomaxDESIGNER*, providing product engineers with the capability to explore the complex interactions between flexible structural components, such as housings and planetary carriers, and the resulting gear, bearing and overall system performance.

"Romax is widely recognized as a leading global provider of integrated software and services for gearbox, bearings and driveline systems. We are extremely pleased to continue building on the development partnership we started last year," said Steve Brown, vice president global sales at Comet Solutions. "Comet further extends the capabilities of *RomaxDESIGNER*, creating an integrated and automated design and analysis environment.»

"Romax and Comet have extended their development partnership, with Romax now securing the rights to supply Comet SimApps to its customers. Our customers want to see the whole stack working, and this new arrangement enables Romax and Comet to work together as closely as needed during an engagement for the design automation flow to be fully captured and validated," said Dan Poon, head of partners at Romax Technology.

September 26–28—MINExpo International 2016 Las Vegas Convention Center. MINExpo boasts 12 indoor and outdoor halls and more than 1,800 companies involved in the global mining industry. Opening sessions allow the industry to come together to debate global challenges, market fluctuations and the future of mining. 20+ education sessions will tackle the most timely and pressing issues in mining today. Resources include exploration, mine site development, open pit mining, underground mining, smelting and refining, processing and preparation and reclamation. Attendees will see live demonstrations they can use today and emerging technology for tomorrow. For more information, visit *www.minexpo.com*.

September 26–29—Gear Dynamics and Gear Noise Short Course Ohio State University. The purpose of this unique short course is to provide a better understanding of the mechanisms of gear noise generation, methods by which gear noise is measured and predicted and techniques employed in gear noise and vibration reduction. Over the past 37 years more than 1,950 engineers and technicians from over 360 companies have attended the Gear Noise Short Course. A popular feature of this course is the interspersing of demonstrations with lectures. The extensive measurement and computer software capabilities of the Gear and Power Transmission Research Laboratory allow instructors to do this in a simple and non-commercial manner. Course instructors include Dr. Donald Houser and Dr. Rajendra Singh. For more information, visit *www.nvhgear.org*.

October 2–5—GMRC Gas Machinery Conference 2016 The GMRC Gas Machinery Conference provides three days of technical training and presentations by the industry's leading experts. The conference includes a vendor exhibit showcasing the latest equipment, technology and services. Educational sessions and networking opportunities are valuable for design engineers, facility engineers, technicians and others, with an emphasis on the operation, maintenance and testing of gas compression machinery. The Gas Machinery Research Council (GMRC) is a not-for-profit research corporation that was founded in 1952. GMRC provides its member companies and industry with the benefits of an applied research and technology program directed toward improving reliability and cost effectiveness of the design, construction and operation of mechanical and fluid systems. For more information, visit *www.gmrc.org/gmc*.

October 5–7—Mechanical Components and Materials Technology Expo Osaka, Japan. M-Tech Osaka is Western Japan's largest exhibition gathering all kinds of mechanical parts such as bearings, fasteners, mechanical springs and metal and plastic processing technology. M-Tech Osaka attracts a significant number of professionals from design, development, manufacturing, production engineering, procurement and quality control departments, who are looking to buy solutions for their businesses. Products and services featured include motors, drivers, controllers, bearings, shafts, mechanical parts, springs, compressor and hydraulic equipment, testing and measuring and more. For more information, visit *http://www.mtech-kansai.jp/en*.

October 11–13—MCMA TechCon 2016 New Orleans, Louisiana. The Motion Control & Motor Association's annual TechCon provides technical training by industry experts, great networking opportunities and a table top exhibition where attendees can see the latest technologies from leading suppliers. New this year is the addition of MCMA's Certified Motion Control Professional Training. Attend to learn and keep up-to-date on motion control, motor and related automation technologies. Breakout session topics include motor design, magnetic materials and electrical steels, motion control, drives and feedback systems and network systems and software tools for engineers. For more information, visit *www.motioncontrolonline.org*.

October 18–21—Northeast Mechanical Fair of Mechanical Industry, Metallurgical and Electrical Material Pernambuco Convention Center, Olinda, Brazil. This year's theme is "Industrial Automation and Energy Efficiency - The Future of Industry." With an exhibition that includes products and services, workshops and training events, the Mechanical Fair will bring together industries such as automation, machinery and equipment, renewable energy, and electronics. "Thanks to the diversity of the exhibitors and program of seminars and workshops offered by the Mechanical Northeast, visitors will have access to a wide range of appropriate solutions for their enterprises and opportunities for expansion. In addition, the event will provide exhibitors a valuable opportunity to do business," said the president of Simmepe Alexander Valencia. Exhibitors include Gates, Parker, SEW and Tsubaki. For more information, visit *www.mecanicane.com.br*.

October 23–27—Materials, Science & Technology 2016 Salt Lake City, Utah. MS&T16 is the most comprehensive forum for materials science and engineering technologies. Attendees learn from materials specialists, explore diverse materials applications and experience the synergy of this materials community. MS&T crosses the boundaries of most materials events by bringing together a broad range of technical sessions and expertise through the strengths of six major materials organizations: The American Ceramic Society (ACerS), Association for Iron & Steel Technology (AIST), ASM International, Metallurgy and Materials Society of CIM (MetSoc), NACE International, and The Minerals, Metals & Materials Society (TMS). Topics include additive manufacturing, ceramic composites, failure analysis, light metal technology, next generation biomaterials, surface protection, high performance metals and more. For more information, visit *www.matscitech.org*.

October 25–27—The Assembly Show Rosemont, Illinois. This focused trade show will help assembly equipment suppliers, buyers and users connect, learn and share the latest technologies and industry advancements. Workshops include collaborative robotics and managing assembly lines. The keynote presentation, "The Herman Miller Performance System Journey: Overcoming the Challenges of Implementing a People Focused Production System," will take place Wednesday October 26. A panel discussion, "Rosie the Riveter 2.0: Recruiting and Retaining Women in Manufacturing," will take place on Thursday October 27. Additional presentations from Festo, Destaco, Balluff, Bosch Rexroth and others will take place during the show. For more information, visit *www.theassemblyshow.com*.

CALL FOR PAPERS!

Are you sitting on an idea for a technical paper but wondering where to present it? Do you have one already written, sitting on your desk, gathering machine dust?

How about *Power Transmission Engineering*? We are always looking for gearing- and power transmission component-relevant technical papers for publication in the magazine and in its digital version. Having your work appear in *Power Transmission Engineering* guarantees you an audience of the most experienced and discriminating industry players. You say your work has not been peer-reviewed? Not a problem, as we are lucky—and thankful—to have on-hand some of the most experienced and brilliant minds in the industry—our technical editors. So if your work "passes muster" and is published, you'll know you were reviewed by the best—and most demanding.

Chances are you'll be creating the paper under the auspices of the company for whom you work or own, or for one of the various industry-relevant associations. That means they as well will bask in the reflected glory that accrues with publication in *Power Transmission Engineering*.

For publication guidelines and more information, please contact Jack McGuinn at *jmcguinn@powertransmission.com*.

ADVERTISING INDEX

Power Transmission Engineering

Power Transmission Engineering is Your KEY to understanding Gears, Gear Drives, Bearings, Motors, Clutches, Couplings, Brakes, and other Power Transmission Components.

Unlock your FREE subscription by filling out this form.

FREE SUBSCRIPTION

1

☐ **YES** I want to receive/continue to receive ***Power Transmission Engineering*** FREE!

☐ No thank you.

Name:______________________________ (print) JobTitle/Position: ____________________

Signature ______________________________ (required) Date: ____________________

2 → E-mail ______________________________ (So we can notify you when the online edition is available)

SAVE a TREE!
☐ I ONLY want the digital edition (e-mail required)

3 → Please update your contact information or attach you business card here. (No Staples)

Company Name:______________________________

Address: ______________________________

____

____

City:______________________________

State/Province: ____________ ZIP+4/Postal Code: ____________

Country: ______________________________

Telephone: ____________ Fax: ____________

E-mail: ______________________________

Website: ______________________________

4 → How is THIS LOCATION involved with power transmission products? (Check all that apply)

☐ WE MAKE power transmission products (10)
☐ WE BUY power transmission products (12)
☐ WE SELL power transmission products (Distributors, sales reps. etc.) (14)
☐ WE DESIGN products with power transmission components in them. (16)
☐ Other (please describe) (15)______________________

5 → My company's principal product or service is:______________________

6 → What is your primary job function responsibility? (Check one)

❏ Corporate Management (1
❏ Plant Engineering (2)
❏ Design Engineering (3)
❏ Marketing & Sales (4)
❏ Manufacturing Engineering (5)
❏ Purchasing (6)
❏ Quality Control (7)
❏ Factory Automation (8)
❏ Maintenance (9)
❏ Other (10)
____

Is there a colleague within your company that might benefit from having their own copy of ***Power Transmission Engineering*** magazine?

Name: ______________________________

Title: ______________________________

DIGITAL SUBSCRIPTIONS

❏ **YES, I want to be notified each issue when *Power Transmission Engineering* is available online**

❏ **YES, I would like to receive *Power Transmission Engineering's* monthly e-mail newsletter**

❏ **YES, I would like to receive *Power Transmission Engineering's* twice monthly e-mail Product Alerts**

❏ **YES, I would like to receive 3rd-party e-mails from *Power Transmission Engineering's* advertisers and partners**

❏ **YES, I would like to receive subscription renewal notices by e-mail**

❏ **No, I do not wish to be contacted by e-mail.**

FAX TO 1-847-437-6618 or
VISIT US ONLINE AT
www.powertransmission.com/subscribe.htm

Mind Sport

Stronghold Competition Puts the Fun in FIRST Robotics

Matthew Jaster, Senior Editor

Here's what we know about Tremont, Illinois: It's a small village in Tazewell County, (population 2,400+), holds an annual summer turkey festival (quite popular) and the courthouse is a famous historic site where politician James Shields challenged an "up-and-coming" lawyer named Abraham Lincoln to a duel with cavalry broad swords (they showed up, but the duel never materialized). In 2016, you can add FIRST Robotics Competition World Champion to the village's rather eccentric list of accomplishments.

Tremont High School's robotics team (Roboteers Team 2481) has been battled-tested since this season's competition kicked-off back on January 9, 2016. "The game this year was called FIRST Stronghold. It had a medieval theme that was comprised of attacking your opponent's castle by crossing defenses and shooting boulders (foam balls) into scoring openings in the tower. Disney Imagineering came up with this year's theme," said Team Mentor Tim Koch.

For those new to robotic engineering competitions, these events are played with robots that can weigh almost 150 lbs. and have a 120" maximum perimeter. The robots can travel 10–14 feet per second at top speed and play in three robot alliances on a 27' wide by 54' long carpeted playing field. "The FIRST Robotics Competition is designed to be a spectator sport and is played in arenas where hundreds or thousands of spectators cheer as the robots play the game," Koch said.

FIRST Stronghold is a medieval themed robotics competition where teams attack their opponent's castle by crossing defenses and shooting boulders (foam balls) into scoring openings in the tower.

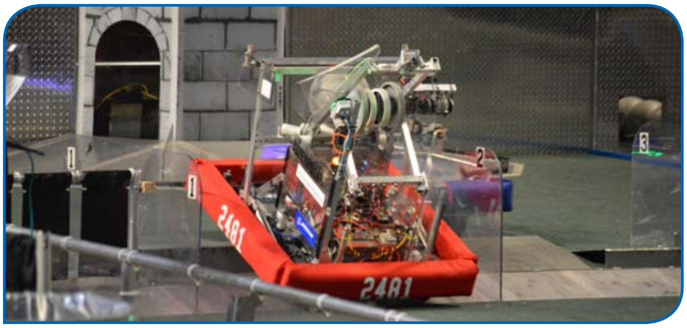

Tremont High School's Roboteers Team 2481took 1st place in the FIRST Robotics Competition World Championship in St. Louis with their robot nicknamed Broadside.

Team 2481 designed, built, programmed and tested their robot during a six-week build period. They also built a second identical robot to use for driver practice and to continue to refine the controls software. During the build season, Koch said it is common for students to work 20–30 hours per week *over and above* time in school and other extracurricular activities. "We also spend a lot of time learning about the teams we are playing with and against to develop a game strategy," he added.

The Roboteers built a robot with two, 2-speed transmissions (one for each side of the robot powering the wheels that are shifted by small pancake air cylinders). The intake roller has a 3:1 planetary transmission reduction using a VexPro transmission. The shooter wheels are direct drive off the motor. There is also an in-line encoder that provides direct feedback via a PWM cable to the motor controller. The team used a proportional-integral-derivative (PID) controller to spin the shooter up to its target speed in the shortest possible time and maintain target speed without significant oscillation.

After winning regional events in Central Illinois and Knoxville, Tennessee, Team 2481 took part in the May 2016 World Championship in St. Louis. They were one of a four-team coalition that took first place in the FIRST Robotics Competition World Championship, beating over 2,800+ teams to capture the world title. And they did it utilizing a robot they affectionately nicknamed, *Broadside*.

While skilled labor continues to be a huge problem in manufacturing, the data Koch has collected on the high school robotics team looks promising. "We track metrics on our team's involvement in STEM. Over the last eight years, 82 percent of our participating students have gone into STEM fields."

The Roboteers will participate in several off-season events where they will re-play Stronghold, sometimes with slightly different rules to keep things interesting. "We now have the opportunity to spread the word about FIRST in our surrounding communities and state, allowing more students to participate," Koch said. "We agree with FIRST Co-founder Woodie Flowers, that this is the hardest fun we ever had!" **PTE**

For more information:

FIRST Robotics
Phone: (603) 666-3906
www.firstinspires.org

Roboteers Team 2481
matt@team2481.com
www.team2481.com


Don't get torqued off.
Assembly
Disassembly
Get TorqLOC®!
Can't remove your corroded gear unit from your machine shaft? Well, stop fretting about it. Man up and get TorqLOC® from SEW-EURODRIVE.
With its stainless steel construction, keyless hollow shaft, and taper bushings, TorqLOC® disassembly is fast and easy. The same bolts used for assembly are used for disassembly.
Not only does TorqLOC® reduce your maintenace headaches, it also eliminates belts, chains, and sprockets to reduce energy costs.
SEW EURODRIVE
seweurodrive.com / 864-439-7537
— Driving the World —